Sequence specific recruitment of proteins to the inner membrane complex of the malaria parasite *Plasmodium falciparum* (Welch, 1897)

Dissertation

Zur Erlangung des Doktorgrades an der Fakultät für Mathematik,
Informatik und Naturwissenschaften,
Fachbereich Biologie
der Universität Hamburg

vorgelegt von
Johanna Wetzel

Hamburg, 2014

Date of oral defense: 19 December 2014

The following evaluators recommend the admission of the dissertation:

Prof. Dr. Tim-Wolf Gilberger

Prof. Dr. Christian Voigt

Table of contents

List of figures

List of tables

I Abstract

Plasmodium falciparum causes malaria tropica, the most severe form of this disease. There are about 250 to 500 million infections annually and about 600'000 deaths per year, the majority being children younger than five years in sub-Saharan Africa. Drug resistance is widespread and there is no vaccine available. The intra-erythrocytic developmental cycle of this parasite causes all symptoms associated with malaria. *Plasmodium* belongs to the infra-kingdom Alveolata, which consists of single-celled organisms that are unified by the existence of an endomembrane system that underlies the plasma membrane, termed "inner membrane complex " (IMC). The IMC has distinct and crucial functions for the respective organisms in cytokinesis and host cell invasion. More than 30 structurally and phylogenetically distinct proteins are embedded in the IMC membranes, where a portion of these proteins displays N-terminal acylation motifs. While N-terminal myristoylation is catalyzed co-translationally within the cytoplasm of the parasite, palmitoylation takes place at specific membranes and is mediated by palmitoyl acyltransferases (PATs). Here, for the first time, a PAT (PfDHHC1) is identified that exclusively localizes to the IMC. It is shown that this enzyme has an identical distribution during schizogony like two putative substrates; the dual acylated IMC proteins (PfISP1 and PfISP3). Using a comprehensive mutagenesis approach, both proteins were used to probe into specific sequence requirements for IMC membrane recruitment, and their interaction with differentially localized PATs of the malaria parasite.

II Abbreviations

2BP	2-bromopalmitate
3xHA	triple hemaglutinin
A	alanine
aa	amino acid
ABE	acyl biotin exchange assay
ACT	artemisinin combination therapy
AKR1/2	ankyrin repeat-containing protein 1/ 2
AMA1	apical membrane protein 1
Amp	ampicillin
AP2	Apetala2
ApiAP2	apicomplexan AP2
APS	ammonium persulphate
APT	acyl protein thioesterase
ARO	armadillo repeats only protein
ATP	adenosine triphosphate
BiP	binding immunoglobulin protein
BNI	Bernhard-Nocht-Institute for Tropical Medicine
bp	base pair
BMCC	1-Biotinamido-4-[4'-(maleimidomethyl)cyclohexane-carboxamido]butane
BSA	bovine serum albumin
BSD	blasticidin deaminase
C	cysteine
C-	Carboxy-
cam	calmodulin
cDNA	complementary DNA
CD36	cluster of differentiation 36
CDPK1	calcium-dependent phosphokinase 1
ChAd63/MVA	chimpanzee adenovirus 63 / modified vaccinia virus Ankara
CRD	cysteine-rich domain
CSP	circumsporozoite protein

D	asparagine
Da	Dalton
DAPI	4′,6-Diamidino-2-phenylindol
DBD	DNA-binding domain
dd	double distilled
DDT	dichlorodiphenyltrichloroethane
DHHC	asparagine-histidine-histidine-cysteine
DMSO	dimethyl sulfoxide
DNA	desoxyribonucleic acid
dNTP	deoxyribonucleotide triphosphate mix
DRM	detergent-resistant membrane
dsDNA	double stranded DNA
DTT	4,4'-(2,2,2-trichloroethane-1,1-diyl)bis(chlorobenzene)
E	glutamic acid
E. coli	*Escherichia coli*
EBA	erythrocyte binding antigen
EDTA	ethylenediaminetetraacetic acid
ERD2	ER lumen protein retaining receptor 2
ER	endoplasmatic reticulum
ERF2	effect on Ras function
EtBr	ethidium bromide
EtOH	ethanol
F	phenylalanine
fw	forward
G	glycine
g	9.81 m/s^2
gDNA	genomic DNA
GAP	genetically attenuated parasite
GAP45/50	glideosome-associated protein 45/50
GAPDH	glyceraldehyde 3-phosphate dehydrogenase
GFP	green fluorescent protein
GRASP	Golgi re-assembly stacking protein
GTF	general transcription factor
H	histidine

h	hour
H3	histone 3
H4	histone 4
HA	hydroxylamine
HCl	hydrogen chloride
hDHFR	human dihydrofolate reductase
HeLa cells	Henrietta Lacks cells
HEPES	N-2-hydroxyethylpiperazine-N-2 ethansulphonic acid
HP1	heterochromatin protein 1
hpi	hours post invasion
HRP	horseradish peroxides
I	isloleucine
ICAM1	intracellular adhesion molecule 1
IDC	intra-erythrocytic developmental cycle
IFA	immuno fluorescence assay
IgG	immunoglobulin G
IMC	inner membrane complex
IP	immunoprecipitation
IPTG	isopropyl-β-D-thiogalaktopyranosid
iRBC	infected red blood cell
ISP	IMC sub-compartment protein
K	lysine
kb	kilobase
kDa	kilo dalton
L	leucine
l	litre
LB	luria broth
M	molar, methionine
MBOAT	membrane-bound -acyl transferase
mCherry	Cherry fluorescent protein
MCS	multiple cloning site
MDCL	Michael G. DeGroote Center for Learning and Discovery
MeOH	methanol
min	minutes

ml	millilitre
MLC	myosin light chain
mM	millimolar
mRNA	messenger RNA
MSP	merozoite surface protein
MTIP	myosin tail interacting protein
MW	molecular weight
MyoA	myosin A
Myr-CoA	myristoyl-CoA
N	asparagines
N-	Amino-
NaAc	sodium acetate
NaCl	sodium chloride
NEM	N-ethylmaleimide
ng	nanogram
NMT	N-myristoyl transferase
NP-40	nonidet P-40
OD	optical density
ORF	open reading frame
P	proline
P. falciparum	*Plasmodium falciparum*
PAT	palmitoyl acyl transferase
PBS	phosphate-buffered saline
PBS-T	PBS-Tween
PCR	polymerase chain reaction
pDNA	plasmid DNA
PFA4/5	protein fatty acyltransferase
PfEMP1	*Plasmodium falciparum* erythrocyte membrane protein
PM	plasma membrane
PMSF	phenylmethylsulfonyl fluoride
PPT	protein palmitoyl thioesterase
PV	parasitophorous vacuole
PVM	parasitophorous vacuole membrane
Q	glutamine

R	arginine
RALP	rhoptry associated leucine-rich protein
RAP	rhoptry associated protein
RAS	radiation attenuated sporozoite
RBC	red blood cell (erythrocyte)
RESA	ring-infected erythrocyte surface antigen
RNA	ribonucleic acid
RON1	rhoptry neck protein 1
ROP	rhoptry protein
rpm	rounds per minute
RPMI	Rosswell Park Memorial Institute
RT	room temperature
rv	reverse
S	serine
S. cervisiae	*Saccharomyces cerevisiae*
sec	seconds
SDS	sodium dodecyl sulfate
SDS-PAGE	sodium dodecyl sulfate polyacrylamide gel electrophoresis
SP	signal peptide
STET	sucrose, Tx-100, EDTA, Tris
Swiss TPH	Swiss Tropical and Public Health Institute
SWF1	spore wall formation protein 1
T	threonine
TAE	tris acetate
TCA	trichloroacetic acid
TE	tris-EDTA
TEMED	tetramethylethylenediamine
TF	transcription factor
TMD	transmembrane domain
TRAP	trombospondin related adhesion protein
TVN	turbovesicular network
TX-100	Triton X-100
U	units

UAS	upstream activation sequence
5’ UTR	5’ untranslated region
UV	ultraviolet
V	volt, valine
VAC8	vacuole related protein
Y	tyrosine
W	tryptophan
WHO	world health organization
WR	WR99210
µF	microfarad
µg	microgram
µL	microliter

1. Introduction

The causative agent of malaria is an obligate intracellular apicomplexan parasite of the genus *Plasmodium.* Among over 200 *Plasmodium* species, only five of them are pathogenic to humans: *P. falciparum* and *P. vivax*, but *P. ovale, P. malariae* and the monkey malaria *P. knowlesi* can cause infections (Singh et al., 2004). *Plasmodium falciparum* causes malaria tropica (also termed falciparum malaria), the most severe form of human malaria that is responsible for 80 % of all cases (Mendis et al., 2001). *Plasmodium falciparum* is most prevalent in Africa, whereas *P. vivax* is mainly present in Southeast Asia. In other parts of Asia and South America, prevalences of *P. falciparum* and *P. vivax* are equal, since transmission rates are lower.

Malaria tropica represents one of the major human health problems in endemic countries and also causes an economical and social burden (Sachs and Malaney, 2002). There are three billion people at risk, 150 to 300 million people are affected annually and about 600'000 die per year due to malaria (WHO World Malaria Report, 2013). Children under five years in sub-Saharan Africa are mostly affected, representing 80 % of all cases (Snow et al., 2005). This disease is widespread among subtropical and tropical countries, and its highest burden is in Africa, but as well in Southeast Asia and South America (Fig. 1.1). Poverty has been and still remains a major reason for the disease (Sachs and Malaney, 2002). Transmission of parasites takes place by *Anopheles* mosquitoes, which also represent the definitive hosts where the sexual reproduction takes place. *Anopheles gambiae* is a major vector since it is especially robust and effective, however 41 of the more than 400 species of the family of anopheline mosquitoes are dominant vectors for malaria transmission to humans (Hay et al., 2010). A recently established global map shows the highly complex variety of *Anopheles* species distribution (Sinka et al., 2012): the situation in Africa is characterized by co-dominance of fewer species compared to the Asian-Pacific or Central-America, where numerous species co-exist (Sinka et al., 2012).

The lack of an effective vaccine, spreading resistances of the parasite to antimalarial chemotherapeutics and problematic vector control measurements are the basis for the urgent need for new intervention approaches in the fight against this disease.

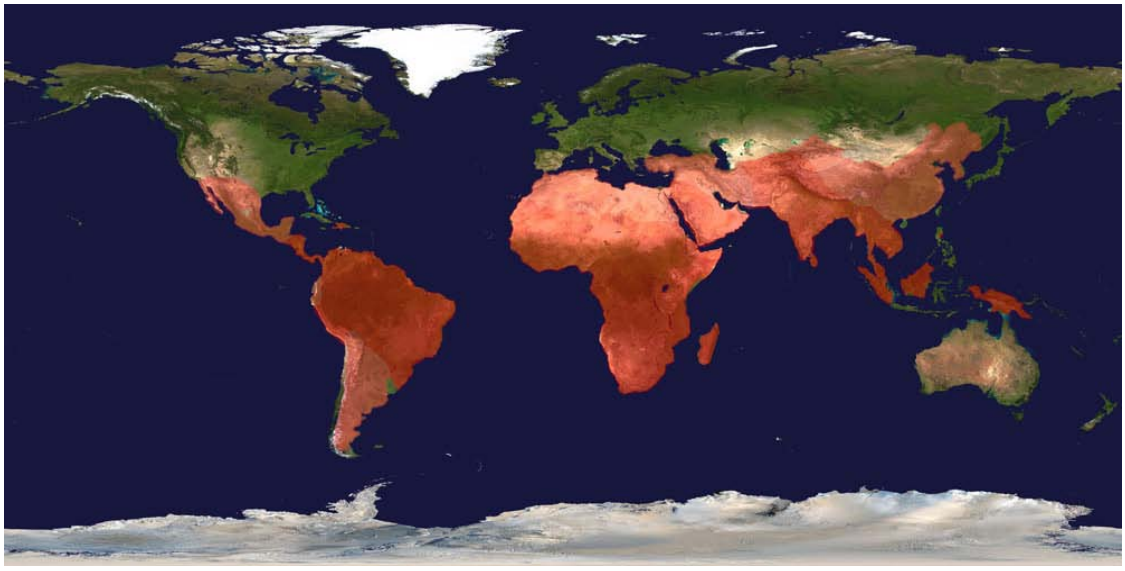

Figure 1.1 World map representing *P. falciparum* prevalence. Nowadays, malaria is endemic to over 100 nations, mostly affected are tropical and subtropical countries. Highly endemic regions are indicated in red, less endemic regions are in lighter shades of red. Image was adapted from sanger.ac.uk.

1.1 Symptoms, treatment and prevention of malaria

The word "malaria" originates form the Italian words "mala" (bad) and "aria" (air). It was believed that foul gasses released from the soil and water of the swamps cause the disease. This idea persisted throughout the 19th century until Laveran discovered the parasite (Laveran, 1880).

1.1.1 Symptoms

It generally takes about two weeks (Bartoloni and Zammarchi, 2012) for humans to develop malaria symptoms after infection, but the incubation period can range from 9 to 30 days. Typically, individuals suffer from paroxysmal attacks – shivering and coldness follow periods of fever and sweating in characteristic intervals. The attacks usually consist of a phase of coldness where the surroundings are perceived as extremely cold even though the body temperature is steadily increasing. Then, a phase of extreme heat arises where patients feel extremely hot and sick for several hours, but without sweating. Temperatures of more than 40° C can be reached. Subsequently, the body temperature is slowly going back to normal, while patients go through a period of extreme sweating. According to the timing of the fever

intervals malaria infections are categorized. Malaria quartana (or quartan fever) is caused by *P. malariae* and occurs every three days with fever on the first and forth day with 2 days without fever in between. Malaria tertiana (tertian fever) occurs every two days and is caused by *P. vivax* or *P. ovale*. Paroxysms are less prominent in *P. falciparum* infections (malaria tropica), since the parasites grow asynchronously with mostly uninterrupted fever and sometimes waves of fever every 48 hours (White, 2013).

The WHO categorizes malaria cases into "uncomplicated" and "severe", based on the severity of symptoms. Common symptoms of uncomplicated malaria include fever, headaches, chills, vomiting, muscle pains and anemia. However, uncomplicated malaria cases can develop into severe malaria, which is characterized by symptoms that are much more serious such as acute renal failure, severe anemia and respiratory failure that can lead to coma and death. Mortality increases when the parasitaemia of an infected individual is greater than 2 %. Most severe malaria cases occur in non-immune individuals that acquire malaria tropica (White, 2013). This is mostly due to the fact that the parasite exports *P. falciparum* erythrocyte membrane protein 1 (PfEMP1) to the erythrocyte surface, which mediate sequestration of the parasites within the capillaries, which has particularly severe effects in organs and the peripheral bloodstream (see below, 1.2.2; Kayser et al., 2005; Kyes et al., 2007). Non-falciparum severe malaria is rare, but has been observed in individuals infected with *P. vivax*. In these cases, death is usually caused by severe anemia, renal failure or coma. Cerebral malaria is a form of severe malaria that shows further neurological symptoms like seizures and coma. Particularly infants are prone to severe malaria, since they are very vulnerable and semi-immunity has not built up yet. Older individuals living in high-transmission areas usually develop semi-immunity over the years, protecting them against severe malaria, but not against infection or mild symptoms. This semi-immunity cannot be transferred through pregnancy and can only be acquired over time after exposure to different strains, although complete protection from disease will never be achieved (White, 2013).

1.1.2 Treatment

European settlers and their slaves brought malaria to the Americas in the 16th century, but the earliest treatment was discovered shortly afterwards. Quinine, which is found in the bark of the Peruvian Cinchona tree, was recognized to be very effective and the dried powder was usually consumed, mixed with red wine. This natural compound is still comparably effective, but since the 1930ies additional synthetic compounds with good anti-malarial activity are

available, although the parasite developed resistance against all of them (Dondrop et al., 2009; Phyo et al., 2012).

Besides the natural compounds described above, there are several classes of synthetic compounds used for malaria treatment (Fidock et al., 2004; Greenwood et al., 2008; Delves et al., 2012). The most prominent class, the 4-aminoquinolines (including chloroquine, amodiaquine and piperaquine), consists of usually fast-acting drugs (Greenwood et al., 2008). Moreover, the 8-aminoquinolines (e.g. primaquine), and the 4-methanol-quinolines (e.g. quinine, quinidine, halofantrine and mefloquine) and antibiotics (such as azithromycin, doxycycline, tetracycline and clindamycine) are effective to treat malaria (Draper et al., 2013). Antifolates such as atovaquone, pyrimethamine, sulphadoxine and proguanil are schizonticides and are also often used for treatment (Delves et al., 2012).

The natural compound artemisinin and its derivatives are the drug of choice since the year 2000, because it is very potent and effective, especially in combination with other antimalarials with longer half-life, known as artemisinin combination therapy (ACT). Even though resistance against artemisin developed 5 years ago, it is still effective in ACT (Dondrop et al., 2009; Phyo et al., 2012).

First choice for treatment consists of administration of ACT: I) coartem (artemether and lumefantrine), II) artesunate and amodiaquine, III) artesunate and sulphadoxin/pyrimethamine (SP), intravenously) SP and amodiaquine. Severe malaria is usually treated with artesunate, artemether or quinine. Vivax malaria can still be successfully treated with chloroquine. SP is the preferred drug to cure chloroquine-resistant malaria and to treat pregnant women.

Since resistance developed in 2008 at the border of Western Cambodia and Thailand-Myanmar (Noedl et al., 2008), new antimalarials are needed to treat the disease. One promising new candidate is the spiroindolone NITD609, which completely cures mice at a single oral dose of 100 mg/kg and an IC_{50} of 1 nM (Rottmann et al., 2010). Furthermore, NITD609 is the second gametocytocidal drug discovered besides primaquine and is currently undergoing phase IIa clinical trials (van Pelt-Koops et al., 2012).

1.1.3 Prevention

Vector control and chemoprophylaxis

Attempts to prevent malaria infection by controlling the vector have been reasonably successful over the past years. Among only four classes of insecticides, dichlorodiphenyltrichloroethane (DDT) and pyrethroids are the most well known. It was once widely used to kill mosquitoes, but numerous reports informed about toxic effects on humans and other animals, as well as being an endocrine disruptor, which led to a stop of use in 1972 (Turusov et al., 2002). Between 1947 and 1952, malaria was eliminated from the North America by spraying DDT. Nowadays, DDT is still used in endemic countries as a chemical for indoor residual spraying (Enayati et al., 2010; Pluess et al., 2010). In contrast to DDT, pyrethroids are safer for vertebrates, but toxic to insects and invertebrates, and are a widespread component of household insecticides (Maund et al., 2012). However, the mosquito vector developed resistance against both chemicals by mutations of the sodium channel (Hemingway et al., 2004; Enayati and Hemingway, 2010). Furthermore, mosquitoes developed metabolic resistance by overexpressing glutathione-S-transerase, which confers resistance through detoxification of both chemicals (Enayati and Hemingway, 2010).

Especially in high-transmission areas, the combination of a physical biting barrier that consist of insecticide-treated mosquito nets and indoor residual spraying have been shown to be highly effective (Lengeler, 2004; Pluess et al., 2010). Their use has increased significantly over the last years, since several organizations expanded the distributions over the last years. It was reported that up to 73 % of the households in sub-Saharan Africa use bed nets, which evidently contributed to reduction of malaria prevalence in recent years (WHO, 2013). Use of insect repellents is another method to protect oneself from mosquito bites, but it is not very feasible for people living in endemic regions due to the high cost. It is, however, rather suitable for travelers. Removal of open water, the breeding ground for mosquito larvae is key to reduce transmission and decrease *Anopheles* density in rural areas. Furthermore, health education is needed in order to recognize early symptoms.

Additionally, many of the available antimalarials can also be used as chemoprophylaxis. Once again, this method is only suitable for travelers, because of severe side effects and high costs. Depending on the area and endemicity, there are different recommendations for chemoprophylaxis. In case of uncertainty, malarone (atovaquone-proguanil), doxycycline, primaquine or mefloquine are recommended.

Towards the development of a malaria vaccine – RTS,S

The low level of commercial interest, the complex, mostly intracellular life cycle of the parasite, its antigenic variation of surface proteins, large gaps in understanding *Plasmodium* biology and its interaction with the human immune system are some reasons why a malaria vaccine is not yet available (Gardner et al., 2002; Florens et al., 2002).

Besides all these adversities, the first malaria vaccine called RTS,S is expected to be available for the public next year (Hill, 2011). RTS,S is a subunit vaccine, consisting of the hepatitis B surface antigen fused to the central repeat region and thrombospondin domain of the circumsporozoite protein (CSP), the main surface protein of sporozoites. It is the most advanced malaria vaccine currently in development. However, it seems to be a "leaky" vaccine, which protects only against a certain number of bites and seems to be especially unreliable in hyperendemic regions. The phase III clinical trial conducted from 2009 to 2012 in 5 to 17 months olds revealed a 56 % reduction in acquisition of clinical malaria and a 47 % reduction of progression into severe malaria 12 months after vaccination (Agnadji et al., 2011; RTS,S Clinical Trials Partnership 2012). These numbers even further decreased after 18 months, when protection against malaria was 46 % and only 36 % for protection against severe malaria.

The Malaria Vaccine Technology Roadmap, funded by the Bill and Melinda Gates Foundation, aims to accelerate the licensing of a malaria vaccine. It is the aim to produce a vaccine that is 50 % protective against severe malaria by 2015 and to further achieve an efficacy of 80 % by 2025 (Hill, 2011; Malaria Vaccine Technology Roadmap, 2013). However, this depends on the outcome of the results from phase III clinical trials in late 2014 (Malaria Vaccine Technology Roadmap, 2013).

WPV – whole parasite-based vaccine

The idea to produce a vaccine based on attenuated, whole parasites was first realized about 50 years ago (Nussenzweig et al., 1967). They showed that vaccination with radiation-attenuated sporozoites (RAS) protect mice from malaria infection and were able to show protection in humans (Nussenzweig and Nussenzweig, 1989). Further studies investigating this method showed that the vaccine is well-tolerated and safe, but showed a relatively low level of protection, probably due to the high diversity of *Plasmodium* strains in the field. When administered by mosquito bite, the vaccine showed a higher level of protection (Khan et al.,

2012). The vaccine shows sterile immunity in animals and almost complete protection in humans when administered by bite, although more than 1000 mosquito bites are needed to achieve this result. A major concern is to produce a balanced level of radiation dose to ensure DNA damage without reducing infectivity and immunogenicity of the sporozoites too much (Ménard, 2013). The production of high numbers of infective sporozoites is commercialized by the company SANARIA and clinical trials using cryopreserved sporozoites injection are ongoing (Seder et al., 2013; Shekalaghe et al., 2014).

More recently, this old idea has gained more attention, but a modern twist has been put to it: genetically attenuated sporozoites (GAPs) harbor gene deletion, which leads to an arrest of parasite growth at the late liver stage. In rodents, this approach seems promising and GAPs have shown a higher potency in inducing protective immunity than radiation-attenuated sporozoites (Butler et al., 2012). Those parasites are genetically homogeneous and defined and preliminary data indicated that GAPs are highly efficacious in producing sterile protection in mice (Labaied et al., 2007; Khan et al., 20012; Butler et al., 2012). Production of *P. falciparum* late-arresting GAPs and their evaluation in humans showed some potential (VanBuskirk et al., 2009; Epstein et al., 2011). However, there was one breakthrough parasite that caused disease, even though the genome still contained the respective gene deletions (Spring et al., 2013). Clinical trials comparing these new methods are needed to evaluate and to directly compare them and to further test the efficiency in highly endemic regions.

Future directions, control and elimination

Low-transmission areas with seasonal malaria episodes have great potential for future malaria elimination. Spreading resistance to artemisinin and its derivatives threatens global malaria control, which makes monitoring and containment of the spread of resistance necessary. Mass drug administration might be a possible measure to contain resistance and eliminate malaria from hypoendemic regions.

1.2 Biology and life cycle of the parasite

1.2.1 Life cycle

Parasites are transmitted via the bites of infected female *Anopheles* mosquitoes, which necessitate blood meals for their oogenesis. In the human host, the injected sporozoites migrate through the blood stream to the liver, where they infect hepatocytes. During the following 1-2 weeks, the intra-hepatic liver-stage parasites multiply asexually and differentiate via schizogony into merosomes that contain merozoites (Prudêncio et al., 2006). This stage is called exo-erythrocytic schizogony whereas schizogony refers to nuclear divisions without cytoplasmic division. This development takes usually 6 (*P. falciparum*) to 15 (*P. malariae*) days (Collins and Jeffery, 2007; White, 2013). From the host cells emerge merosomes, which then rupture and release thousands of merozoites into the blood stream, where they infect erythrocytes (Ménard, 2013). Within the erythrocytes, the merozoites grow first into a ring-shaped form and develop further into trophozoites. At the subsequent schizont stage, the parasite nuclei divide several times within a common cytoplasm. The parasite feeds by ingesting hemoglobin, which is metabolized into amino acids in the food vacuole. The toxic by-product α-hematin (ferriprotoporphyrin IX) is stored as a biologically inert hemozoin crystal. Late schizonts are called segmenters, in which new merozoites develop after completion of cytokinesis that finally leave the red blood cells and invade additional erythrocytes (Fig. 1.2). This asexual intra-erythrocytic developmental cycle (IDC) is completed within 48 hours (in *P. malariae* within 72 hours) and causes all symptoms associated with malaria. Such massive proliferation can lead to a parasite load of 100 billion in the blood of an adult.

Besides schizogony a small percentage of parasites differentiate into sexual forms, male and female gametocytes (micro- and macrogametocytes) (Dixon et al., 2008). Gametocytes do not cause pathology in the human host and will disappear from the circulation after 3 weeks (*P. falciparum*) if not taken up by a female anopheline mosquito (Drakeley et al., 2006). However, these numbers can differ (reviewed in Drakeley et al., 2006). In the mosquito's midgut, the gametocytes develop into gametes and fertilize each other, forming motile ookinetes. The resulting ookinete traverses the mosquito gut wall and encysts on the exterior of the gut wall as an oocyst. Here, they undergo several divisions producing a large number of sporozoites that cross the basal lamina into the mosquito's body cavity and migrate to the

salivary glands. During the next blood meal, the sporozoites are injected into the subcutaneous tissue of the human host (Fig. 1.2). A proportion is ingested by macrophages and others are taken up by the lymphatic system where they are presumably destroyed (Amino et al., 2006). The sporozoites, which successfully enter the blood stream, move to the liver where they begin the cycle again.

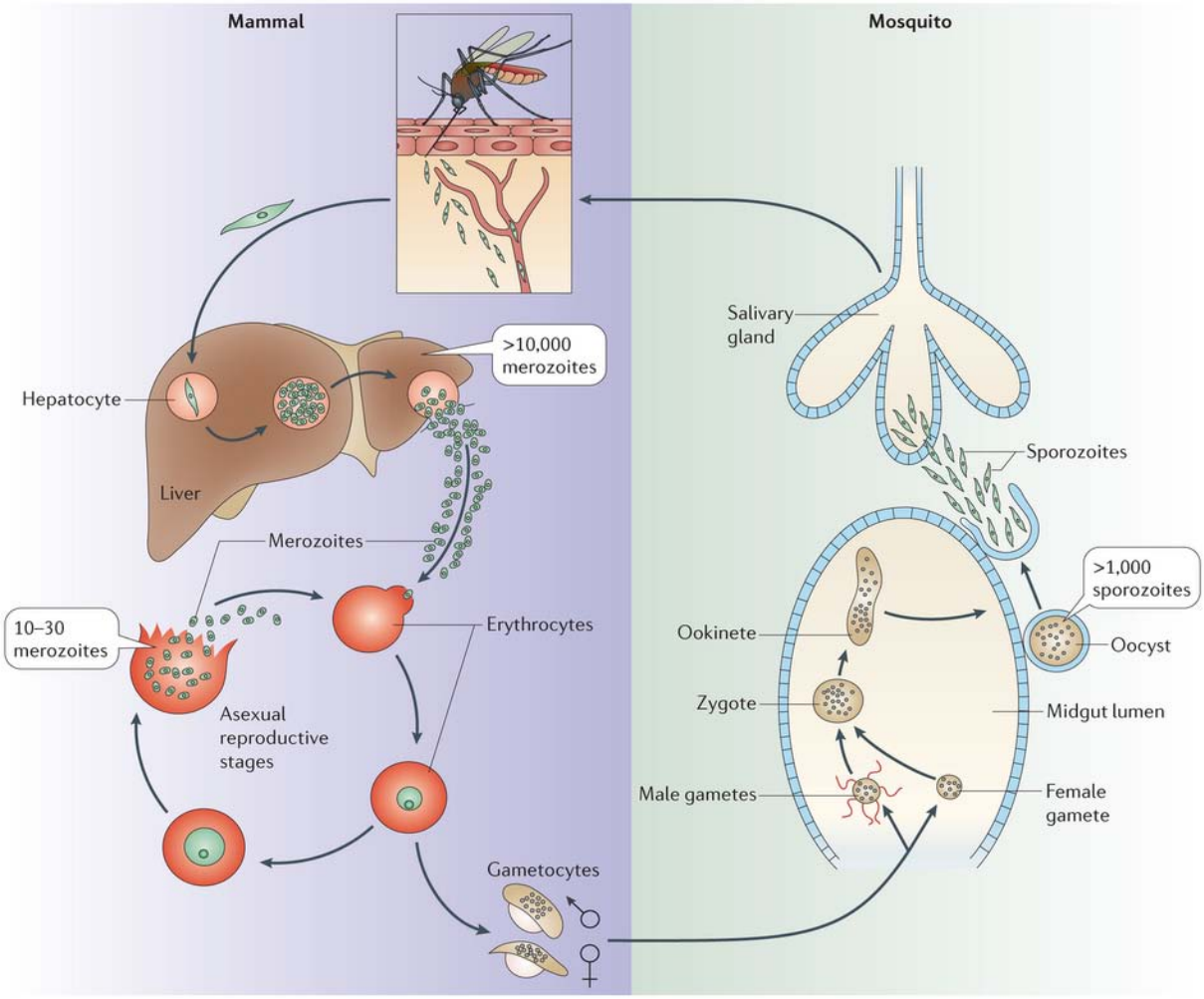

Figure 1.2 Overview over the life cycle of *Plasmodium* between the human host and the anopheline vector. From an anthropocentric point of view, the most important part of the parasite's complex life cycle is the asexual, intra-erythrocytic, developmental cycle, which causes all of the symptoms associated with malaria. It is initiated by the invasion of the human red blood cell. Adapted from Ménard, 2013.

1.2.2 Species-specific aspects of parasite biology

Blood stage schizogony in *P. falciparum* differs from that of the other human malaria parasites with respect to the trophozoite- and schizont-infected erythrocytes, which adhere to capillary endothelial cells (Kayser et al., 2005). Furthermore, infected red blood cells (iRBCs)

are also able to adhere to uninfected erythrocytes, so-called “rosetting”. PfEMP1 surface molecules that are encoded by the *var* gene family are known to mediate this sequestration (Kyes et al., 2007). The *var* multigene family consists of 60 members, which undergo antigenic variation, regulated by mutually exclusive expression of only one gene at a time (Scherf et al., 1998). PfEMP1 attaches to different endothelial receptors in capillaries, like ICAM1 in the brain, chondroitin sulphate A in the placenta or CD36 in many other organs. As a consequence, only early ring stage parasites circulate in the bloodstream. On one side, sequestration is an advantage for the parasite, because it prevents elimination of infected red blood cells (iRBCs) by the spleen. On the other side, sequestration interferes with blood circulation in vital organs and causes severe complications such as cerebral and placental malaria. Additionally, *P. falciparum* infects all erythrocyte stages and can, therefore, reach a higher parasitaemia than other *Plasmodium* species (Kayser et al., 2005).

During the development of the *P. ovale* and *P. vivax* parasites in the liver, so-called hypnozoites can emerge from sporozoites. These small, mononuclear stages may persist in hepatocytes for several months or even years and develop into merosomes in numerous episodes. In these cases, malaria-relapses are due to reactivation of hypnozoites, or due to recrudescence of persisting erythrocytic stages (Kayser et al., 2005).

1.2.3 The *P. falciparum* genome

The haploid genome of *P. falciparum* has a size of 22.8 megabases and consists of 14 linear chromosomes. The mitochondrial genome has a size of approximately 6 kilobases (kb), the circular apicoplast genome has a size of 35 kb. The genome sequencing project revealed that *P. falciparum* contains 5409 open reading frames (ORFs), of which 60 % code for hypothetical proteins with an unknown function and no orthologous proteins in other eukaryotic species (Gardner et al., 2002; Aravind et al., 2003). With an AT-richness of 80.6 %, the genome of *P. falciparum* is the most AT-rich genome sequenced to date (Gardner et al., 2002).

1.2.4 Molecular architecture of the merozoite

DNA containing and secretory organelles

Not only their highly adapted and extraordinary life cycle and immune evasion strategies make *Plasmodium* such an interesting study subject – their evolutionary origin and cellular architecture display many features that are not found outside the phylum (Cowman and Crabb, 2006). The most remarkable organelle is the apicoplast, which was acquired through secondary endosymbiosis (endo = within; syn = with; biosis = living) during evolution (Keeling, 2009; Van Dooren and Striepen, 2013). This ancient plastid-like organelle has 4 membranes surrounding the 35 kb genome, part of which is integrated into the parasite's nuclear genome (Wilson et al., 1996). The apicoplast's functions include fatty acid biosynthesis and it is additionally involved in major biochemical pathways (Yeh and DeRisis, 2011). The mitochondrial genome, in contrast, is only 6 kb small and lacks the characteristic cristae (van Dooren et al., 2005). Not all apicomplexan parasites have an apicoplast (e.g. *Cryptosporidium*; Abrahamsen et al., 2004), but they all share the presence of an apical complex. This aggregation of secretory organelles is important for invasion and consists of micronemes, rhoptries and dense granules. Micronemes emerge during schizogony from the Golgi complex and translocate alongside the microtubules and dock with the rhoptry tips (Bannister et al., 2003). Although it is still unknown how many different proteins are stored, some of the adhesines the parasite is using during erythrocyte invasion are stored in these organelles. The former include members of the erythrocyte binding antigens (EBAs), apical membrane antigen 1 (AMA1), and the trombospondin-related adhesion proteins (TRAPs). All of these proteins are targeting surface structures of the host cell (Malpede and Tolia, 2014). Compared to micronemes, the rhoptries are much bigger in size and less in numbers. Like micronemes they are Golgi-derived organelles and their protein contents are also involved in invasion, e.g. the family of reticulocyte-binding homologues (RH proteins) and the rhoptry neck proteins (RONs), but some also promote formation of the parasitophorous vacuole (PV) (Cowman et al., 2012; Counihan et al., 2013). The dense granule proteins function later during invasion and modify the host cell, e.g. RESAs. Rhoptries and micronemes localize apically, whereas dense granules are distributed throughout the cell's cytosol.

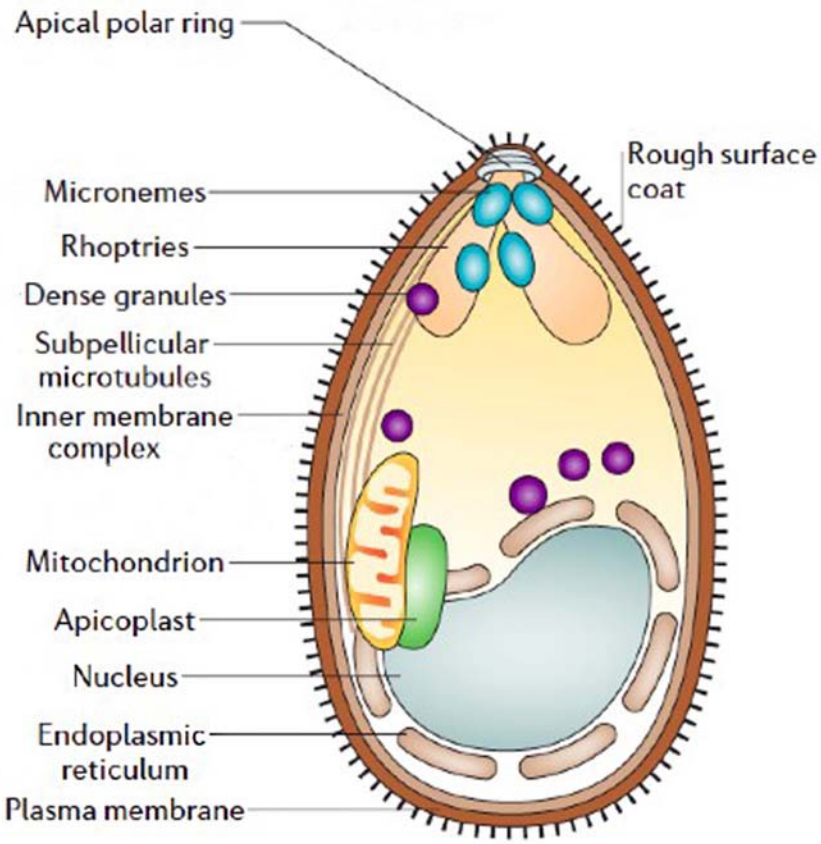

Figure 1.3 Schematic representation of the ultrastructure of the merozoite. The merozoite is with 1 to 2 µm the smallest life cycle stage and also one of the smallest eukaryotic cells in general. It is equipped with a full set of organelles, including micronemes, rhoptries and dense granules. These secretory organelles contain proteins that are crucial for invasion. In addition to the phylum-specific organelles (micronemes, rhoptries, dense granules, apicoplast), the parasite possesses all typical eukaryotic organelles. Cellular features are not according to scale. Schematic was adapted from Bannister et al., 2003.

The cytoskeleton

In general, membrane skeletons are required for cell shape, strength and maintenance, internal organization of subpellicular organelles, cell division and movement. They consist of filamentous protein networks that are linked to membranes through interactions with integral membrane proteins. Apicomplexan parasites need a robust but also dynamic cytoskeletal architecture to maintain structural integrity during the fast intra-erythrocytic growth phase and especially during host cell invasion. As described above, during the late phase of schizogony the parasite builds up its invasion machinery. Beside the secretory organelles, a highly complex endomembrane system is synthesized that lies underneath the merozoite's plasma membrane (PM) in mature merozoites. This membrane system is termed the inner membrane complex (IMC, please refer to section 1.3) (Dubremetz and Torpier, 1978; Morrissette et al.,

1997; Raibaud et al., 2001; Morrissette and Sibley, 2002; Kono et al., 2012). PM and IMC are jointly form a triple bilayer called the pellicle. Below the PM and the IMC lie 2-3 sub-pellicular microtubules. Together, the subpellicular microtubules and the IMC form the subpellicular network, which also contains interwoven 8-10 nm filaments that provide the cell with strength and stability. The subpellicular microtubules are organized form the apical polar ring (Bannister et al., 2003). The filaments of the SPN are linked together by intermembrane particles (IMPs).

The motor unit: The "glideosome"

Parasite motility is referred to as "gliding motility". It is defined as an amoeboid-like movement of sporozoites (Steward and Vanderberg, 1988; Morrissette and Sibley, 2002; Baum et al., 2006). Extracellular adhesins from the thrombospondin-related anonymous protein (TRAP) family are linked to the IMC via the motor complex (Bullen et al., 2009). This sophisticated actin-myosin machinery is termed "the glideosome" (Fig. 1.4). Some of the characterized protein elements are the glideosome-associated proteins (GAPs; GAP45 and GAP50) that in association with myosin A (MyoA) and myosin light chain 1 (MLC1) (Cowman et al., 2012) are linked to the outer membrane of the IMC, potentially by interacting with transmembrane proteins of the IMC (Fig. 1.4) (Mann and Beckers, 2001; Gaskins et al., 2004; Baum et al., 2008; Bullen et al., 2009; Rayavara et al., 2009). The N-terminal domain of MLC1 serves as a tail for MyoA and brings the motor to its site of action by association with the C-terminus of GAP45. Depletion of GAP45 results in impaired gliding motility, invasion and egress in *Toxoplasma gondii* (Frénal et al., 2010). GAP45 has been implicated in the recruitment of the motor complex as well as in the maintenance of pellicle cohesion (Frénal et al., 2010). The N-terminus of GAP45 has acyl modification sites and mutational analysis indicated that these are essential for the insertion of the protein into the IMC (Rees-Channer et al., 2006; Frénal et al., 2010).

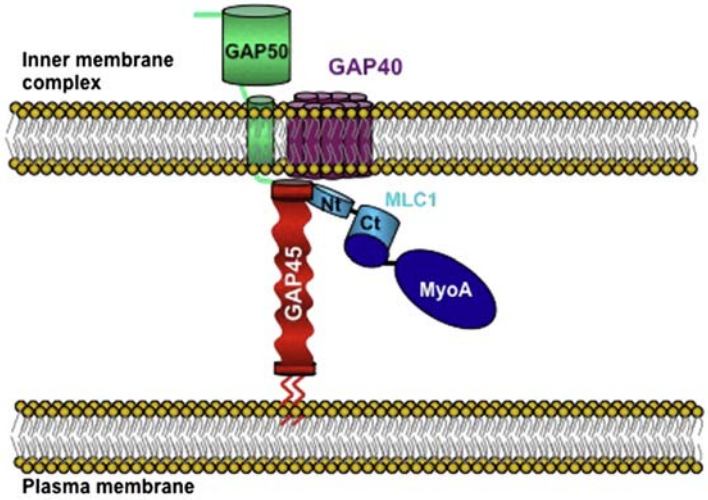

Figure 1.4 Schematic of the glideosome complex. This model visualizes some of the currently known glideosome proteins and their interaction with each other. This schematic was adapted from Frénal et al., 2010.

1.2.5 Merozoite invasion of erythrocytes

After rupture of the host cell, it takes less than 30 seconds for a released merozoite to invade a new erythrocyte (Treeck et al., 2009). After encounter of an erythrocyte, it reorients on the surface of the erythrocyte to position its apical tip in direct contact with the targeted membrane and subsequently invades (Fig. 1.5). This invasion is crucial for the parasite's survival and the invasion process is therefore generally accepted as a target for vaccine or drug development. Even though the merozoite is capable of invading a new host cell very quickly – speed alone is not enough. The cell further harbors several immune-evasion mechanisms that make it so successful. The proteinaceous surface coat of the merozoite is characterized through the presence of the merozoite surface protein 1 (MSP1), being the most abundant one. Different variants of MSP1 exist, indeed, with its particularly high level of polymorphism it is one of the most highly polymorphic eukaryotic proteins known (Volkmann et al., 2002). MSPs mediate the initial reversible attachment followed by a reorientation (Cowman and Crabb, 2006). The latter process is carried out by proteins of the EBA and RH protein families, which bind the red blood cell tightly (Wright and Rayner, 2014). One key player of the invasion process is the microneme protein apical membrane antigen 1 (AMA1) that is released onto the parasite's surface just after egress of the merozoite from the iRBC. AMA1 forms a complex with the RONs, which are secreted from the rhoptries onto the iRBC surface (Lamarque et al., 2011). The newly formed molecular seal, the so-called tight junction, allows other rhoptry contents to get passed into the erythrocyte

(Fig. 1.5) (Cowman et al., 2012). Active invasion of the parasite is then powered by the "glideosome" (please refer to section 1.2.4). Merozoite surface proteins are shed off and the parasitophorous vacuole starts forming. The sealing of the vacuole and dense granule secretion marks the end of invasion. Although about 50 proteins are implicated in invasion (Cowman et al, 2012), the invasion-related processes might be mediated by a complicated protein network. Using transcriptional profiling approach in combination with phylogenetic profiles, domain-domain interactions and yeast two-hybrid datasets a high confidence protein network was constructed that governs invasion (Hu et al., 2010). This sub-network harbors about 400 proteins, wherefrom 260 are unknown hypothetical proteins.

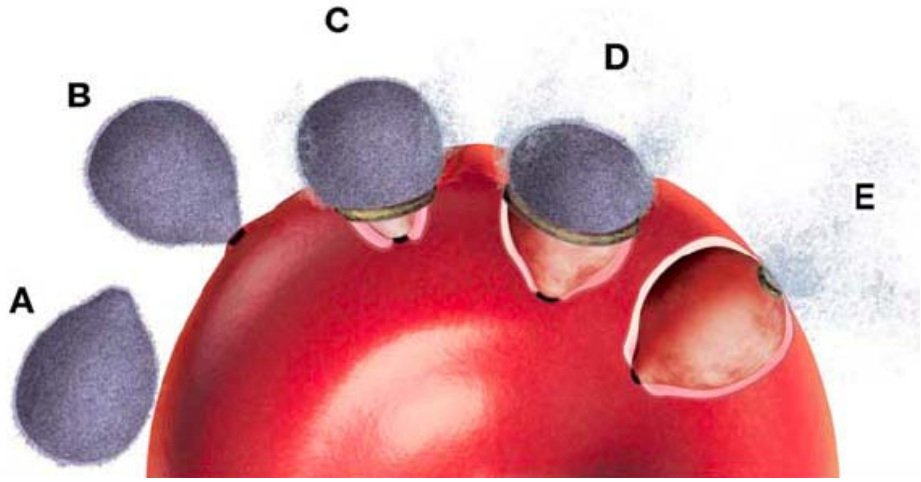

Figure 1.5 Schematic of the different steps during merozoite invasion. A. Initial recognition is followed by **B.** reorientation and tight junction formation. **C,D.** Active invasion takes place while the tight junction (brown) is moving towards the basal end of the merozoite while the surface coat is shed. **E.** After complete invasion, the parasite starts growing and remodeling its host cell. Adapted from Cowman et al., 2012.

1.3 The inner membrane complex (IMC)

1.3.1 Evolution of the IMC

While the secretory organelles are characteristic of all organisms belonging to the apicomplexan phylum (Levine; 1980), the IMC is a morphological trait of a large phylogenetic group called Alveolata (Adl et al., 2005). This phylogenetic group comprises three traditional main phyla: I) Dinoflagellata being typically marine flagellates; II) Ciliata comprising common protozoa like *Paramecium spp*., and; III) Apicomplexa, representing

mostly parasitic species, including the genera of *Theileria, Eimeria* and *Toxoplasma*, which are important human and animal pathogens with significant impact (Wolters, 1991; Adl and Leander, 2007). A fourth group has been identified recently – the Chromerida consisting of marine, photosynthetically active protozoa (Moore et al., 2008). An exceptional characteristic of alveolates is the possession of the IMC also called alveoli (Cavalier-Smith, 1993; Gould et al., 2002; Adl et al., 2005; Bullen et al., 2009; Kono et al., 2012). This endomembrane system appears to possess taxon-specific functionality, exemplified above in the invasion process of the apicomplexan parasites. In dinoflagellates and ciliates the alveoli predominantly play a structural role. In all phylogentic clades it might also have a role as an important scaffolding element during cytokinesis (Gaskins et al., 2004; Sibley, 2004; Soldati et al., 2004).

1.3.2 Protein composition of the IMC

As a reflection of its multifunctional roles the IMC is composed of a phylogenetic, function and structural diverse set of proteins (Kono et al., 2012, 2013). They can be categorized into transmembrane proteins (like the glideosome-associated protein with multiple membrane spans 2, GAPM2), small acylated proteins (IMC sub-compartment proteins, PfISPs), alveolins (Alveolin 5; PF10_0039), alveolin like proteins (PF08_0033) and others (MAL13P1.228), which do not fit in any of the categories (Kono et al., 2013). A unique multigene family of proteins, the alveolins (Mann and Beckers, 2001; Gould et al., 2002; Gubbels et al., 2006; Gould et al., 2008; Bullen et al., 2009), is restricted to alveolates and, therefore, recognized as one molecular nexus of the Alveolata (Gould et al., 2008). So far, using proteomics (Gould et al., 2011), system biological approaches (Hu et al., 2010) and phylogenetic profiling (Kono et al., 2012) 28 IMC proteins have been identified. In addition to a common core set of conserved proteins, the IMC includes many lineage-specific proteins reflecting additional specialized roles. For instance, MAL13P1.228 is a *Plasmodium*-specific protein and is not found in any other species (Kono et al., 2012). Only a few IMC proteins are functionally characterized, most of them belong to the glideosome complex. Besides the GAPs, other peripheral IMC membrane proteins were identified. The ISPs belong to the group of small acylated IMC proteins. They were originally identified in *Plasmodium* (Hu et al., 2010) and described in greater detail in *T. gondii* (Beck et al., 2010; Fung et al., 2012). The IMC in *T. gondii* tachyzoites consists of 3 sub-compartments, the basal, central and apical part. TgISP1 is localized to the apical cap, TgISP2 and TgISP4 are localized centrally in the tachyzoite, and, ISP3 is localized to central and basal regions (Beck et al., 2010; Fung

et al., 2012). TgISP1 was found to have a gate-keeping function as it excludes the localization of other TgISPs to the apical cap (Beck et al., 2010). The gate-keeping function of TgISP1 may be accomplished by its C-terminal domain, because the C-terminal domain of TgISP2 could not complement it (Beck et al., 2010). TgISP2 seems to be the only vital ISP in *T. gondii*, disruption of TgISP2 leads to defects in cell division (Beck et al., 2010). This data suggests that this family of proteins, in contrast to GAP45, plays a role in cytokinesis. Some structural insights were delivered by recent work from Tonkin and colleagues, which revealed that TgISP1 possesses a small core domain with several cysteines (Tonkin et al., 2012). Moreover, crystallization of TgISP1 and TgISP3 showed that both proteins have a pleckstrin homology (PH) domain (Tonkin et al., 2014). PH domains mediate protein-lipid and protein-protein interactions. Mutational analysis of selected amino acids of the PH fold and biochemical characterization implicate that TgISP PH domains do not bind phospholipids, but possibly function in binding proteins (Tonkin et al., 2014). The *P. falciparum* homologues PfISP1 (PF10_0107) and PfISP3 (PF14_0578) also possess N-terminal acyl modification motifs (Hu et al., 2010; Cabrera et al., 2012), but the sequence homology compared to the TgISPs is relatively low. However, both PfISPs contain a PH fold (predicted by SMART; Schultz et al., 1998; Letunic et al., 2012), indicating that PfISPs might play an important role in recruiting interaction partners to the IMC, which might fulfill a so far uninvestigated function.

1.3.3 IMC biogenesis

The duplication of the Golgi is among the earliest visible events of parasite replication and shortly precedes the onset of IMC biogenesis (Hu et al., 2002). The establishment of a polarized secretory system might be a prerequisite for daughter cell formation of the daughter cell IMC. The IMC is derived from clathrin-coated vesicles of the ER-Golgi complex (Bannister et al., 2000; Gordon et al., 2008; Yeoman et al., 2011). During *Plasmodium* schizogony the nuclei move to the periphery of the mother cell. Daughter cell formation is initiated by the formation of the IMC beneath the mother cell's PM and an intact pellicle forms while the daughter cells grow about six hours before merozoite egress (Kono et al., 2012). In early schizonts, the IMC is visible as two cramp-like structures per nucleus (T1). They form while the mitotic spindles are still present. They further extend into small ring-like structures, about 630 nm in diameter (T2). Towards the end of schizogony the rings quickly expand and the IMC grows beyond the nuclei (T3) (Kono et al., 2012). Proteins that display

this typical dynamic are called “type A” proteins (Kono et al., 2012). In addition, a second IMC structure becomes visible about 3.5 hours prior egress, proteins showing this distinct localization pattern are called “group B” proteins. This group includes the alveolins (e.g. PF10_0039, PFE1285w) and the *Plasmodium*-specific MAL13P1.228. The later appearance of the group B proteins points towards a highly regulated mechanism through which proteins are recruited to the IMC. Moreover, the two different groups likely fulfill distinct functions.

IMC in gametocytes

The pre-sexual parasite forms, the gametocytes, show a characteristic development over five distinct stages. The earliest stage is hardly distinguishable from mature schizonts. After stage II, the gametocytes grow into stage III forms with a similar size to schizonts. Stage IV parasites represent the largest of the gametocyte stages with a size of 10.9 µm (Dearnley et al., 2012). Stage V gametocytes are the most mature stage and are the only stage that is found in the bloodstream to eventually getting taken up by a mosquito. About 900 proteins are expressed in gametocytes, 315 of them are exclusive (Baker et al., 2011; Silvestrini et al., 2010).

Generally speaking, the IMC protein composition is very similar in asexual merozoites and presexual gametocytes. GAP50 forms a complex with GAP45 and MTIP and shows similar solubility profiles of the proteins (Dearnley et al., 2012). Even though the glideosome components are still present, the actin-myosin motor does not play a role in gametocyte elongation, but may be implicated in important structural tasks. In contrast to the architecture of the IMC in merozoites that appears to be formed of only one cistern (Kono et al., 2012), the IMC in gametocyte contains 10 – 15 cisternae that are connected at transverse sutures (Meszoely et al., 1987; Dearnley et al., 2012; Kono et al., 2012). Those sutures sub-divide the IMC into several plates, giving the parasite a segmented appearance. Moreover, they connect the IMC with the PM (Meszoely et al., 1987; Kono et al., 2012). Underneath the IMC lie the microtubules, which are spaced at intervals of approximately 10 nm (Dearnley et al., 2012).

1.4 Modifications of proteins

A variety of cellular functions is controlled by a range of different protein modifications. Small functional groups are often added to a specific amino acid residue, which is the case for one of the most common modifications, phosphorylation. Ubiquitination and nitrosylation are other well-studied modifications that regulate protein function. However, the attachments of lipid moieties to proteins like myristoyl, palmitoyl, stearoyl or farnesyl also play important roles in protein function and regulation. The most common forms of protein fatty acylations in eukaryotes are N-myristoylation and S-palmitoylation (Resh, 1999). The two fatty acylations can modify proteins both separately and concertedly with other lipid modifications. These modifications have become increasingly recognized to be of major importance for a better understanding of how sub-cellular localization, trafficking and enzymatic activity of membrane-associated proteins are regulated (Resh, 1999).

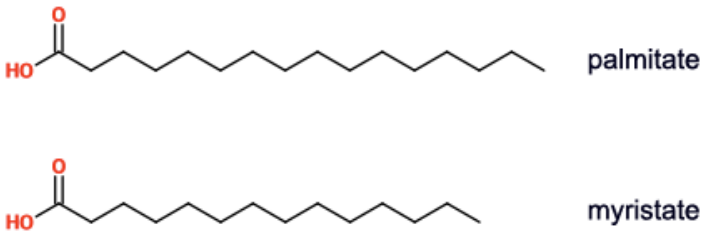

Figure 1.6 Chemical structure of palmitate and myristate. The enzyme-available form of both palmitate and myristate consists of coenzyme A (CoA) linked to the lipid by replacing the hydrogen.

1.4.1 Myristoylation

Myristoylation is characterized by the co-translational addition of myristic acid, a 14-carbon fatty acid (Fig. 1.6). 0.5 % of all eukaryotic proteins are myristoylated (Maurer-Stroh et al., 2002). This irreversible process is catalyzed by cytosolic N-myristoyl transferases (NMTs) and can occur co- and post-translationally. Protein myristoylation is a well-understood process and a consensus motif has been identified as MGxxC/S/T (Resh et al., 1999; Maurer-Stroh et al., 2002). 10 to 14 carbons are inserted hydrophobically into the hydrocarbon core of the bilayer. Even though myristoylation is required for membrane association, it is not sufficient for stable and permanent membrane anchoring (Maurer-Stroh et al., 2002; Aicart-

Ramos et al., 2011). A second signal is needed for myristoylated proteins to become stably attached to a membrane. This can be a polybasic cluster or palmitate.

N-myristoyl transferase (NMT) mechanism and inhibition

There is little data on how myristoylation is regulated in vivo. NMTs can become phosphorylated by tyrosine kinases that, in turn, are myristoylated by NMTs (Selvakumar and Sharma, 2006). However, the mechanism of NMTs has been investigated in great detail and is composed of several steps: First, an amino peptidase cleaves off the initializing methionine. Myristoyl-CoA binds NMT with very high affinity and induces a conformational change so that the peptide substrate can bind. Nucleophilic substitution leads to attachment of myristoyl-CoA to the N-terminal glycine and a stable amide bond is formed. The CoA is then released, followed by the myristoylated peptide (Rudnick et al., 1991; Wright et al., 2010). The NMT of the fungus *Candida albicans* was crystallized already in 1998 (Weston et al., 1998) and shown to have internal twofold symmetry, the "NMT fold". Its core domain is constructed predominantly of several α-helices (Weston et al., 1998).

Using myristic acid analogues, binding of different acyl chains has been investigated in great detail. The findings include that:

- chain length is important for binding of myristoyl-CoA to NMT (Heuckeroth et al., 1988)
- functional and polar groups only have minor effects on NMT activity (Heuckeroth et al., 1990; Devadas et al., 1992)
- myristoyl-CoA is bound in a bent conformation (Heuckeroth et al., 1988)
- the myristoyl-CoA binding site is highly conserved across species (Heuckeroth et al., 1988; Kishore et al., 1993)
- peptide recognition occurs within the first 10 N-terminal amino acids (Heuckeroth et al., 1988)

Maurer-Stroh and co-workers predicted a consensus motif by using the first 17 N-terminal amino acids of a protein to calculate whether a protein becomes myristoylated or not (Maurer-Stroh et al., 2002). Furthermore, they propositioned that there are three regions of a peptide that are needed for proper interaction with the enzyme: the very N-terminal region (residues 2 to 7) is bound by the active site, the central region of a peptide (residues 8 to 11) interact with

the surface opening of the catalytic pocket, and the last region (residues 12 to 18) act as a hydrophilic linker (Maurer-Stroh et al., 2002). NMTs have been characterized in several parasitic species, because the enzyme is essential to the survival within their host. Since the initial publication, crystal structures of the *S. cerevisiae* as well as *P. falciparum* NMT were revealed (Bhatnagar et al., 1998; Gunaratne et al., 2000). Several research groups have probed into selective inhibition of parasite NMTs (Panethymitaki et al., 2006; Bowyer et al., 2007; Bowyer et al., 2008; Frearson et al., 2010; Crowther et al., 2011; Tate et al., 2013). However, the high homology between human and parasitic NMTs and the conserved binding site for myristoyl-CoA complicates the process of finding specific inhibitors. Nonetheless, the protein substrates are different. This fact can be exploited to create pathogen-specific NMT inhibitors. N-myristoylation is vital to a cell's survival. Especially promising was the discovery of an inhibitor of the NMT of *Trypanosoma brucei*, since it is among very few *T. brucei* proteins that were shown to be selectively inhibited (Frearson et al., 2010). Furthermore, a recent study showed that the plasmodial NMT is essential and can be targeted by various drugs (Wright et al., 2014). Compound 2a is a very promising candidate since it reduces parasitaemia in mice. Several substrates were identified as well, including IMC proteins like ISP1, ISP3, CDPK1, GAP45, MTIP, MyoA, alveolin 5. One phenotype of NMT inhibition is the failure of IMC assembly and failure to progress into merozoites (Wright et al., 2014).

1.4.2 Protein palmitoylation

Protein palmitoylation is the only reversible post-translational lipid modification known and it is characterized by the addition of the 16-carbon fatty acid palmitate (Fig. 1.6) to cysteine residues, forming a thioester linkage (Resh, 1999; Dietrich and Ungermann, 2004). As a consequence, palmitoylation is also called thioesterification. Palmitoylation is a regulatory mechanism that mediates protein-membrane attachment and sub-cellular trafficking of proteins. Furthermore, it plays an important role in protein-protein interactions, protein stability and enrichment of proteins in microdomains of membranes. Palmitoylation is the most common form of fatty acylation in eukaryotes and it is catalyzed by palmitoyl acyltransferases (PATs).

Palmitoyl acyltransferases (PATs)

Regardless of the discovery of palmitoylation several decades ago, the enzyme family of PATs, catalyzing this post-translational modification has only been discovered in recent times (Lobo et al., 2002; Roth et al., 2002). PATs reside in different tissues and sub-cellular localizations and usually act on intracellular proteins (Ohno et al., 2006; Mitchell et al., 2006; Batistic, 2012; Frénal et al., 2013). Some sequence requirements in PAT-substrates have been discovered and palmitoylation can be predicted using CSS-Palm (Ren et al., 2008; www.csspalm.biocuckoo.org). The prediction tools are based on a clustering and scoring strategy (CSS) algorithm. Through searching the scientific literature and collecting experimentally verified data on palmitoylation sites this tool was generated. 263 palmitoylation sites were analyzed and 4-, 6-, 8-, and 10-fold cross-validations and leave-one-out validation were calculated (Ren et al., 2008). Nevertheless, a clear general sequence motif has not yet been identified, although it has been shown that leucines, lysines and additional cysteines are favored amino acid residues surrounding palmitoylated cysteines (Lobo et al., 2002; Roth et al., 2002; Bartels et al., 1999; Babu et al., 2004; Smotrys and Linder, 2004; Roth et al., 2006; Xue et al., 2006; Ohno et al., 2006; Hou et al., 2009).

PATs are polytopic membrane proteins with four or more transmembrane domains (TMDs) and typically share a DHHC-motif (A: asparagine; H: histidine; C: cysteine), which is flanked by cysteine-rich domains (CRDs; 51 aa in length) and faces the cytosolic side of membranes, usually between TMD 2 and TMD 3 (Greaves et al., 2011; Mitchell et al., 2006). This motif is directly involved in the palmitoyl transfer and was found in all eukaryotic species examined so far. Particularly, H1 and C have been identified to be important for substrate binding (Mitchell et al., 2006). Experiments in yeast showed that interchange of DHHC motifs between different PATs cannot restore a PATs' function (Mitchell et al., 2006). Therefore, the DHHC motif itself is required for substrate specificity, function and folding. Even though the general topology and the DHHC-CRD region seems to be rather conserved among PATs, they vary significantly at the sequence level (Batistic, 2012). Besides the DHHC-CRD motif, there is also a DPG (D: asparagine, P: proline; G: glycine) motif next to TMD2 and a TTxE (T: threonine; E: glutamate) motif next to TMD3, all of them facing the cytosolic side of the membrane. Whereas it is unclear whether or not those other domains have vital functions for enzyme activity, the C-terminal domains of PATs seem to be important for localization and substrate identification (González-Montoro et al., 2009; Beck et al., 2013). A second class of PATs exists; the membrane-bound O-acyl transferases (MBOATs) usually act on proteins that

are modified in the lumen of the secretory pathway. The number of PATs can vary from over 20 in metazoans (22 in *Homo sapiens*, 12 in *P. falciparum* and 18 in *Toxoplasma gondii*) to seven in the budding yeast *Saccharomyces cerevisiae* (Roth et al., 2006; Frénal et al., 2013). *Plasmodium falciparum* expresses twelve proteins containing the DHHC motif (Jones et al., 2012), of which six show distinct upregulation in late stages (Cabrera et al., 2012; www.plasmodb.org). Of note, using complementary palmitoyl protein purification approaches and quantitative mass spectrometry, over 400 palmitoylated proteins were identified in asexual blood stages of the parasite, including those involved in cytoadherence, drug resistance, signaling, development, and invasion (Gavin et al., 2002). Importantly, the physiological role of palmitoylation of these proteins is for the most part unknown and is not necessarily connected to membrane association. PATs reside in different sub-cellular localizations and might play a role in specific membrane recruitment of proteins such as VAC8 to vacuole membrane in yeast, RAS2 into the plasma membrane and ARO to the rhoptry membrane of *T. gondii* (Dietrich and Ungermann, 2004; Beck et al., 2013). Furthermore, it was reported that some PATs show dual localization patterns being localized to two organelles simultaneously (Ohno et al., 2006; Batistic, 2012). PATs are not only expressed in different cellular compartments, but may also be localized to different tissues (Ohno et al., 2006). Moreover, while some PATs are ubiquitously expressed, the expression pattern of others seems to be highly regulated.

A comprehensive localization map of PATs in *T. gondii* was recently established, where two of these PATs (TgDHHC2, TgDHHC14) could be localized to the IMC (Beck et al., 2013, Frénal et al., 2013). This study also identified two IMC-localized PATs in *P. berghei* (PbDHHC3, PbDHHC9), whereas only one out of 11 PATs has been localized to the rhoptries (PfDHHC7) in an over-expression approach (Frénal et al., 2013). Based on the fact that PATs localize to different organelles in Apicomplexa, it is tempting to speculate that PAT-substrate pairs exist. However, the most intriguing question is how substrate specificity of PATs is achieved.

Membrane targeting of dual acylated proteins

Membrane attachment mediated by the addition of lipophilic groups to proteins usually takes place when a protein gets modified by two or more lipids. Protein myristoylation is not sufficient for permanent membrane association, and at least one other lipid group is needed for membrane localization, as two lipid modifications are better than one. The kinetic bilayer-trapping hypothesis describes how a dual acylated protein becomes membrane associated (Shahinian and Silvius, 1995): myristate is attached co-translationally to the N-terminal glycine and, therefore, increases its lipophilicity. The single lipid group leads to transient interactions of the protein with intracellular membranes. Eventually, the protein encounters its determined PAT and becomes rapidly palmitoylated. The strong hydrophobicity promotes stable membrane binding and "traps" the protein in the membrane bilayer.

Even though palmitate and myristate only differ in length by two carbons, they are not confused by the respective enzymes. Palmitoyl-CoA is found in a 5- to 20-fold higher concentration within a cell than myristoyl-CoA (Rudnick et al., 1991). Occasionally, palmitoyl-CoA is bound by NMTs, but it is not transferred to the particular peptide. The hydrophobicity of palmitoyl-CoA is significantly higher than myristoyl-CoA.

Depalmitoylation

While some proteins are permanently palmitoylated, others undergo cycles of palmitoylation and depalmitoylation (Linder and Deschenes, 2007). This process is catalyzed by cytoplasmic acylprotein thioesterases (APTs). Moreover, during protein degradation, proteins are broken down into peptides by proteases and subsequently depalmitoylated by lysosomal palmitoyl thioesterases (PPTs). Hydrolysis of palmitate from the protein is an essential step during protein degradation. The process is catalyzed by 2 sets of enzymes: proteases first cleave proteins into peptides, which is followed by cleavage of palmitate by protein palmitoyl thioesterases (PPTs). Failure to successfully hydolyze fatty acids from proteins can lead to neurodegenerative disorders (Vesa et al., 1995). Mutations in human PPTs have been linked to neuronal ceroid lipofuscinosis and disruption of the genes in mice showed the same effect (Gupta et al., 2001; Mitchison et al., 2004). Palmitoyl proteins exist in different states as some membrane proteins are palmitoylated at the cytoplasmic face of membranes shortly after their synthesis and remain permanently palmitoylated. Many proteins are palmitoylated by PATs and depalmitoylated by APTs one or more times during their lifetime (Fig. 1.7). In *P.*

falciparum, APTs have not been characterized, whereas in *T. gondii* inhibitors of the depalmitoylation machinery have been investigated in more depth recently (Kemp et al., 2013). The APTs in *T. gondii* were named "PPTs", since "APT" was already assigned to an unrelated gene (Child et al., 2013; Kemp et al., 2013). Interestingly, a high-throughput screen in *T. gondii* identified not only inhibitors but also enhancers of parasite invasion (Child et al., 2013). A chloroisocoumarin was identified that targets TgPPT1 and increases microneme secretion, parasite motility and invasion.

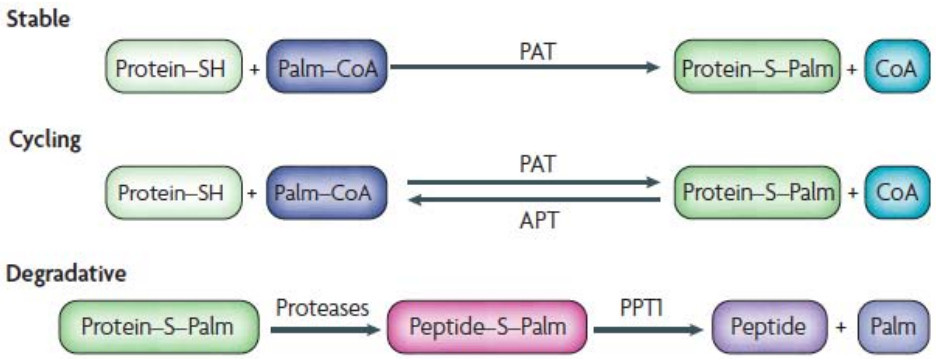

Figure 1.7 Dynamic states of palmitoyl proteins. Proteins are usually either stably palmitoylated or undergo dynamic cycles of palmitoylation and depalmitoylation. During protein degradation removal of palmitate is an essential step. Schematic was adapted from Linder and Deschenes, 2007.

Palmitoylation inhibitors

Palmitoylation has become increasingly recognized as a potential therapeutic target. However, identification of palmitoylation inhibitors has been complicated, since high-throughput screening is not possible for most assays. Two large groups of inhibitors exist: lipid-based and non-lipid compounds (Draper and Smith, 2009). Even though both groups inhibit palmitoylation, those compounds also act on other cellular processes and their mechanism of action is largely unknown. 2-bromopalmitate (2BP) inhibits palmitate incorporation in a non-specific manner (Resh, 1999; Draper and Smith, 2009). 2BP was used to study the *P. falciparum* motor complex proteins (Jones et al., 2012). While GAP50, CDPK1 and MyoA remained unaffected by 2BP treatment, GAP45 and MTIP were affected. Specifically, the localization of GAP45 to the IMC was impaired and showed a diffuse staining. But not only IMC proteins are affected by 2BP treatment, the drug has a pleiotropic effect and leads to mislocalized rhoptries (Jones et al., 2012). In *T. gondii*, 2BP also affects palmitoylation and, therefore, several cellular functions including gliding motility and invasion (Alonso et al.,

2012). Additionally, 2BP also prevents depalmitoylation, since it inhibits the human APTs (Pedro et al., 2013). Thus, several cellular functions are likely to be affected by 2BP treatment.

Tunicamycin is another inhibitor of palmitoylation and likely functions by competing with palmitoyl-CoA for binding to PATs (Planey and Zacharias, 2010). This antibiotic has a non-specific effect on *P. falciparum* during the second cell cycle after adding the drug (Naik et al., 2001). One more lipid-based, non-specific inhibitor of palmitoylation is cerulenin. Non-lipid based palmitoylation inhibitors include compound I-V, which likely act on the substrate binding site (Ducker et al., 2006; Planey and Zacharias, 2010). Compound V has been found to be particularly potent and inhibits both myristoylation and palmitoylation (Draper and Smith, 2009).

Implication of palmitoylation in disease

Huntingtin's disease is a neurodegenerative disorder, which is caused by accumulation of the huntingtin protein (HTT) in the nucleus and cytoplasm. HTT is usually membrane-bound, mediated by palmitoylation by HIP14 at Cys214 (Huang et al., 2004; Yanai et al., 2006; Young et al., 2012). Healthy individuals have a N-terminally located poly-glutamine stretch of up to 35 amino acids. In disease, this stretch is extended to more than 40 glutamines. Even though the mechanism of how disease is promoted is still unclear, it is likely, that the change of amino acid sequence in length leads to an abolishment of interaction with HTT's PAT HIP14 and, therefore, abolishment of membrane localization of HTT, leading to those neurotoxic cytoplasmic inclusions.

Other human PAT genes are connected to disease, mostly cancer, such as DHHC2 in colorectal and liver cancer (Oyama et al., 2000); DHHC8 in schizophrenia (Mukai et al., 2004; Young et al., 2012); DHHC9 in cancer and mental retardation (Raymond et al., 2007) and DHHC15 in x-linked mental retardation (Mansouri et al., 2005); DHHC11 in bladder cancer (Yamamoto et al., 2007) and lung cancer (Kang et al., 2008); and DHHC17 in Huntington's disease and cancer (Ducker et al., 2004; Yanai et al., 2006). In most cases, deletion or over-expression of the respective DHHC genes leads to cancer formation (Oyama et al., 2004; Ducker et al., 2004). Palmitoylation of certain proteins is also impaired, but these proteins are mostly unidentified.

1.4.3 Approaches used to detect fatty acylated proteins

Approaches used to detect myristoyl proteins

Traditional approaches to detect myristoylated proteins include metabolic labeling with ($_3$H)myristate and detection by fluorography, metabolic labeling with iodo-fatty acid analogues containing ($_{125}$I) and direct mass spectrometry (Resh, 2006). These methods are not always straightforward, and the identification of modified proteins in complex cell lysates can be laborious. A more recent approach is chemical labeling by using bioorthogonal probes. Bioorthogonal fatty acid probes are isosteric analogues of myristic acid that are accessible for cytoplasmic NMTs (Heuckeroth et al., 1988). This method is highly specific and uses myristate analogues with a highly reactive azide group. After metabolic labeling and the incorporation of the azidofatty acid analogues, the protein can be pulled down using the Staudinger Ligation (Saxon and Bertozzi, 2000). Capture of proteins is carried out using a biotinylated or fluorescently labeled phosphine, which allows further purification. Alternatively, proteins can be captured using copper-catalyzed click chemistry, depending on the tag used (Roth et al., 2006; Kang et al., 2008). This approach was recently adapted to apicomplexan parasites (Child et al., 2013; Child, 2014) and has also successfully been used for the detection of palmitoyl proteins (Kostiuk et al., 2008; Jones et al., 2012). This method is highly sensitive, rapid and quite specific compared to *in vitro* radiolabeling (Kostiuk et al., 2007).

Approaches used to detect palmitoyl proteins

Similar to the above-mentioned methods, approaches to identify palmitoylated proteins include *in vitro* radiolabeling and chemical labeling (Planey and Zacharias, 2009). Since palmitic acid is attached to cysteines via a thioester bond, this can be used as an advantage over myristate, which is attached via a stable amide bond that cannot be selectively cleaved. The acyl-biotin exchange assay (ABE) uses this property as a basis for palmitoyl protein purification (Drisdel and Green, 2004). ABE followed by mass spectrometry was used to analyze the palmitoyl proteome of several species including *S. cerevisiae* and *P. falciparum* (Roth et al., 2006; Jones et al., 2012).

The palmitoyl proteome of the parasite was published in 2012 (Jones et al., 2012). Before that, only three parasite proteins had been confirmed to be palmitoylated: CDPK1 (Möskes et al., 2004), GAP45 (Rees-Channer et al., 2006) and calpain (Russo et al., 2009). This recent

large-scale study used 2 sets of approaches to analyze the putative *Plasmodium* palmitome: the acyl-biotin exchange assay (Drisdel and Green, 2004; Wan et al., 2007) and metabolic labeling followed by click-chemistry (MLCC). Both assays were followed by mass spectrometry, which detected a total of 400 proteins. 55 of them were enriched in both assays, including several scaffolding, cytoskeletal, adhesion, metabolism, signaling, and transport proteins.

1.6 Aims of this study

The IMC of the malaria parasites is an essential structural element for motility, invasion and cytokinesis and is therefore an essential structure. It is the purpose of this thesis to:

- identify IMC specific PATs,
- to investigate how membrane specificity of dual acylated proteins is achieved and discover essential sequence requirements for IMC membrane attachment of PfISPs and
- to probe into specific sequence requirements for interaction of PAT-substrate pairs.

2. Materials

2.1 Chemicals, equipment and software

2.1.1 Chemicals

Acetic acid glacial	VWR, Canada
Acetone	VWR, Canada
Acrylamide/bis-acrylamide solution (29/1)	VWR, Canada
Agar	VWR, Canada
Agarose	Invitrogen, Canada
Albumax II	Invitrogen, Canada
6-aminohexanoic acid	Sigma, USA
Ammonium persulfate	VWR, Canada
Ampicillin sodium salt	VWR, Canada
Biotin-BMCC	Thermo Scientific, Canada
Blasticidin-S-Hydrochloride 15205	Invitrogen, Canada
Bromphenolblue	VWR, Canada
Bovine serum albumin	Sigma, USA
Calcium chloride dihydrate	VWR, Canada
Chemiluminescent HRP substrate Immobilon™ Western	Milipore, USA
Chloroform	VWR, Canada
Chelex	BioRad, Canada
CO_2 gas mixture	Air Liquide, Canada
Coomassie	VWR, Canada
DAPI	VWR, Canada
D(+)-Glucose monohydrate	VWR, Canada
DMSO	Sigma, USA
DTT	Sigma, USA
dNTPs	Sigma, USA
Amersham ECL™ Western Blotting Analysis System	GE Healthcare, UK

EDTA	VWR, Canada
EGTA	VWR, Canada
Ethanol anhydrous	Commercial alcohols, Brampton, ON
Ethidium bromide	VWR, Canada
Formaldehyde solution 10 %	VWR, Canada
Gentamicin	Sandoz, Canada
Giemsa solution	Sigma, USA
Glutaraldehyde solution 25 %	VWR, Canada
Glycerol anhydrous	VWR, Canada
Glycine	VWR, Canada
HCl	VWR, Canada
HEPES	VWR, Canada
Hydrochlorc acid	VWR, Canada
Hypoxanthine	VWR, Canada
Immersion oil Type A	Cargille Laboratories, USA
Immersol 518F	Zeiss, Germany
Isopropanol	VWR, Canada
Lysozyme	Sigma, USA
Methanol	VWR, Canada
Magnesium chloride hexahydrated	VWR, Canada
Manganous chloride	VWR, Canada
Neutravidin agarose resin	Thermo Scientific, Canada
Peptone	VWR, Canada
Phenol-Chloroform	VWR, Canada
Phusion buffer HF	New England Biolabs, USA
Phusion polymerase	New England Biolabs, USA
Ponceau S	VWR, Canada
Potassium acetate	VWR, Canada
Potassium chloride	VWR, Canada
Potassium hydroxide	VWR, Canada
Protease inhibitor	Invitrogen, Canada
Potassium phosphate monobasic	VWR, Canada
Potassium phosphate dibasic	VWR, Canada

RPMI 1640 +L-glutamine +25mM HEPES -$NaHCO_3$	Invitrogen, Canada
Saponin	Sigma, USA
Sodium acetate	VWR, Canada
Sodium bicarbonate	VWR, Canada
Sodium cabonate	Amresco, USA
Sodium chloride	VWR, Canada
Sodium dodecyl sulfate (SDS)	VWR, Canada
Sodium hydroxide	VWR, Canada
Sodium phosphate monobasice	VWR, Canada
Sodium phosphate dibasice	VWR, Canada
D-Sorbitol	Sigma, USA
N,N,N,N-Tetramethylethylenediamine	VWR, Canada
Trichloroacetic acid	VWR, Canada
Tris hydrochloride	VWR, Canada
Tris (hydroxymethyl)aminomethane	VWR, Canada
TritonX-100	VWR, Canada
L-Tryptophan	VWR, Canada
Tween 20	VWR, Canada
WR99210	Jacobs Pharmaceuticals, USA
Xylencyanol FF	VWR, Canada
Yeast extract	BD, USA

2.1.2 Kits and Standards

PureLink ™ PCR Purification Kit	Invitrogen, Canada
PureLink ™ Quick Gel Extraction Kit	Invitrogen, Canada
PureLink ™ Quick Plasmid Miniprep Kit	Invitrogen, Canada
PureLink ™ HiPure Plasmid Midiprep Kit	Invitrogen, Canada
DNA size marker	Frogga Bio, USA
PageRuler™ Prestained	Fermentas, USA

2.1.3 Equipment and laboratory supplies

Agarose gel running apparatus	BioRad, Canada
Analytical balance SI-234	Denver Instruments, USA
Cell spreader, disposable	VWR, Canada
Centrifuge Avanti J-E (JA-14, JA-20 rotors)	Beckman Coulter, USA
ChemiDoc XRS+ system	BioRad, Canada
Electroporator (CE Module, GenePulser Xcell, PC Module)	BioRad, Canada
Eppendorf CF 5424 (FA-45-24-11 rotor)	Eppendorf, Canada
Excella E24 Incubator Shaker Series	New Brunswick Scientific, USA
Falcon tubes (15, 50 ml, sterile)	Sarstedt, Canada
Filtropur filters S 0.2	Sarstedt, Canada
Filtropur V50 0.2	Sarstedt, Canada
Freezer -20° C Frigidaire	Electrolux, USA
Freezer -80° C Forma 900 Series	Thermo Scientific, Canada
Fridge	Thermo Scientific, Canada
Gene pulser cuvette 2.0 cm	BioRad, Canada
Hamamatsu Digital camera (Model C4742-95) (Camera controller C10600 Orca R)	Carl Zeiss Canada Ltd., Canada
Incubator	Thermo Scientific, Canada
Laboratory scale	Denver Instruments, USA
Laminar flow cabinet 1300 Series A2	Thermo Scientific, Canada
Latex gloves	Microflex, USA
Liquid nitrogen tank Locator 6 Plus	Thermo Scientific, Canada
Magnetic stirrer Hei-Standard	Heidolph Instruments, USA
Maximum protection mask	VWR, Canada
Microwave oven	Mabe Canada Inc., Canada
Micro cover glass	VWR, Canada
Microscope slides (1, 1.2 mm)	VWR, Canada
Nanodrop® 2000c Spectrophotometer	Thermo Scientific, Canada
Needles, disposable	BD, USA
Nitrocellulose Protran BA 85 membrane	GE Healthcare, UK
Pasteur pipettes	VWR, Canada
PCR C1000 thermal cycler	Thermo Scientific, Canada

PCR tubes	Sarstedt, Canada
Petri dish 92x16 mm	Sarstedt, Canada
pH meter Seven easy	Mettler Toledo AG, Switzerland
Pipettes	Gilson, Mandel, Canada
Pipette gun	Thermo Scientifc, USA
Pipette tips (2, 20, 200, 1000 µl)	Sarstedt, Canada
Plastic pipettes (5, 10, 25 ml, sterile)	Sarstedt, Canada
Power source 300 V	VWR, Canada
Rocker	VWR, Canada
SafeSeal tubes (1.5, 2 ml, sterile)	Sarstedt, Canada
Scalpels, disposable	Miltex, USA
SDS-Gel Preparation Equipment, Mini-PROTEAN® Tetra Cell	BioRad, Canada
Semi-Dry Blotting Unit FB-SDB-2020	Thermo Scientific, Canada
Syringe (15, 30 ml)	BD, USA
Thermomixer	Eppendorf, Canada
Vacuum pump BVC 21	Vacuubrand, USA
VarioMACS	Miltenyi Biotec GmbH, Germany
Vortex mixer SRT6D	Stuart Equipment, UK
Water bath WA10V11B	VWR, CANADA
Wet transfer system	BioRad, Canada
Zeiss AXIO Scope.A1	Carl Zeiss Canada Ltd., Canada
Zeiss Axioskop 2plus (Power supply 232)	Carl Zeiss Canada Ltd., Canada

2.1.4 Software and databases

Software

Adobe Illustrator CS 11.0.0	Adobe, USA
Adobe Photoshop CS5.1 12.1x64	Adobe, USA
FinchTV 1.4.0	Geospiza Inc.
Image Lab ®	BioRad, Canada
Mendeley Desktop 1.11	Mendeley Ltd.
MS Office	Microsoft
Nanodrop 2000/2000c 1.4.1	Thermo Scientific, Canada

SnapGene Viewer 1.2	GSL Biotech LLC

Databases

CSS-Palm 3.0	http://csspalm.biocuckoo.org/online
Expasy proteomic tools	www.expasy.org
Myristoylator	www.expasy.org/myristoylator
NCBI Blast	http://blast.ncbi.nlm.nih.gov/Blast.cgi
PlasmoDB	www.plasmodb.org
PRALINE ™	http://www.ibi.vu.nl/programs/pralinewww/
NetPhos 2.0	http://www.cbs.dtu.dk/services/NetPhos/
SMART	http://smart.embl-heidelberg.de/

2.1.5 Enzymes

FirePol® DNA Polymerase	Fermentas, USA
Phusion Polymerase	New England Biolabs Inc., Canada
5x Phusion Buffer HF	New England Biolabs Inc., Canada
dNTPs (2 mM each)	Sigma, USA
*Avr*II	New England Biolabs Inc., Canada
*Bam*HI	New England Biolabs Inc., Canada
*Cla*I	New England Biolabs Inc., Canada
*Eco*RI	New England Biolabs Inc., Canada
*Kpn*I	New England Biolabs Inc., Canada
*Not*I	New England Biolabs Inc., Canada
*Sal*I	New England Biolabs Inc., Canada
*Xho*I	New England Biolabs Inc., Canada
10x NEB Buffer 1, 2, 3 and 4	New England Biolabs Inc., Canada
Fast digest buffer	New England Biolabs Inc., Canada
100x BSA	New England Biolabs Inc., Canada
T4 DNA ligase (400 U/µl)	New England Biolabs Inc., Canada
10x T4 DNA ligase buffer	New England Biolabs Inc., Canada

2.2 Buffers and reagents for molecular biology techniques

2.2.1 Stock Solutions

1 M Tris-HCl

12.11 g tris[hydroxymethyl]aminomethan were dissolved in 80 ml ddH_2O. After having adjusted the pH to 8 with HCl, ddH_2O was added to a final volume of 100 ml.

0.5 M EDTA

18.61 g ethylenedinitril tetra-acetic acid was dissolved in 80 ml ddH_2O. The pH was adjusted to 8 with 10 M NaOH. ddH_2O was added to a final volume of 100 ml.

10x PBS

70.0 g NaCl (120 mM), 35.6 g $Na_2HPO_4 \cdot 2H_2O$ (20 mM) and 6.25 g NaH_2PO_4 (5.2 mM) were dissolved in ddH_2O, adjusted to 1 l.

2.2.2 Solutions for Polymerase chain reaction (PCR)

TE-buffer (10 mM Tris-HCl/1 mM EDTA)

0.2 ml 0.5 M EDTA and 1 ml 1 M Tris-HCl (pH 8) were added to 80 ml ddH_2O and adjusted to a final volume of 100 ml.

3 M sodium acetate (NaAc)

24.6 g sodium acetate (anhydrous; $CH_3COOHNa$) or 40.8 g sodium acetate (trihydrate; $CH_3COOHNa \cdot 3H_2O$) were dissolved in 80 ml ddH_2O. The pH was adjusted to 5.2 with acetic acid. ddH_2O was added to a final volume of 100 ml.

Table 2.1 List of oligonucleotides used in this study. Restriction enzyme cut sites are underlined.

***P. falciparum* ISP3 primers**	
Primer	**Sequence**
PfISP3_FL_fw	GCGCGGTACCATGGGAAATTTATGTTGTAGT
PfISP3_FL_rv	GCGCCCTAGGTGCATTCAAACAATATTTTTG
PfISP3_3'_fw	CGATGCGGCCGCTATGTTGTAGTAATAATG
PfISP3_int_fw	GTTTCAGTCTGAATATTACC
PfISP3_FL_mCh_fw	GAGAGGATCCATGGGAAATTTATGTTGTAG
PfISP3_FL_mCh_fw	GAGAGCGGCCGCTGCATTCAAACAATATTTTTG
PfISP3_G2A_FL_fw	GCGCGGTACCATGGCAAATTTATGTTGTAGT
PfISP3_C5AC6A_FL_fw	GCGCGGTACCATGGGAAATTTAGCTGCTAGT
20_PfISP3_1-10A_fw	GCGCGGTACCATGGGAGCTGCATGTTGTGCTGCTGCTGCT ATAAAAAAC
20_PfISP3_1-10A_rv	GCGCCCTAGGTATATCTATATTTGATTTACTGTTTTTTATAGCAGCAGCAGC
20_PfISP3_11-20A_fw	GCGCGGTACCATGGGAAATTTATGTTGTAGTAATAATGATGCAGCAGCCGC TGCAGCAGCT
20_PfISP3_11-20A_rv	GCGCCCTAGGTGCAGCTGCTGCTGCTGCAGCGGCTGCTGCATCATT
20_PfISP3_C5AC6A_fw	GCGCGGTACCATGGGAAATTTAGCTGCTAGT
20_PfISP3_C5AC6A_rv	GCGCCCTAGGTGCATTCAAACAATATTTTTG
20_PFISP3_C5A_fw	GCGCGGTACCATGGGAAATTTAGCTTGTAGTAATAATGATATAAAAAACA GTAAATC
20_PfISP3_C5A_rv	GCGCCCTAGGTATATCTATATTTGATTTACTGTTTTTTATATCATTATTACT
20_PfISP3_C6A_fw	GCGCGGTACCATGGGAAATTTATGTGCTAGTAATAATGATATAAAAAACA GTAAATC
20_PfISP3_C6A_rv	GCGCCCTAGGTATATCTATATTTGATTTACTGTTTTTTATATCATTATTACT
10_PfISP3_N9RD10K_fw	GGCCGGTACCATGGGAAATTTATGTTGTAGTAATAGAAAAGCAGCAGC
10_PfISP3_N9RD10K_rv	GGCCCCTAGGTGCTGCTGCTGCTGCTTTTCTATTACTAC
10_PfISP3_N9D10K_fw	GGCCGGTACCATGGGAAATTTATGTTGTAGTAATAAAAAAGCAGCAGC
10_PfISP3_N9D10K_rv	GGCCCCTAGGTGCTGCTGCTGCTGCTTTTTTATTACTAC
10_PfISP3_N9D_fw	GATCGGTACCATGGGAAATTTATGTTGTAGTAATGATGATGCAGCAGC
10_PfISP3_N9D_rv	GGCCCCTAGGTGCTGCTGCTGCTGCATCATCATTACTAC
10_PfISP3_fw	GGCCGGTACCATGGGAAATTTATGTTGTAGTAATAATGATGCAGC
10_PfISP3_rv	GGCCCCTAGGTGCTGCTGCTGCTGCATCATTATTACTAC
10_PfISP3_D10G_fw	GGCCGGTACCATGGGAAATTTATGTTGTAGTAATAATGGAGCAGC
10_PfISP3_D10G_rv	GGCCCCTAGGTGCTGCTGCTGCTGCTCCATTATTACTAC
10_PfISP3_D10K_fw	GGCCGGTACCATGGGAAATTTATGTTGTAGTAATAATAAAGCAGC
10_PfISP3_D10K_rv	GGCCCCTAGGTGCTGCTGCTGCTGCTTTATTATTACTAC
10_PfISP3_D10R_fw	GGCCGGTACCATGGGAAATTTATGTTGTAGTAATAATAGAGCAGCAGC
10_PfISP3_D10R_rv	GGCCCCTAGGTGCTGCTGCTGCTGCTCTATTATTACTAC
***P. falciparum* ISP1 primers**	
Name	**Sequence**
PfISP1_fw	GGCCGGTACCATGGGGAATATTGTATCATGTTGTTC
PfISP1_FL_rv	GATCCCTAGGCGAATTTTTTTTATAATCTTTC
PfISP1_3'_fw	GATCGCGGCCGCGTATCATG TTGTTCATTAGACG
PfISP1_int_fw	GAAAAATTACAAGTGTG
20_PfISP1_C7A,C8A_fw	GGCCGGTACCATGGGGAATATTGTATCAGCTGCTTCATTAG
20_PfISP1_C7A,C8A_rv	GGCCCCTAGGGTCGTCGTTTAAATATTTTTTATTTTCGTCTAATGAAGCAGC TGATAC
20_PfISP1_G2A_fw	GATCGGTACCATGGCAAATATTGTATCATG
20_PfISP1_G2A_rv	GGCCCCTAGGGTCGTCGTTTAAATATTTTTTATTTTCGTCTAATGAACAACA TGATAC
10_PfISP1_fw	CATGGGTACCATGGGGAATATTGTATCATGTTGTTCATTAGC
10_PfISP1_rv	GTACCCTAGGTGCTGCTGCTGCTGCTAATGAACAACATGATAC
11_PfISP1_fw	GATCGGTACCATGGGGAATATTGTATCATGTTGTTCATTAGACGC
11_PfISP1_rv	GTACCCTAGGTGCTGCTGCTGCTGCGTCTAATGAACAACATGATAC
11_PfISP1_D11K_fw	CATGGGTACCATGGGGAATATTGTATCATGTTGTTCATTAAAAGC
11_PfISP1_D11K_rv	CATGCCTAGGTGCTGCTGCTGCTGCTTTTAATGAACAACATGATAC
***P. falciparum* PAT primers**	
Name	**Sequence**
PfDHHC1_3'_fw	GGCCGCGGCCGCCTGTGTATGGGTTGATAACTGC
PfDHHC1_3'_FL_rv	CCGGCCTAGGTGTGTTTGATATTAATGTATAACACACATC
PfDHHC1_int_fw	GGATGAGGACTACAGAAATGC
PfDHHC1_FL_fw	CCGGGGTACCATGAATGATAATGAGAGCTTAGACAGC
PfDHHC2_FL_fw	CCGGGGTACCATGAGACCTAAATATGTTC
PfDHHC2_FL_rv	CCGGCCTAGGAACAGGATTTTCATGTGC
PfDHHC9_FL_fw	ATGGGGATCCATGAATAATTATTTGGC

PfDHHC9_FL_rv	GATCGCGGCCGCATGAATAATTATTTGGC
PfDHHC3_FL_fw	GATCGGATCCATGAATAATCACATTTGTGC
PfDHHC3_FL_rv	GATCGCGGCCGCATAATTTTTTAATGTAATTTCTCC
APT1_fw	GATCGGTACCATGAGAATAATAAAATATATATTTTTTGC
APT1_rv	GATCCCTAGGATTAGGTGTATTTGGATTTC

***P. falciparum* CDPK1 primers**	
Name	**Sequence**
20_CDPK1_K10D,K13D,R15D _fw	GATCGGTACCATGGGGTGTTCACAAAGTTCAAACGTGGATGATTTTGATAC GGATAG
20_CDPK1_K10D,K13D,R15D _rv	GATCCCTAGGCGTAAATTTACTTCTATCCGTATCAAAATCATCCACG

***S. cerevisiae* primers**	
Name	**Sequence**
PfDHHC1 _opt_Cla	GATCATCGATTGTGTTGCTAATCAGGG
PfDHHC1_opt_seq	CTTGTCTATATCCTTCTGAAG
PfDHHC3_opt_Bam	GATCGGATCCATGAATAATCACATTTGTGCC
PfDHHC3_opt_Cla	GATCATCGATATAATTCTTCAGAGTAATTTCTC
PfDHHC9_opt_Bam	GATCGGATCCATGAACAATTATCTGGCCTTC
PfDHHC9_opt_Cla	GATCATCGATGTCTCCATCCTCCTTAATGTTC
20_PfISP3_opt_fw	GATCCATGGGCAATCTGTGTTGCTCTAACAACGATATCAAGAATAGCAAAT CCAACATAGACATTG
20_PfISP3_opt_rv	AATTCAATGTCTATGTTGGATTTGCTATTCTTGATATCGTTGTTAGAGCAAC ACAGATTGCCCATG
20_PfISP3_C5C6_opt_fw	GATCCATGGGCAATCTGGCCGCCTCTAACAACGATATCAAGAATAGCAAAT CCAACATAGACATTG
20_PfISP3_C5C6_opt_rv	AATTCAATGTCTATGTTGGATTTGCTATTCTTGATATCGTTGTTAGAGGCGG CCAGATTGCCCATG
20_PfISP3_D10D10K_opt_fw	GATCCATGGGCAATCTGTGTTGCTCTAACAACAAGATCAAGAATAGCAAAT CCAACATAAAGATTG
20_PfISP3_D10D19K_opt_rv	AATTCAATCTTTATGTTGGATTTGCTATTCTTGATCTTGTTGTTAGAGCAAC ACAGATTGCCCATG

2.2.3 Solutions for gel electrophoresis

50x TAE buffer

242 g Tris-Base, 57.1 ml acetic acid glacial, 37.2 g $Na_2EDTA{\cdot}2H_2O$ were dissolved in 0.8 l ddH_2O and the total volume adjusted to 1 l.

Agarose gels

Agarose was added to 1x TAE buffer to reach concentrations of 0.7 – 1.5 %. The suspension was boiled in the microwave oven until the agarose was completely dissolved. After the solution cooled down to ~ 60° C, 0.6 µg/ml ethidiumbromide was added and the gels were poured.

6x Gel loading buffer

40 % glycerol (6 ml), 0.1 g (0.25 %) of each bromphenolblue and xylencyanol FF were dissolved in 15 ml ddH_2O.

2.2.4 Solutions for cloning and plasmid amplification

10x LB (luria broth) medium

50 g peptone, 100 g Yeast extract and 100 g NaCl were dissolved in 1 l ddH_2O and autoclaved.

Ampicillin

5 g ampicillin sulphate were dissolved in to obtain a final concentration of 100 mg/ml and stored at -20° C.

Kanamycin

500 mg kanamycin were dissolved in 10 ml ddH_2O to obtain a final concentration of 50 mg/ml. The solution was aliquoted and stored at -20° C.

LB Amp+/Kan+ agar plates

500 ml of autoclaved LB medium containing 1.5 % Bacto™-agar were boiled and cooled down to at least 60° C before adding 500 µl ampicillin (100 mg/ml) or 500 µl ampicillin (50 mg/ml), respectively. The agar was then poured into Petri dishes (~25 ml/100 mm plate), allowed to cool to room temperature and stored at 4° C.

STET buffer

80 g saccharose, 18.61 g EDTA, 5 ml Triton X-100 and 1.2 g Tris-Base were dissolved in 1 l ddH_2O.

Lysozyme

0.1 g lysozyme were dissolved in 10 ml TE buffer and stored at 4° C.

2.2.5 Bacteria, vectors and yeast strains

Bacteria

E. coli DH5α cells	McMaster University (Ana Cabrera, Tatianna Wong, Johanna Wetzel)
E. coli BL21	McMaster University (Ana Cabrera)

Vectors

pARL-1a-GFP	Struck et al., 2005
pBcam-mCherry	Flueck et al., 2010
pBcrt-dsRed	Struck et al., 2008
S. cerevisiae vector pRS406	Hou et al., 2009
S. cerevisiae vector pRS403	Hou et al., 2009

***Saccharomyces cerevisiae* strain**

NDY (lacks five of the seven yeast DHHC genes: *akr1*Δ *akr2*Δ *pfa3*Δ *pfa4*Δ *pfa5*Δ	Roth et al., 2006; Hou et al., 2009

2.2.6 Sequencing primers

Primer	**Sequence (5'→3')**
*gfp*272 rv	CCTTCGGGCATGGCACTC
ama1 fw	CCTAATAATTTATTTGATAATTTTTC
mCh rv	GCGCATGAACTCCTTGATGATGGC
6583 fw	GTTGTGTGGAATTGTGAGCGG
2161 fw	CTTATTCAAATGTAATAAAAG
581 fw	GTCCGCCCTGAGCAAAGACC
ProtA rv	GTAAGATCTCATAGAACGC

2.2.7 Solutions for generation of chemocompetent *Escherichia coli* DH5α or BL21 cells

TFB I Buffer

1.5 g KOAc, 4.9 g $MnCl_2 \cdot 4H_2O$, 6.1 g RbCl, 0.74 g $CaCl_2$ and 75 ml glycerol were dissolved in 500 ml ddH_2O. pH was adjusted to 5.8 with 0.2 N acetic acid. Solution was sterile filtered and stored at 4° C.

TFB II buffer

1.1 g MOPS, 0.6 g RbCl, 5.5 g $CaCl_2$ and 75 ml glycerol were dissolved in 500 ml ddH_2O. pH was adjusted to 7.0 with 1 M NaOH. Solution was sterile filtered and stored at 4° C.

2.3 Buffers and reagents for biochemical techniques

2.3.1 Solutions for SDS-polyacrylamide gel electrophoresis (SDS-PAGE)

5x Laemmli buffer (sample buffer)

1.5 g SDS, 1.16 g DTT, 3.75 ml 1M Tris pH 6.8, 0.015 g bromophenol blue were dissolved in 7.5 ml ddH_2O. 7.5 ml glycerol were added and mixed. Solution was aliquoted and stored at -20° C.

10x SDS PAGE running buffer

144 g glycine, 10 g SDS and 30.2 g Tris-Base were dissolved in 1 l ddH_2O.

Separating gel buffer (pH 8.8)

45.4 g Tris-Base were dissolved in 250 ml ddH_2O to get a concentration of 1.5 M Tris-Base. The pH was adjusted to 8.8.

Stacking gel buffer (pH 6.8)

1.85 g Tris-Base and 37 g Tris-HCl were dissolved in 250 ml ddH_2O. The pH was adjusted to 6.8.

10 % ammonium persulfate (APS)

0.2 g APS were dissolved in 2 ml ddH_2O.

Coomassie

25 ml acetic acid glacial and 0.125 g Coomassie blue G-250 were dissolved in 225 ml ddH_2O and mixed for 1 h. Solution was filtered with Whatman paper and stored at room temperature.

Coomassie-destaining solution

50 ml tap water, 40 ml MeOh and 10 ml acetic acid glacial were mixed and stored at room temperature.

Ponceau S

1 g Ponceau was mixed with 5 ml acetic acid glacial and 495 ml ddH_2O and stored at room temperature.

2.3.2 Solutions for Western Blot

Transfer buffer for wet transfer

5.8 g Tris-HCl and 2.9 g glycine were dissolved in 700 ml ddH_2O, 200 ml methanol was added and the final volume adjusted to 100 ml.

Transfer buffers for semi-dry blotting

Cathode buffer

3.03 g Tris-Base (25 m M) and 5.25 g 6-aminohexanoic acid (40 mM) were dissolved in 800 ml ddH_2O. 200 ml MeOH were added to a final volume of 1 L.

Anode I buffer

3.63 g Tris-Base (30 mM) were dissolved in 800 ml ddH_2O. 200 ml MeOH were added to a final volume of 1 L.

Anode II buffer

36.33 g Tris-Base were dissolved in 800 ml ddH_2O. 200 ml MeOH were added to a final volume of 1 L.

PBS-Tween (PBS-T)

0.5 ml Tween 20 was dissolved in 500 ml PBS.

Membrane blocking

Blocking was performed using 10 % skim milk in PBS-T.

Antibodies

Primary antibodies

Name	dilution in 1% Milk	Manufacturer
Rabbit polyclonal anti GAP45	1:3000	Dr. Sharma, NII, New Delhi, India
Mouse monoclonal anti-GFP	1:1000	Roche, USA
Rat monoclonal anti mCherry	1:2000	Chromotek, USA
Mouse monoclonal anti GAPDH	1:3000	Dr. Daubenberger, Swiss TPH, Basel, Switzerland
Mouse monoclonal anti GAPM2 C-ter	1:2000	Dr. Kono, BNITM, Hamburg, Germany

Secondary antibodies

Name	dilution in 1% Milk	Manufacturer
Goat anti-rat HRP	1:3000	Rockland Immunochemical, USA
Goat anti-mouse HRP	1:3000	Rockland Immunochemical, USA
Goat anti-rabbit HRP	1:3000	Rockland Immunochemical, USA

Wash buffer

0.1 % skim milk/PBS-T.

2.3.4 Buffers for solubility assay

Bicarbonate buffer

0.1 M Na_2CO_3 was prepared freshly each time in ddH_2O by dissolving 0.106 g Na_2CO_3 in 10 ml ddH_2O.

Triton X-100 buffer

1 % Triton X-100 in ddH_2O was prepared by dissolving 100 µl Tx-100 in 10 ml ddH_2O.

2.3.5 Solutions for biotin switch assay

LB buffer (50mM Tris, 150mM NaCl, 5mM EDTA, pH 7.4)

5 ml 1 M Tris pH 7.4, 15 ml 1 M NaCl, 1 ml 0.5 M EDTA and 79 ml ddH_2O were mixed and stored at 4° C.

LB buffer + 20 mM NEM + 3.4 % Triton X-100

100 µl 1 M NEM (prepared freshly each time: 0.125 g in 1 ml 100 % ethanol) were added to 1.7 ml 10 % TX100/LB buffer and 3.3 ml LB buffer.

LB buffer + 1 mM NEM + 0.2 % Triton X-100

5 µl 1 M NEM, 100 µl 10 % TX100/LB buffer in 4.95 ml LB buffer were prepared freshly each time.

LB buffer + 0.2 % Triton X-100

200 µl 10 % TX100/LB buffer were added to 10 ml LB buffer and stored at room temperature.

4 SB buffer (4 % SDS, 50 mM Tris, 5 mM EDTA, pH 7.4)

2 ml 20 % SDS, 0.5 ml 1 M Tris pH 7.4, 100 µl 0.5 M EDTA and 7.4 ml ddH_2O were mixed and stored at room temperature.

4 SB + 10 mM NEM

30 µl 1 M NEM and 2.97 ml 4 SB buffer were mixed freshly.

LB buffer + 0.1 % SDS + 0.2 % Tx100

1 ml 10 % Tx100/H_2O, 250 µl 20 % SDS and 49 ml LB buffer were mixed and stored at room temperature.

+ Hydroxylamine buffer (0.7 M hydroxylamine, 1 mM biotin-BMCC, 0.2 % Triton X-100, pH 7.4)

	For 3 ml:	For 1 ml:
50 mM biotin-BMCC	60 µl	20 µl
10 % TX-100/water	60 µl	20 µl
1 M Hydroxylamine pH 7.4	2.1 ml	700 µl
ddH_2O	780 µl	260 µl

1 M hydroxylamine buffer

1M hydroxylamine was prepared freshly and kept on ice all the time. 0.69 g hydroxylamine were dissolved in 8.0 ml ddH_2O. The pH was adjusted to 7.4 with 5M NaOH and the final volume was adjusted to 10 ml with water.

50 mM biotin-BMCC stock in DMSO

26.989 mg/ml biotin-BMCC were dissolved in DMSO, aliquoted in 50 µl and stored at -80° C

- Hydroxylamine buffer (50 mM Tris, 1 mM biotin-BMCC, 0.2 % Triton X-100, pH 7.4)

	For 3 ml:	For 1 ml:
50 mM biotin-BMCC	60 µl	20 µl
10 % TX-100/water	60 µl	20 µl
1 M Tris pH 7.4	150 µl	50 µl
ddH_2O	2.73 ml	910 µl

Low biotin-BMCC buffer (50 mM Tris, 150 mM NaCl, 5 mM EDTA, 0.2 mM biotin-BMCC, 0.2 % Triton X-100, pH 7.4)

	For 5 ml:	For 2.5 ml:
50 mM biotin-BMCC	20 µl	10 µl
1 M Tris pH 7.4	250 µl	125 µl
1 M NaCl	750 µl	375 µl
10 % TX-100/water	100 µl	50 µl
0.5 M EDTA	500 µl	250 µl
ddH_2O	3.15 ml	1.6 ml

2.3.6 Buffers for NP-40 extraction of proteins

TBS (Tris-buffered saline) contains 50 mM Tris-HCl, pH 7.5; 150 mM NaCl, 0.05 % NP-40 and complete protease inhibitors. The reagents were dissolved in ddH_2O and stored at 4° C.

2.3.7 Solutions for immunoprecipitation

Immunoprecipitation (IP) lysis buffer

Lysis buffer contains 10 mM Tris-HCl (pH 7.5), 150 mM NaCl, 0.5 mM EDTA, 0.5 % NP40 and 1 mM PMSF and protease inhibitor cocktail.

IP dilution buffer

Dilution buffer contains 10 mM Tris-HCl (pH 7.5), 150 mM NaCl, 0.5 mM EDTA, and 1 mM PMSF and protease inhibitor cocktail.

2.4 Buffers and reagents for cellular biology techniques

Complete parasite culture medium

The *in vitro* cultivation of *P. falciparum* parasites was carried out in a medium consisting of RPMI 1640, supplemented with 25 mM HEPES, 50 mg/l hypoxanthine, 0.21 % $NaHCO_3$ (w/v), 0.5 % Albumax (w/v) and 16 mg/l gentamycin. The medium was prepared by dissolving 25 g Albumax II, 80 g RPMI 1640, 10 g D-glucose and 5 g $NaHCO_3$ in 4.75 l ddH_20. 0.14 g hypoxanthine were dissolved in 2 ml NaOH and added to the medium. The pH was adjusted to 7.2 using NaOH. 2 ml gentamycin (40 mg/ml) were added and the total volume was adjusted to 5 l with ddH_20. After further 5 min of stirring, this complete culture medium was sterile filtered through a 0.22 µm filter into sterile glass bottles and stored at 4° C.

Erythrocytes

Human erythrocytes were obtained from the McMaster University Children's Hospital as a ready-to-use erythrocyte concentrate of blood type O+.

Blasticidin-S-HCl

50 mg Blasticidin-S-Hydrochloride 15205 was dissolved in 10 ml culture medium to receive a final concentration of 5 mg/ml, sterile filtered and stored in Eppendorf tubes at -80° C.

WR99210

15 µl 20 mM WR99210 in DMSO was dissolved 1:1000 in culture medium to 20 µM, sterile filtered and stored in Eppendorf tubes at -80° C.

Giemsa solution

15 ml of Giemsa stock solution were added to 200 ml of tap water.

D-Sorbitol

25 g D-sorbitol were dissolved in 450 ml ddH_2O. The solution was adjusted to 500 ml with ddH_2O, sterile filtered and stored at 4° C.

Saponin

Saponin was dissolved in PBS to receive a concentration of 0.03 % and stored at 4° C.

Freezing solution

21 g sorbitol and 4.5 g NaCl were dissolved in 360 ml ddH_2O and complemented with 140 ml glycerol. The solution was sterile filtered solution and stored at 4° C.

Thawing solution

17.5 g NaCl were dissolved in 500 ml ddH_2O, sterile filtered and stored at 4° C.

Cytomix

Sterile filtered cytomix contains 120 mM KCl, 0.15 mM $CaCl_2$, 2 mM EDTA, 5 mM $MgCl_2$, 10 mM K_2HPO_4/KH_2PO_4 (pH 7.6), 25 mM Hepes in ddH_2O. Aliquots and stock solution were stored at 4° C.

2.4.1 Buffers and reagents for immunofluorescence assays (IFAs) on formaldehyde/glutaraldehyde fixed cells

Antibodies

Primary antibodies

Antibody	Dilution in 3% BSA	Manufacturer
Mouse monoclonal anti GFP	1:1000	Roche, USA
Rat monoclonal anti mCherry	1:1000	Chromotek, USA
Mouse monoclonal anti GAPM2	1:2000	Dr. Kono, BNITM, Hamburg, Germany
Rabbit monoclonal anti RALP C-ter	1:1000	Dr. Haase, BNITM, Hamburg, Germany

Secondary antibodies

Antibody	Dilution	Excitation	Manufacturer
Alexa Fluor goat anti-mouse FITC	1:1000	488 nm	Invitrogen (A11001)
Alexa Fluor goat anti-mouse FITC	1:1000	594 nm	Invitrogen (A11005)
Alexa Fluor goat anti-rabbit FITC	1:1000	488 nm	Invitrogen (A11008)
Alexa Fluor goat anti-rabbit FITC	1:1000	594 nm	Invitrogen (A11012)
Alexa Fluor goat anti-rat FITC	1:1000	488 nm	Invitrogen (A11006)
Alexa Fluor goat anti-rat FITC	1:1000	594 nm	Invitrogen (A11007)

Fixation buffer

2 ml 10 % formaldehyde and 1.5 µl 25 % glutaraldehyde were dissolved in 2.5 ddH_2O and 500 µl 10x PBS.

Triton X-100

The fixed cells were permeabilised with 0.1 % Triton X-100 in PBS. 50 µl Triton X-100 were added to 50 ml sterile PBS.

Blocking buffer

Cells were blocked with 3 % bovine serum albumin (BSA). 1.5 g BSA was dissolved in 50 ml PBS and sterile filtered.

2.4.2 Solutions and reagents for gDNA isolation

Buffer A

4.1 g sodium acetate (500 mM), 0.58 g NaCl (100 mM) and 0.0037 g EDTA (1 mM) were dissolved in 100 ml ddH_2O.

10 % SDS

SDS was dissolved in ddH_2O to a concentration of 10 %.

3. Methods

3.1 Molecular biology techniques

3.1.1 Primer design

Primers were designed to be as heterogeneous as possible at a length of approximately 20 bases. Primer pairs preferably carried similar annealing temperatures. Primers were designed to start with four random bases adjacent to the required restriction enzyme site. The last four bases of the 3' end were selected to include at least two guanine and/or cytosine bases, respectively. Full-length, truncated and mutant versions of PF14_0578 (PfISP3), PF10_0107 (PfISP1), PFL1090w (GAP45), PFB0815w (CDPK1), PfAPT1 and PfPATs were cloned using primers summarized in Table 2.1.

3.1.3 Polymerase chain reaction (PCR)

Generally, PCR was performed in 50 µl containing 5x concentrated reaction buffer. The reaction mixture was prepared on ice; nucleotides and DNA polymerase were the last reagents to be added. Previously cloned and sequenced constructs were used as templates whenever possible.

28.8 µl	ddH_2O
10 µl	5x Phusion buffer HF
2.5 µl	forward primer (10 µM)
2.5 µl	reverse primer (10 µM)
1 µl	template DNA (approximately 0,1 ng/µl gDNA)
5 µl	dNTPs (dGTP, dATP, dCTP, dTTP; 2 mM each)
0.2 µl	Phusion DNA polymerase (0.1 – 0.5 U)

The reactions were cycled for 35 times using the following standard settings:

Initial denaturation	95° C	5 min	
Denaturation	95° C	30 sec	35x
Annealing	42 – 60° C	30 sec	
Extension	65° C	20 sec – 2 min	
Final elongation	65° C	5 min	

Optimal annealing and primer extension temperatures were determined using temperature-gradient PCR.

Mutagenesis

Mutations were introduced using primers carrying the desired base substitutions. Primers contain additional 6 bases after the last mutated one. Ideally, primer pairs share a 16 bp overlapping region to obtain desired PCR products by minimizing the extension time to 15 sec. Mutation of gene-internally localized amino acids was done using overlap PCR, where primer pairs share a 16 bp overlapping region.

PCR of codon-optimized genes

Codon-optimization for optimal expression *P. falciparum* genes in *S. cerevisiae* was done by ordering the entire gene at MWG operon, containing both desired restriction enzyme overhangs. Both DNA strands were amplified and ligated into the desired vector directly.

3.1.4 Gel electrophoresis

PCR products were analyzed by agarose gel electrophoresis. 3 µl of the PCR product were supplemented with 2 µl 6x loading buffer. The samples were loaded on a 1 % agarose gel containing ethidium bromide (0.6 µg/ml) together with 4 µl of a 1 kb DNA size marker (100 ng/µl). Gel electrophoresis was performed at 80 V for 30 min. The gel was examined under UV light using the ChemiDoc XRS+ system (BioRad) and documented with a digital camera using the Image Lab ® software.

3.1.5 Purification of PCR products and DNA digestion

PCR products were purified using the PureLink ™ PCR Purification Kit (Invitrogen) or the PureLink ™ Quick Gel Extraction Kit (Invitrogen). The vast majority of constructs contain *Kpn*I and *Avr*II restriction enzyme cut sites.

Typically, DNA was digested in a 50 µl reaction volume. *Dpn*I was added to the reaction when cDNA or pDNA was used as a template for PCR, to ensure digest of bacterial DNA, but not PCR product. The following reagents were mixed in an Eppendorf tube and incubated at 37° C for 1 h:

30 µl	DNA in TE buffer
0.5 µl	Enzyme 1
0.5 µl	Enzyme 2
5 µl	10x digestion buffer
5 µl	10x BSA
9 µl	ddH_2O

3.1.6 Ligation

DNA concentration was estimated using gel electrophoresis comparing band intensities with reference bands from the 1 kb DNA ladder. Ligation was performed in a 10 µl reaction volume using 10 ng of plasmid and the insert fragment at a 20 – 50 fold molar excess.

1 µl	10x ligation buffer
1 µl	plasmid vector
7 µl	insert
1 µl	T4 DNA ligase (40 U/µl)

The ligation was incubated for at least 20 min at room temperature or at 4° C overnight.

3.1.7 Transformation of *Escherichia coli*

Chemocompetent DH5α *E. coli* cells were transformed by heat shock. 100 µl of competent cells were thawed on ice and mixed with 10 µl ligation product. The cells were incubated on

ice for 10 min, heat-shocked for 1 min at 42° C, and transferred back on ice for 2 min. 650 µl pre-warmed LB (without ampicillin) was added and the cells were allowed to recover shaking for 20 min at 900 rpm at 37° C on a Thermomixer (Eppendorf). After centrifugation for 1 min at 3400 g, 2/3 of the supernatant were removed, the pellet was resuspended and plated on an Amp+ agarose plate and incubated at 37° C overnight.

3.1.8 Colony screen PCR of transformed DH5α

Several bacterial colonies were screened by PCR to verify the presence of the desired transfection construct. PCR was set up using forward primer of the respective insert and a reverse primer that binds to the 5' end of the *gfp*- or *mCherry*-tag, respectively; or alternatively with the reverse primer binding to the insert and a forward primer located at the 3' end of the *ama1* promoter. With a sterile pipette tip, single colonies were transferred onto an Amp+ agar masterplate followed by transfer of the colony into a PCR tube containing 10 µl reaction mixture. The masterplate was then incubated at 37° C for at least 6 h.
PCR conditions were as follows:

5.8 µl	ddH_2O
1 µl	10x Taq Buffer
1 µl	forward primer (10 µM)
1 µl	reverse primer (10 µM)
1 µl	dNTPs (dGTP, dATP, dCTP, dTTP; 2 mM each)
0.2 µl	Taq DNA polymerase (0.1 – 0.5 U)

The reactions were cycled 30 times using the following standard settings:

Initial denaturation	95° C	5 min	
Denaturation	95° C	30 sec	30x
Annealing	42° C	30 sec	
Extension	65° C	1 – 2 min	
Final elongation	65° C	3 min	

PCR products were checked for correct fragment size on a 1 % agarose gel. Positively screened clones were selected from the masterplate and inoculated into 4.5 ml LB medium

containing 4 µl ampicillin (100 mg/ml) and incubated at 37° C overnight in a rotating incubator at 250 rpm (New Brunswick Scientific Excella E24 Incubator Shaker Series).

3.1.9 STET method for Minipreps

2 ml overnight bacterial culture was centrifuged at 10'000 g for 1 min. The pellet was resuspended in 500 µl STET buffer. 50 µl lysozyme (10 mg/ml) was added and the sample was incubated for 3 min at room temperature followed by 2 min incubation at 95° C. After centrifugation for 5 min at 21'000 g, the supernatant was transferred to a new tube. 50 µl 6.5 M NaAc and 500 µl isopropanol were added and the sample was vortexed. The samples were centrifuged for 5 min at 21'000 g, the supernatant was removed and the pellet was air-dryed. The pellet was resuspended in 50 µl TE buffer containing RNAse A (50 µg/ml) and the plasmids were digested with an appropriate set of enzymes followed by agarose gel electrophoresis.

3.1.10 Plasmid DNA Isolation from recombinant *Escherichia coli* cultures

Escherichia coli overnight cultures were harvested and processed using the PureLink™ Quick Plasmid Miniprep Kit according to protocol. To confirm presence of the desired plasmid, the isolated DNA was digested with a set of appropriate restriction enzymes. The resulting digestion pattern was then compared to the calculated digested plasmid construct.

3.1.11 Sequencing

20 µl of plasmid DNA at a concentration of 100 ng/µl and 10 µl primers (2 µM) were sent to Eurofins MWG Operon for sequencing. Most transfection constructs were checked for integration of the desired insert by a two-primer based sequencing reaction: the *ama1* forward primer or the *gfp/mCherry* reverse primer allowed to sequence across both the ATG start codon the 3' end of the gene. Correct plasmids were stored at -20° C.

3.1.12 Glycerol stabilates

Glycerol stabilates were prepared from positive *E. coli* clones. 0.5 ml of overnight culture was resuspended in 0.5 ml of 80 % glycerol/water. These bacterial stocks were stored at -80° C.

3.1.13 Large-scale plasmid production

200 ml of Amp+ LB medium were inoculated with ~ 5 µl bacteria from glycerol stock and grown overnight at 37° C in a rotating incubator (250 rpm; New Brunswick Scientific Excella E24 Incubator Shaker Series). Plasmid DNA was isolated using the PureLink ™ HiPure Plasmid Midiprep Kit according to protocol. Purified plasmid DNA was dissolved in 100 µl TE and plasmid concentration was determined using a Nanodrop® 2000c Spectrophotometer (Thermo Scientific, USA). To confirm presence of the desired plasmid, the isolated DNA was diluted 1:20 and digested with a set of appropriate restriction enzymes and checked by agarose gel electrophoresis. The resulting digestion patterns were then compared to the calculated digested plasmid construct. Appropriate DNA volumes from DNA midi preps were taken for precipitation to yield 100 µg. Plasmids were precipitated by adding 0.1 vol 3 M NaAc and 3 vol 100 % EtOH and incubated at -20° C for 1 h. After 20 min of centrifugation at 21'000 g and washing with 500 µl 70% EtOH, the plasmid pellet was dissolved in 15 µl sterile TE buffer. This DNA was used for parasite transfection.

3.1.14 Preparation of chemocompetent *Escherichia coli* DH5α cells

Bacteria were plated on LB agar plate (without ampicillin) from frozen stock to get single colonies. After overnight growth at 37° C, a single colony was picked and grown in 5 ml LB without ampicillin at 37° C overnight in a rotating incubator (250 rpm; New Brunswick Scientific Excella E24 Incubator Shaker Series). 2 ml of the overnight culture were inoculated into 200 ml LB without ampicillin and grown for approx. 2 h at 37° C and 250 rpm until the OD_{600} reached 0.5 – 0.6. Then, the cells were chilled for 10 to 20 min on ice and split into four pre-chilled 50 ml Falcon tubes and centrifuged for 15 min at 4000 g and 4° C. The supernatant was removed and each pellet was resuspended in 15 ml cold TFB I buffer and incubated on ice for 10 min. The bacteria were spun at 4000 g for 15 min at 4° C. The supernatant was removed and each pellet was resuspended with 2 ml cold TFB II buffer. Cells were aliquoted in 100 µl, snap frozen in liquid nitrogen and stored at -80° C. The newly made cells were checked for competency by transforming them with a test plasmid and calculating the colony forming units.

3.2 Biochemical techniques

3.2.1 SDS-polyacrylamide gel electrophoresis and Western Blotting

Preparation of 10 % Tris-glycine gels

Glass and porcelain plates were cleaned using ddH_2O and ethanol. The gel sandwich was assembled and placed into the caster. For 1 gel, a 10 % tris-glycine separating gel was prepared by mixing 2 ml 40 % polyacrylamide/bis-acylamide solution (37.5/1), 1.5 ml separating gel buffer (pH 8.9), 2.5 ml ddH_2O, 60 µl 10 % SDS, 25 µl 10 % APS and 5 µl TEMED in a 15 ml falcon tube. The separating gel was mixed well and poured into each gel sandwich (~ 4.5 ml per gel). To get a smooth surface, the gel was overlaid with isopropanol. After polymerization, the isopropanol was poured off. Then, the stacking gel was prepared using 334 µl 40 % polyacrylamide/bis-acylamide solution (37.5/1), 0.5 ml stacking gel buffer (pH 6.8), 1.1 ml ddH_2O, 20 µl 10 % SDS, 10 µl 10 % APS and 2.5 µl TEMED in a 15 ml falcon tube, mixed well and poured over the separating gel into the gel sandwich (~ 1.5 ml per gel). A comb was introduced avoiding any air bubbles and the gels were allowed to completely polymerize. Wrapped in moist tissues, they were stored at 4° C until use.

Electrophoresis

The electrophoresis tank with the gel sandwiches was set up and 1x SDS-PAGE running buffer was added in the upper and lower chamber. The gels were fixed with positioning clips and the combs were removed. Thawed protein samples were diluted in an appropriate volume of ddH_2O, 15 µl 5x SDS sample buffer was added and the samples were heated to 95° C for 5 min. After boiling, the samples were centrifuged 5 min at 21’000 g. 5 – 25 µl of protein samples were loaded alongside 4 µl of a protein standard marker. The gel was run for 1 h at 200 V.

Coomassie staining of protein gels

SDS-PAGE gels were stained with Coomassie for 5 to 60 min at room temperature on a rocker.

Destaining of protein gels

The Coomassie was poured off and replaced by tap water. Gels were allowed to destain overnight at room temperature on a rocker. Alternatively, gels were destained for 10 min using destaining solution.

Protein transfer

Gel sandwiches were dismantled and the stacking gel was cut off. Blot sandwiches were set up as follows in a tray filled with transfer buffer (from bottom to top): sandwich device (black side), 6 mm sponge, 3 MM Whatman paper, polyacrylamide gel, nitrocellulose membrane, 3 MM Whatman paper, 6 mm sponge and sandwich device (white side). Sponges, papers and membrane were pre-wet in transfer buffer. The transfer sandwich was placed into the blotting tank loaded with cold transfer buffer. Transfer was carried out at 100 V for 1 h.

Ponceau-S staining of blotted proteins

To test for proper transfer of proteins, membranes were stained with Ponceau-S for approximately 15 min on a rocker. Membranes were destained in tap water for 5 min.

Blot procedure

The membrane was transferred into a 50 ml Falcon tube and blocked with 10 ml blocking buffer rotating for 1 h at room temperature. The blocking solution was discarded and the first antibody diluted in 3 ml 1 % milk in PBS-T was added. After 1 h incubation at room temperature the first antibody was removed and the membrane washed twice for 5 min in 0.1 % milk in PBS-T. The second antibody diluted in 3 ml 1 % milk in PBS-T was added and incubated for 1 h at room temperature. The blot was washed 3 times for 5 min in wash buffer and rinsed with PBS. Blocking and incubation steps were alternatively carried out at 4° C overnight.

Antibody detection

The blot was dried on a tissue and placed on a polythene film. The enhanced chemo luminescence reagents were mixed 1:1 and applied to the blot covering the entire surface (0.5 ml per blot). After 1 min incubation the blot was dried again, wrapped in polythene film. The

blot was developed using the ChemiDoc XRS+ system (BioRad) using Image Lab ® software.

3.2.2 TCA precipitation

Proteins were precipitated by mixing 1 ml sample with 1 ml 20 % trichloroacetic acid. After incubation for 30 min at 4° C, the sample was centrifuged at 21'000 g for 5 min. The supernatant was removed and the pellet was washed twice with 200 µl ice-cold acetone. The pellet was air-dried and resuspended in 5x loading dye. The sample was boiled for 5 min at 95° C and centrifuged 5 min at 21'000 g before performing SDS-PAGE.

3.2.3 Solubility Assay

Plasmodium falciparum proteins were extracted using 0.03% saponin (Sigma) from a synchronized, late stage parasite culture (10 ml). Extraction was done sequentially: the lysate was resuspended in 100 µl ddH_2O, freeze-thawed 3 times (at -80° C or using liquid nitrogen) and centrifuged at 21'000 g for 5 min. The supernatant containing soluble proteins was transferred to a new tube. Hot (80° - 90° C) 5x loading dye was added to that fraction and subsequently frozen at -20° C. After the hypertonic lysis, the pellet was washed 3 times with 500 µl ddH_2O and twice with 100 µl PBS, then it was resuspended in 100 µl freshly prepared 0.1 M Na_2CO_3 and kept on ice for 30 min to extract peripheral membrane proteins. After incubation, the tube was centrifuged at 21'000 g for 5 min and the supernatant was transferred to a new tube. Hot (80° - 90° C) 5x loading dye was added to that fraction and subsequently frozen at -20° C. The pellet was washed 3 times with 500 µl PBS and extracted for 30 min with 100 µl 1% Triton X-100 and centrifuged at 21'000 g for 5 min to obtain the integral membrane protein fraction in the supernatant. The supernatant was transferred to a new tube and hot (80° - 90° C) 5x loading dye was added to that fraction and subsequently frozen at -20° C. The final pellet was washed once with PBS and resuspended in 100 µl PBS containing insoluble proteins. 5x loading dye was added to the pellet and boiled at 90° C for 5 min. After centrifugation for 5 min at 21'000 g, the tube was stored at -20° C. Equal amounts of all supernatants were analyzed by immunoblotting with adequate amounts of 5x SDS loading dye. Proteins were detected using anti-GFP antibodies, the cytosolic protein GAPDH was used as a control.

3.2.4 S-acyl biotin exchange assay (ABE)

Saponin lysed parasite pellets derived from 100 ml synchronized late stage parasites were subjected to biotin switch protocol as previously described (Wan et al., 2007; Jones et al., 2012; Cabrera et al., 2012). Saponin-lysed pellets were washed 3x with PBS and 1x with ice-cold LB buffer centrifuging each time at 21'000 g for 1 min (pool pellets while washing). The supernatant was removed, 100 µl protease inhibitors were added, resuspended and all pellets were pooled in 900 µl ice-cold LB buffer (in one 2 ml eppendorf tube). The parasite mixture was 3x freeze-thawed at -80° C (or liquid N_2) to break cells and further disrupted passing through a 27G needle coupled to a 1 ml syringe. 1 ml of ice-cold LB buffer with 20 mM NEM (N-ethylmaleimide) and 3.4 % TX-100 was added and tubes were incubated under rotation for 1 h at 4° C. The lysate was split into 140 µl aliquots and chloroform/methanol precipitate (Wessel Flügge method) was performed. 35 µl 4 SB buffer with 10 mM NEM was added to the pellets and placed at 37° C shacking on a thermomixer (Eppendorf) at 1400 rpm until the pellet is fully re-solubilized. 105 µl of LB with 1 mM NEM, 0.2 % TX-100 and protease inhibitors was added, mixed and incubated overnight at 4° C with rotation. NEM was removed by 3x chloroform/MeOH precipitation (first 2x add 35 µl 4 SB buffer, incubate at 37° C shaking until fully re-solubilized, then add 105 µl LB + 0.2 % TX-100). After the third chloroform/methanol precipitation the pellet was resuspended in 35 µl 4 SB buffer and the parasite material was pooled when fully re-solubilized and vortexed. The samples were split into 30 µl aliquots and 120 µl + hydroxylamine buffer was added to half of the tubes and 120 µl – hydroxylamine buffer was added to the other half of the samples. Tubes were incubated 1 – 2 h at RT under rotation. Then, all proteins were chloroform/methanol precipitated. Pellets were resuspend in 30 µl 4 SB and fully solubilized. 120 µl low-biotin-BMCC buffer was added to all samples and incubated for 1 – 2 h at RT under rotation. All proteins were 3x chloroform/methanol precipitated (first 2x resuspend in 35 µl 4 SB buffer, incubate at 37° C until is fully re-solubilized and then add 105 µl LB with 0.2 % TX-100). The final pellet was resuspended in 35 µl 4 SB buffer and diluted in SDS to 0.1 % by addition of 665 µl LB with 0.2 % TX-100 and protease inhibitors. Samples were incubated at room temperature for 30 min under rotation. Afterwards, tubes were spun at 21'000 g for 1 – 2 min. One of each tubes (both – and + hydroxylamine) were set aside as loading controls and subject to TCA precipitation. The rest like samples were pooled in 15 ml tubes. 15 µl washed NeutrAvidin resin per ml of sample were added and rotated at RT for 1.5 – 2 h (or overnight at 4° C). Beads were pelleted by centrifugation at 21'000 g for 5 min. Beads were washed 4x with 5 ml LB with 0.1 % SDS and 0.2 % TX-100 and incubate 10 min each time.

Wessel Flügge method for precipitation of proteins
To each 140 µl protein aliquot add:
560 µl methanol
210 µl chloroform
420 µl water
Vortex and spin 2 min at full speed at room temperature
Remove supernatant
Add 420 µl methanol
Invert tube carefully 2-3 times and spin 2 min at full speed at room temperature
Remove supernatant and allow pellet to dry for 10-15 min in hood

3.2.5 NP-40 extraction of proteins

NP-40 extraction was achieved by re-suspending a saponin-lysed parasite pellet from a 10 ml dish in 1 ml TBS (50 mM Tris-HCl, pH 7.5; 150 mM NaCl) containing 0.05 % NP-40 and complete protease inhibitors (Roche) for 15 minutes at 4° C. After centrifugation (5 min at 21'000 g) equivalent amounts of supernatant and pellet fractions were resolved on 10 % SDS-PAGE, transferred to nitrocellulose membrane and blotted using mouse anti-GFP (Roche) and rat anti-mCherry antibodies (Chromotek).

3.3 Cellular biology techniques

3.3.1 Parasite culture

Plasmodium falciparum parasites (strain 3D7) were cultured in human O+ erythrocytes according to the protocol of Trager and Jensen (Trager and Jensen, 1976). Cultures were incubated at 37º C in air-sealed desiccators after flushing for about 30 sec with a gas mixture consisting of 94 % N_2, 5 % CO_2 and 1 % O_2. *Plasmodium falciparum*-infected erythrocytes derived from a previously established culture. The parasites were kept at 5 % haematocrit. Culture medium was changed daily or every second day depending on the parasitaemia by gently holding the dish aslope without disturbing settled cells and aspirating the medium with a Pasteur pipette. Fresh medium (pre-warmed in 37º C water bath) and the required drugs

were added before gently resuspending the cells. The parasitaemia was adjusted to suit experimental requirements by splitting or diluting the cultures.

Generation of gametocytes

Gametocytes were produced using a modified version of the established protocol (Fivelman et al., 2007; Kono et al., 2012). Gametocytogenesis was induced by starving parasite cultures by only removing 2/3 of media, leaving 1/3 of used media in the petri dish. The cultures were fed this way every day for approximately 10 days.

3.3.2 Parasite staining

Preparation of blood smears

To estimate the parasitaemia, 200 µl of a resuspended culture were shortly pelleted in a tabletop centrifuge and the medium was removed. 2.5 µl of the pellet was pipetted onto a glass slide and smeared along the surface using a spreader. Alternatively, 1 µl of settled erythrocytes were directly taken from the dish and smeared.

Giemsa staining

The blood film was dried and fixed by dipping the slide into methanol for a few seconds. The slide was then stained for 20 min in Giemsa solution. Microscopy was carried out (using oil immersion) at a magnification of 100x using a Zeiss AXIO Scope.A1 light microscope. 400 RBCs were counted and the percentage of infected cells determined.

3.3.3 Synchronization of parasite growth

Growth of intraerythrocytic *Plasmodium falciparum* parasites can be synchronized using treatment with D-Sorbitol. Only uninfected RBCs and RBCs infected with ring-stage parasites survive this treatment whereas trophozoite- and schizont-infected cells are destroyed by osmotic lysis (Lambros and Vanderberg, 1979).

RBCs were centrifuged at 450 g for 5 min. The supernatant was removed; the pellet was resuspended in six pellet volumes of a pre-warmed 5 % sorbitol solution and incubated in a 37º C water bath for 10 min. After centrifugation for 5 min at 450 g, the pellet with the

surviving ring stage parasites and non-infected erythrocytes was resuspended in the original volume using pre-warmed culture medium, and placed in a new dish. To obtain a tight synchronisation, the procedure was repeated after 36 h.

3.3.4 Freezing parasite stabilates

9 ml of a culture of minimally 3 % ring stage parasites were centrifuged at 450 g for 5 min. The culture supernatant was removed and the erythrocyte pellet resuspended in 1 ml freezing solution. The resuspended parasites were transferred to a Cryo tube and subsequently frozen in liquid nitrogen.

3.3.5 Thawing parasite stabilates

The frozen vial was thawed rapidly by agitation in a 37° C water bath (ca. 2 min) and the solution was transferred to a 10 ml Falcon tube. An equal volume of pre-warmed thawing solution was added, mixed and centrifuged for 2 min at 450 g. The supernatant was discarded and the parasites were washed once in thawing solution. The erythrocyte pellet was resuspended in fresh medium containing 4 % erythrocytes and put into a 10 ml dish. Parasitaemia was checked after two days.

3.3.6 Transfection of *Plasmodium falciparum* parasites

Transfection of parasites was carried out as previously described (Fidock and Wellems, 1997). 5 ml of synchronized 3D7 parasite culture containing at least 10 % RBCs infected with young ring stages were centrifuged for 5 min at 450 g. The erythrocyte pellet was then mixed with DNA/cytomix and transferred to a 2 mm electroporation cuvette (BioRad). The cells were electroporated using single exponential (310 V, 950 µF, ∞ Ω) conditions. Transfected parasites were immediately transferred into a culture dish containing 300 µl fresh erythrocytes in 10 ml of pre-warmed complete culture medium. Parasites were grown for about 4 – 8 hours before exchanging the medium and applying blasticidin-S (BSD) pressure and/or WR99210 (10 nM WR99210 and 30 nM blasticidin final concentrations) depending on the selectable marker gene on the plasmid. For the following ten days, medium and drug were exchanged daily and afterwards every second day. All transfected plasmids contained a selectable marker gene, either the blasticidin-S deaminase gene, conferring resistance to BSD-S-HCl, or the human dihydrofolate reductase (h*dhfr*) gene, which compensates the function of the

endogenous dihydrofolate reductase blocked by the antifolate WR99210. Parasites were maintained as described below under permanent BSD and/or WR pressure until the population reached a parasitaemia suitable for freezing parasite stabilates and further experiments. This usually took about 3 to 4 weeks. Then the amount of BSD was increased to up to 20 µl per 10 ml culture to select for parasites carrying increased plasmid copy numbers (Epp et al., 2008).

Generation of double transgenic parasite cell lines

Double transfectant parasites expressing PF14_0578-mCherry and PFC0160w-GFP were generated by transfecting 100 µg of pB-PF14_0578-mCherry into the stable transgenic cell line expression 3D7-PFC0160w-GFP. Double transfectant parasites expressing PF11_0167-mCherry and PfARO-GFP were generated by transfecting 100 µg of pB-PF11_0167-mCherry into the established cell line PfARO-GFP (Cabrera et al., 2012). Double transfectant parasites expressing PF14_0578-mCherry and PF10_0107-GFP were generated by transfecting 100 µg of pB-PF14_0578-mCherry into the stable transgenic cell line expression 3D7-PF10_0107-GFP.

Selection for plasmid integration into the endogenous locus (3' replacement)

3D7 parasites expressing endogenous PfISPs and PfPATs as a GFP-fusion protein were generated by 3' replacement. To achieve this, the last 1 kb of the coding region of the respective gene (excluding the stop codon) were amplified from 3D7 gDNA and cloned in the *Not*I and *Avr*II restriction sites of the transfection vector pARL-1a-GFP (Struck et al., 2005). *Not*I/*Avr*II restriction digest released the *ama1* promoter in this vector and replaced it with the 3' end of the targeted gene. Therefore, integration of this vector by homologue recombination leads to GFP-tagged gene products. In order to select for the integration of vectors into the genome by single crossover recombination, the plasmid was transfected into *P. falciparum* 3D7 parasites as described above. When the parasites reached a parasitaemia suitable for freezing, parasites were grown for 4 weeks without drug pressure. During this time, the culture was regularly fed and diluted. After these four weeks, the parasites were re-challenged with WR until they showed normal growth. This "ON-and-OFF" cycle was repeated until integration was confirmed by PCR, microscopy and Western Blot. During growth in absence of drug pressure parasites tend to loose their episomally maintained plasmids (Wu et al., 1995). Therefore, re-challenging with WR selects for an enrichment of parasites carrying integrated plasmids.

3.3.7 Isolation of parasite proteins

Saponin lysis

10 ml late stage parasite culture (5 % haematocrit and 5 to 10 % parasitaemia) was centrifuged at 450 g for 5 min. The erythrocyte pellet was resuspended in 5 ml 0.03 % saponin in 1x PBS and incubated for 10 min on ice. After spinning the parasites down for 5 min at 21'000 g and removing the supernatant, the parasite pellet was resuspended in 1 ml 1x PBS, transferred to an Eppendorf tube and washed 3 times in 1 ml PBS or until the supernatant was clear.

3.3.8 Life cell imaging by fluorescence microscopy

Transfected parasite cultures were analysed by live cell imaging. 500 µl resuspended culture at a parasitaemia of approximately 5 % were transferred into an Eppendorf tube. 0.5 µl DAPI (200 µg/ml) was added to stain the nuclei. The samples were incubated at 37° C for 10 min. 8 µl of settled cells were pipetted directly onto a glass slide and covered with a cover slip. Images were taken on a Zeiss Axioskop 2plus microscope with a Hamamatsu Digital camera (Model C4742-95, Zeiss axiovision) using a 100x oil immersion objective. Cells were visualized with a DIC filter. The DAPI-stained parasite nuclei (blue), mCherry signals (red), and GFP signals (green) were photographed.

Fluorescence or dye	Excitation	Emission
mCherry	587 nm	610 nm (red)
DAPI	360 nm (UV)	460 nm (blue)
GFP	395 nm	509 nm (green)

3.3.9 Immunofluorescence assay (IFA)

Formaldehyde / glutaraldehyde fixation

1.5 ml resuspended parasite culture was transferred into an Eppendorf tube and centrifuged at 450 g for 5 min. The supernatant was removed and the pellet was resuspended and washed in 1 ml 1x PBS and centrifuged at 450 g for 5 min. The supernatant was removed and the pellet was resuspended in 5 ml freshly made fixation buffer. After 30 min rotating incubation at room temperature the erythrocytes were centrifuged at 450 g for 1 min and the fixation buffer was removed. The pellet was washed with 1 ml 1x PBS until the supernatant was red, then the

cells were permeabilized in 1 ml 0.1 % TX-100 in 1x PBS under rotation for 10 min at room temperature. After centrifugation at 3400 g for 1 min, the supernatant was removed and the pellet was washed twice with 1 ml 1x PBS. Then, the erythrocytes were resuspended in 1 ml blocking buffer (3 % BSA in 1x PBS) and incubated for 1 h at room temperature. Afterwards the erythrocytes were centrifuged at 3400 g for 1 min, the supernatant was removed and the pellet was resuspended in 500 µl of the primary antibodies diluted in blocking buffer and incubated 1 h at room temperature. The erythrocytes were centrifuged at 3400 g for 1 min and washed three times with 1 ml 1x PBS. Cells were resuspended in 500 µl of the secondary fluorescently labeled antibodies diluted in blocking buffer and incubated for 1 h at room temperature. After centrifugation cells were washed three times with 1 ml 1x PBS. For the last wash, the PBS was supplemented with 0.5 µl DAPI and the cells were incubated under rotation for 10 min. The supernatant was removed, but leaving about in 50 µl the tube for resuspension of the parasite pellet. 8 µl of this suspension were transferred onto a glass slide. A cover slip was gently placed on top and sealed with nail polish. The slides were stored up to two days in the dark at 4° C. All incubation steps carried out for 1 h at room temperature could be carried out as well at 4° C overnight. Images were taken on a Zeiss Axioskop 2plus microscope with a Hamamatsu Digital camera (Model C4742-95, Zeiss axiovision) using a 100x oil immersion objective. Cells were visualized with a DIC filter.

Methanol fixation

Thin blood smears were performed on glass slides by using 3 µl of resuspended parasite culture. The slides were air-dried and then fixed for 2 min in pre-cooled (-20° C) 100 % methanol. The slides were air-dried again and wells were prepared with a hydrophobic pen (diameter ≈ 1 cm). The wells were washed with 1x PBS for 10 min at room temperature in a humidified chamber. After removing the 1x PBS from the wells, 50 µl of the first antibody diluted in 1 % BSA in 1x PBS (sterile filtered) were added an incubated for 30 min at room temperature in a humidified chamber. Then the wells were washed three times for 5 min with 1x PBS. After the slides were dried partially, 50 µl of the secondary (fluorescently labeled) antibody diluted in 1 % BSA were added and incubated for 30 min in a humidified chamber in the dark. The wells were washed again three times for 5 min with 1x PBS and then completely dried. After adding 0.5 µl DAPI (1 µg/ml), a cover slip was added and sealed with nail polish. Images were generated as described above.

3.3.10 Isolation and purification of *Plasmodium falciparum* gDNA

10 ml parasite culture containing a parasitaemia of 3 – 5 % late stage parasites were centrifuged 5 min at 450 g. The supernatant was removed and the iRBCs were lysed with 1 ml 0.03 % saponin and incubated on ice for 10 min. After centrifugation for 5 min at 21'000 g, the parasite pellet was resuspended in cold PBS and transferred to an Eppendorf tube and centrifuged for 1 min at 21'000 g. The parasites were again washed in 1 ml PBS. The parasite pellet was resuspended in 300 µl buffer A. 150 µl 10% SDS were added and mixed well by vortexing. After incubation for 10 min at room temperature, the DNA was extracted by adding 450 µl phenol:chloroform and repeatedly inverting the tube for 1 min. After 5 min of centrifugation at 21'000 g, the upper aqueous phase was transferred to a new tube. 400 µl chloroform was added and the tube was repeatedly inverted for 15 sec. After a further centrifugation step at 21'000 g, the aqueous phase was transferred to a new tube and the DNA precipitated for 1 h on ice after addition of 1 ml 100 % EtOH. After centrifugation for 20 min at 21'000 g, the supernatant was removed and the pellet was washed with 500 µl 70 % EtOH. The tube was centrifuged for 5 min at 21'00 g and the supernatant was completely removed. The DNA pellet was air dried and dissolved in 50 µl TE buffer. 3 µl were analyzed by agarose gel electrophoresis.

4. Results

4.1. Identification of an inner membrane complex (IMC) localized palmitoyl acyltransferase (PAT) in *Plasmodium falciparum*

Putative PfDHHC PATs were identified by BLAST search (www.plasmodb.org) using the conserved DHHC sequence motif. 12 putative PATs with a conserved DHHC region were identified and are summarized in Table 4.1.

Table 4.1 List of *P. falciparum* DHHC proteins. Studied proteins are highlighted in grey. Additional late transcribed PATs that are not part of this thesis are marked in a lighter shade of grey.

Name	Gene ID	Coding sequence (bp)	Molecular weight (kDa)	Protein identity, predicted domain	Signal peptide (SP) Transmembrane domain (TMDs)
DHHC1	PFC01060w	1851	73.8	Palmitoyl transferase, ankyrin repeats	5 TMDs
DHHC2	PFF0485c	855	33.1	putative DHHC-type zinc finger protein	4 TMDs
DHHC3	PF11_0217	882	34.8	putative DHHC-type zinc finger protein	4 TMDs
DHHC4	MAL7P1.68	3966	158.7	putative DHHC-type zinc finger protein	4 TMDs
DHHC5	MAL13P1.126	2031	80.8	putative DHHC-type zinc finger protein, ankyrin repeats	8 TMDs
DHHC6	PFI1580c	1662	67	putative DHHC-type zinc finger protein	4 TMDs, 2 SP
DHHC7	PFE1415w	1221	48.2	putative DHHC-type zinc finger protein	4 TMDs
DHHC8	MAL13P1.117	942	36.5	putative DHHC-type zinc finger protein	4 TMDs
DHHC9	PF11_0167	882	34.7	putative DHHC-type zinc finger protein	4 TMDs, 2 SP
DHHC10	PF10_0273	813	33.8	putative DHHC-type zinc finger protein	4 TMDs
DHHC11	PFB0720c	783	30.8	putative DHHC-type zinc finger protein	4 TMDs, 2 SP
DHHC12	PFB0140w	801	34.8	putative DHHC-type zinc finger protein, prokaryotic membrane lipoprotein lipid attachment site profile	5 TMDs

Since all IMC proteins are exclusively upregulated in late parasite stages, the transcriptional profiles of the PATs were analyzed to identify PATs that have a similar expression and might be localized to the IMC. Analysis of the transcriptional profiles and available mass

spectrometry data showed that six PATs are upregulated in late parasite stages: PfDHHC1, PfDHHC2, PfDHHC3, PfDHHC5, PfDHHC7 and PfDHHC9 (Tab. 4.1). However, only PfDHHC1, PfDHHC2, PfDHHC3, and PfDHHC9 are homologues of the IMC PATs in *P. berghei* and *T. gondii* (Frénal et al., 2013; see below, 4.1.1).

4.1.1 Overexpression of late transcribed PATs

To analyze the localization of the four putative IMC PATs in *P. falciparum* PfDHHC1 (PFC0160w), PfDHHC2 (PFF0485c), DHHC3 (PF11_0217), and PfDHHC9 (PF11_0167) were cloned into the transfection vectors pARL-GFP (Treeck et al., 2006) or pBcam-mCherry (Flueck et al., 2010), circumventing internal restrictions sites in the genes of interest. Constructs were transfected into *P. falciparum* 3D7 wild type parasites. The pARL-GFP vector contains an h*dhfr* resistance cassette to select for parasites that contain the plasmid by adding the drug WR99210. The pBama-mCherry contains a *bsd* resistance cassette, which allows the selection for transfected parasites by adding the drug blasticidin-S-HCl. To mimic the late transcription of the genes of interest, in both plasmids the *ama1* promoter was used (Bozdech et al., 2003). All constructs were sequenced to confirm the absence of any mutations and gene identity.

PfDHHC1 (PFC0106w) is located on chromosome 3, has a size of 1851 basepairs (bp) (molecular weight (MW): 73.8 kilo Dalton (kDa)) and is expressed at high levels in trophozoites and schizonts. It has 8 introns, no signal peptide and 5 transmembrane domains (Tab. 4.1). Peptides corresponding to the gene were detected by mass spectrometry in salivary gland sporozoites. The protein has 2 annotated domains: zf-DHHC palmitoyl acyltransferase domain (predicted by PFAM, E-value: 7.00 E-33) and ankyrin repeats (predicted by SUPERFAMILY, E-value: 2.80 E-35). The PfDHHC1 homologue has been localized to the IMC in *Toxoplasma gondii* (Beck et al., 2013; Frénal et al., 2013).

PfDHHC2 (PFF0485c) is a putative DHHC-type zinc finger protein. The gene is located on chromosome 6 and a size of 855 bp (MW: 33.1 kDa) (Tab. 4.1). It has 4 introns, no signal peptide, and 4 transmembrane domains. Peptides corresponding to that gene were detected by mass spectrometry in ring, schizont and salivary gland sporozoite stage parasites. The expression levels show an upregulation of gene expression in late stage parasites. The protein has 1 annotated domain: zf-DHHC palmitoyl acyltransferase domain (predicted by PFAM, E-

value: 2.30 E-36). PfDHHC2 homologue has been localized to the IMC in *T. gondii* (Frénal et al., 2013).

PfDHHC3 (PF11_0217) is located on chromosome 11, has a size of 882 bp (MW: 34.8 kDa) It has 6 introns, no signal peptide, and 4 transmembrane domains (Tab. 4.1) and is expressed during asexual proliferation with an increased level in late trophozoite and schizont parasite stages, as well as in stage V gametocytes and sporozoites. Peptides corresponding to the gene were detected by mass spectrometry in schizonts and salivary gland sporozoites. The protein has 1 annotated domain: zf-DHHC palmitoyl acyltransferase domain (predicted by PFAM, E-value: 4.80 E-29). The PfDHHC3 homologue has been localized to the plasma membrane in *T. gondii* and to the IMC in *P. berghei* (Frénal et al., 2013).

PfDHHC9 (PF11_0167) is is located on chromosome 11 and has a size of 882 bp (MW: 34.7 kDa) (Tab. 4.1). It harbors 12 introns, 2 signal peptides, 4 transmembrane domains and is highly expressed in late schizont stages and sporozoites. Peptides corresponding to the gene were detected by mass spectrometry in salivary gland sporozoites. The protein has 1 annotated domain: zf-DHHC palmitoyl acyltransferase domain (predicted by PFAM, E-value: 5.40 E-37). The homologue has not been localized in *T. gondii,* but shows IMC localization in *P. berghei* (Frénal et al., 2013).

Localization of the fusion proteins revealed that only PfDHHC1-GFP has a localization pattern, resembling the IMC and shows the IMC-typical dynamics during schizogony (Hu et al., 2010; Yeoman et al., 2011; Ridzuan et al., 2012; Kono et al., 2012): it commences as cramp-like structures (T1), transforming to small ring-shaped formations (T2) that towards the end of schizogony expand (T3) and are then equally distributed underneath the plasma membrane (PM) (Fig. 4.1A). The localization patterns of the other over-expressed PATs are distinct and resemble other membrane systems such as the endoplasmic reticulum (ER) (PfDHHC2-GFP, Fig. 4.1B), the PM (PfDHHC3-mCherry, Fig. 4.1C) and the apical organelles (PfDHHC9-mCherry, Fig. 4.1D).

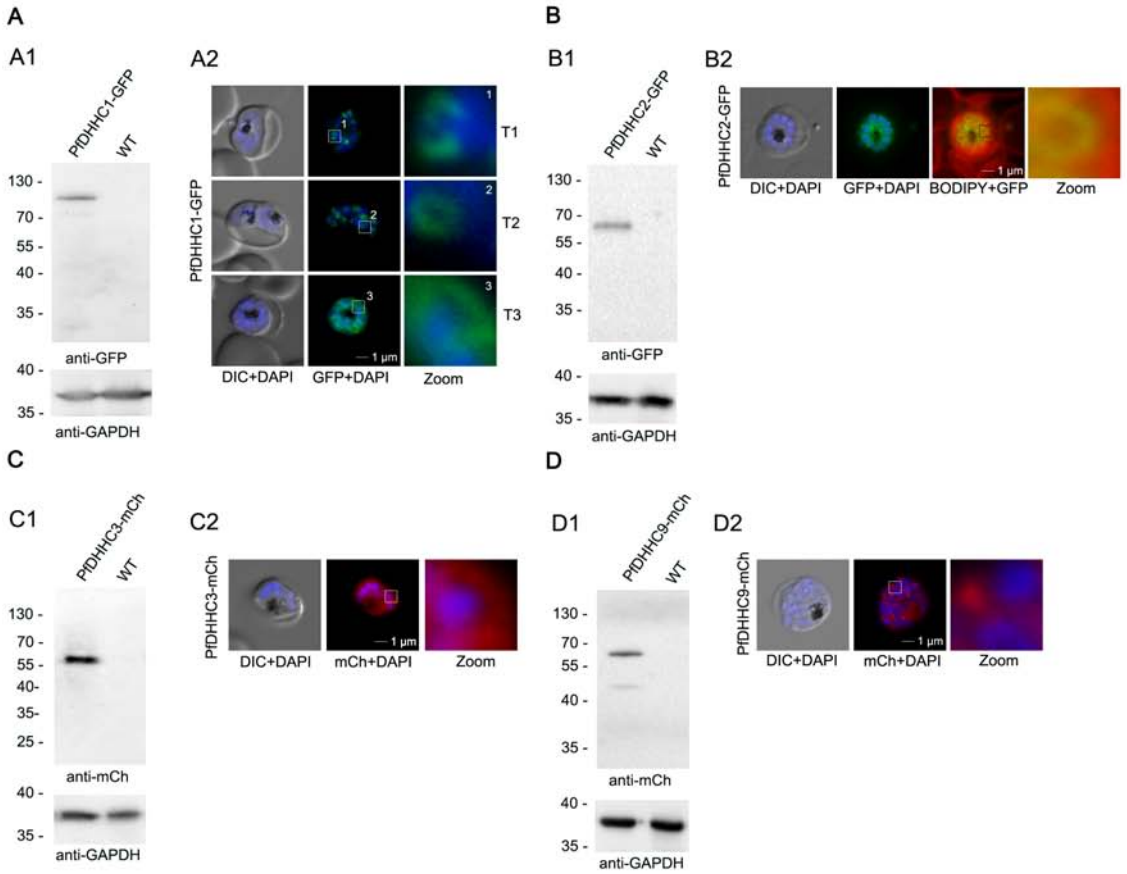

Figure 4.1 Over-expression and localization of PfDHHC1 (PFC0160w), PfDHHC2 (PFF0485c), PfDHHC3 (PF11_0217) and PFDHHC9 (PF11_0167) in late stage parasites. A. Expression of PfDHHC1-GFP. A1. Western blot analysis using anti-GFP antibodies. A single protein band of about 100 kDa (expected MW: 100 kDa) was detected in the transgenic but not in the parental parasite line. A2. Localization of PfDHHC1-GFP in unfixed parasites showing characteristic IMC dynamics during schizogony. Nuclei are stained with DAPI (blue). Enlargement of selected areas are marked with a white square and referred to as zoom. **B.** Expression of PfDHHC2-GFP. B1. Western blot revealed a 65 kDa (expected MW: 59 kDa) protein band detected by anti-GFP antibodies in the transgenic cell line but not in the control. B2. Live microscopy of PfDHHC2-GFP revealed a circular structure around the nucleus of the nascent merozoites reminiscent of the ER. **C.** Expression of PfDHHC3-mCherry. C1. Western blot analysis with anti-mCherry antibody detected a 60 kDa (expected MW: 61 kDa) protein with some degraded protein at about 45 kDa. C2. Microscopic analysis located this GFP-fusion protein in the periphery of the nascent merozoites consistent with PM localization. **D.** Expression of PfDHHC9-mCherry. D1. Expression leads to 65 kDa protein (expected MW: 61 kDa) detected in Western blot analysis using mCherry antibodies. D2. Microscopy localized this fusion protein mainly in apical structures in the parasite. Scale bars, 1 µm.

To further confirm the IMC localization of DHHC1 all proteins were co-localized with the IMC marker glideosome-associated protein with multiple membrane spans 2 (GAPM2; PFD1110w; Kono et al., 2012) in immunfluorescence assays (IFAs) (Fig. 4.2). Only PfDHHC1 showed co-localization in schizont stage parasites (Fig. 4.2A), whereas all other PfPATs did not co-localize with the IMC marker (data not shown).

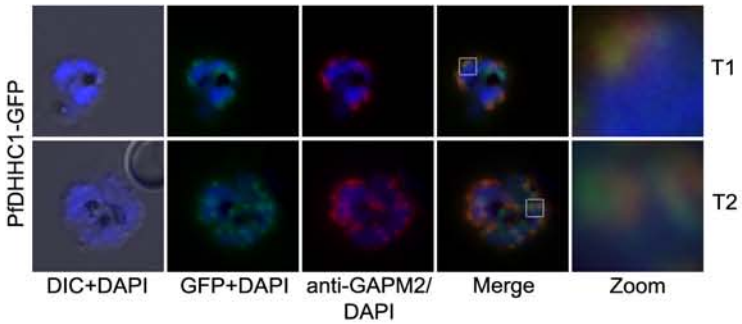

Figure 4.2 Co-localization of PfDHHC1 with the IMC marker GAPM2 in IFAs. Parasites were fixed and incubated with GAPM2-specific antibodies. Localization of PfDHHC1-GFP with GAPM2 in fixed parasites showing characteristic IMC dynamics during schizogony. Nuclei are stained with DAPI (blue). Enlargement of selected areas are marked with a white square and referred to as zoom. Scale bars, 1 µm.

4.1.2 PfDHHC1 is an IMC localized PAT

To confirm the IMC localization of PfDHHC1, the endogenous gene was tagged with GFP (Fig. 4.3). Approximately 1 kb of the very 3' end of the corresponding coding sequence was amplified by PCR, digested with restriction enzymes, purified, and ligated in frame with the GFP tag in the pARL-GFP vector. The *ama1* promoter was replaced by the respective 3' end of the investigated gene. Hence, in absence of a promoter and ATG start codon protein expression can only be visualized after integration of the plasmid into the endogenous locus. This integration event reconstitutes the locus with a gene carrying an in-frame epitope or *gfp* tag at the 3' end (3' replacement, Fig. 4.3A). Importantly, the respective gene locus is still under control of the endogenous promoter. To promote integration of the plasmid the parasites were grown under drug pressure until a resistant population was established. This was followed by four weeks parasite growth without drug. Thereafter, the parasites were re-challenged with WR until they showed normal growth. This "ON-and-OFF" cycle was repeated three times. During growth in absence of drug pressure parasites tend to loose their episomally maintained plasmids leading to an enrichment of parasites carrying plasmids integrated into the genome. Appropriate plasmid integration into the PfDHHC1 locus was shown by PCR (Fig. 4.3B) and expression of the fusion protein was verified by Western blotting (Fig. 4.3C). Stage specific expression was analyzed using tightly synchronized parasite material, which confirmed expression of PfDHHC1 in late stage parasites only (Fig. 4.3D). Microscopy of endogenously tagged PfDHHC1 confirmed IMC localization with its distinct biogenesis during schizogony (Fig. 4.3E). Importantly, the endogenously tagged

PfDHHC1 shows an identical distribution and dynamic like the episomally expressed counterpart (please refer to Fig. 4.1) and again is indicative for an IMC localized protein.

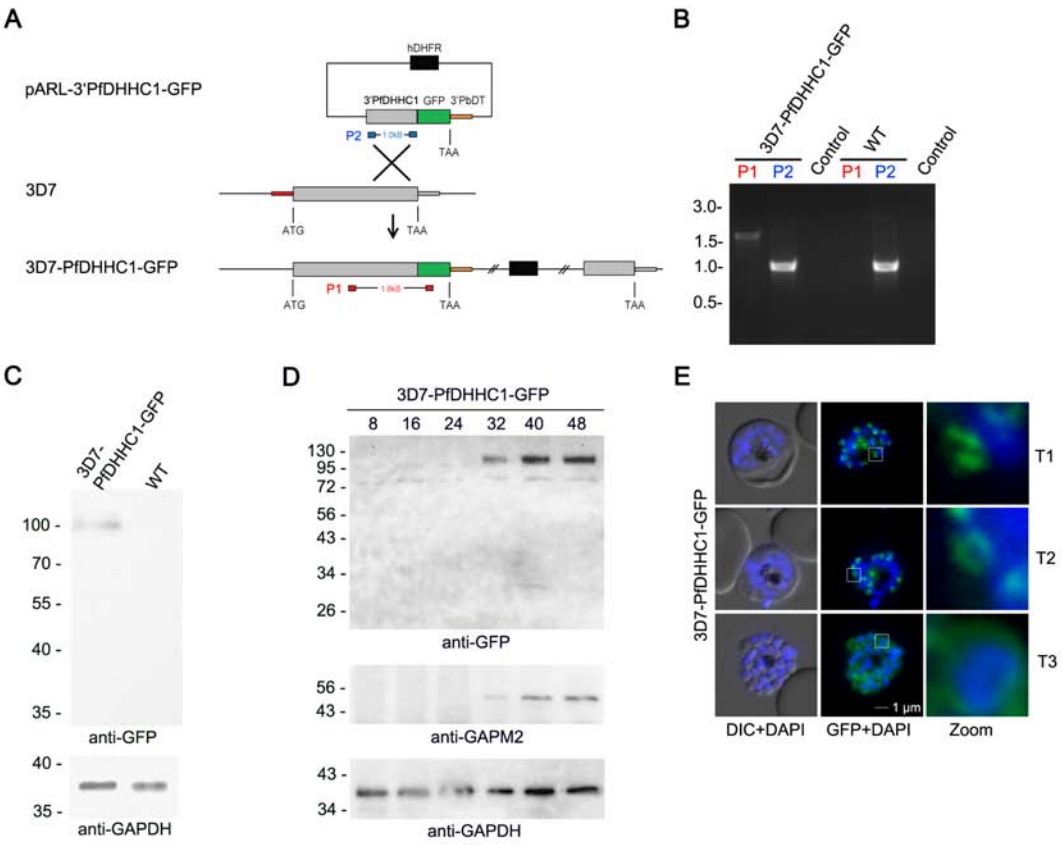

Figure 4.3 PfDHHC1 is an IMC localized palmitoyl acyltransferase. A. Schematic representation of the GFP replacement of the endogenous 3'end of PfDHHC1 creating a 3D7-PfDHHC1-GFP cell line. The vector encompasses the selection cassette (black), 1 kb of the PfDHHC1 gene (grey) was fused to GFP (green) accompanied by the 3'UTR of *Pb*DT (orange) without any promoter. Integration of the vector takes place by homologous recombination (cross) into the PfDHHC1 locus creating a full-length PfDHHC1-GFP fusion under the control of the endogenous promoter. **B.** Integration was confirmed by PCR using two different primer combinations on gDNA. One primer set (red) hybridizes in a PfDHHC1 region upstream of the integration and in the coding region of GFP. This primer combination can only amplify a 1.7 kb DNA fragment after recombination took place. The other set (blue) amplifies 1.1 kb of PfDHHC1 in the parental as well as in the transgenic parasite line. Control indicates PCRs with the red primer set in the absence of parasite DNA. **C.** Expression of the transgene from the endogenous locus was shown by Western blot analysis using anti-GFP antibodies (upper panel) resulting in a fusion protein of approximately 100 kDa (calculated molecular weight 100 kDa). Anti-GAPDH was used as a loading control. **D.** Stage-specific Western blot analysis of 3D7-PfDHHC1-GFP expression. Parasites were synchronized with an 8-hour timeframe and harvested during the following life cycle at 8, 16, 24, 36, 40 and 48 hours post invasion. Membranes were probed with anti-GFP. Stage-specific control: anti-GAPM2. Loading control: anti-GAPDH. **E.** PfDHHC1-GFP was localized in unfixed late stage parasites showing characteristic IMC dynamics during schizogony (T1-T3). Nuclei were stained with DAPI (blue). Enlargement of selected areas are marked with a white square and referred to as zoom. Scale bar, 1 µm.

In order to analyze expression and distribution of PfDHHC1 in pre-sexual stages, gametocytogenesis was induced with a starvation assay (please refer to 3.3.1). In pre-sexual gametocyte stages (Fig. 4.4) PfDHHC1-GFP is not equally distributed within the nascent IMC but accumulates in transversal structures resembling the symmetric meshwork enclosing the gametocyte previously described as the localization of the *Plasmodium*-specific IMC protein MAL13P1.228 (Kono et al., 2012) reflecting the sutures of individual IMC plates (Meszoely et al., 1987).

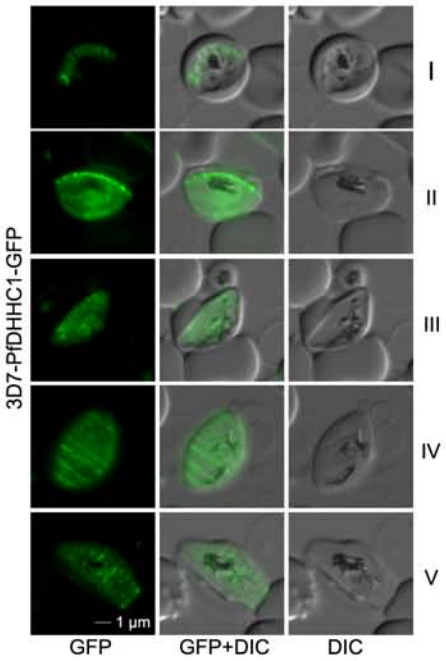

Figure 4.4 PfDHHC1-GFP distribution within the nascent IMC during gametocytogenesis. These symmetric sutures are expanding with ongoing maturation of the gametes (stage I-V). Scale bar, 1 µm.

4.1.3 Co-localization of PfDHHC1 with the IMC protein PfISP3

PfISP3 (PF14_0578) is an inner membrane complex protein (Hu et al., 2010) and categorized as a group A IMC protein (Kono et al., 2012). It is located on chromosome 14 and has a size of 447 bp (MW: 17.1 kDa). It has no introns and neither a predicted signal peptide nor a transmembrane domain. Expression levels of this protein are high in schizont stage parasites. PfISP3-peptides were detected by mass spectrometry in trophozoites, schizonts, merozoites, gametocytes, oocytes and salivary gland sporozoites. PfISP3 is phosphorylated at serine 16 (www.plasmodb.org). PfISP3 is the homologue of TgISP3 (Beck et al., 2010). Most importantly, PfISP3 is predicted to be myristoylated (score: 0.645, predicted by NMT) and palmitoylated (Cys 5, score: 2.167; Cys 6, score 1.49; Cys 145, score 1.058; predicted by

CSS-Palm version 3.0) and displays a similar N-terminal amino acid sequence as PfISP1 (Hu et al., 2010, Kono et al., 2012; Cabrera et al.; 2012 Jones et al., 2012).

PfISP3-mCherry was previously cloned and obtained from Dr. Maya Kono (Gilberger laboratory, BNITM, Hamburg). This chimeric gene was cloned into the pBcam vector (Flueck et al., 2010). The plasmid was transfected into 3D7-PfDHHC1-GFP parasites and selected with blasticidin-S-HCl. Co-localization of PfDHHC1-GFP with PfISP3-mCherry revealed identical dynamics of these two proteins (Fig. 4.5A), which would be congruent with a potentially specific interaction of these proteins.

4.1.4 Co-localization of PfDHHC1 with the *trans*-ER (tER) marker Sec13p

Previous work based on antibodies localized PfDHHC1 to the Golgi complex (Seydel et al., 2005). RNA expression profile, stage-specific Western blot analysis (Fig. 4.3D) and live microscopy (Fig. 4.1A and Fig. 4.3E) argued against this localization. Nevertheless, PfDHHC1 was co-localized with the tER marker Sec13p that resides in close proximity to the *cis*-side of the Golgi (Struck et al., 2008). To achieve this, the 3D7-PfDHHC1-GFP cell line was transfected with Sec13-dsRed plasmids. Sec13-dsRed was previously cloned by Dr. Susann Herrmann (Gilberger laboratory, McMaster University, Canada) fusing the N-terminal part of Sec13p with the sequence encoding *Discosoma* red fluorescent protein (dsRed.). The chimeric gene is driven by the constitutive *crt* promotor and the plasmid contains a *bsd* resistance cassette. Co-localization studies of the two proteins revealed their distinct dynamics (Fig. 4.5B). PfSec13p is localized to distinct regions during parasite development: in ring stage parasites, the protein is visible as a single dot close to the parasite's nucleus, which starts multiplying before the onset of nuclear division (Fig. 4B; Struck et al., 2008). During schizogony, the tER further multiplies, showing similar dynamics to Golgi complex multiplication (Struck et al., 2008). Shortly before newly formed merozoites are released from the erythrocyte, the tER is visible as a single dot per nucleus (Fig. 4B, bottom panel).

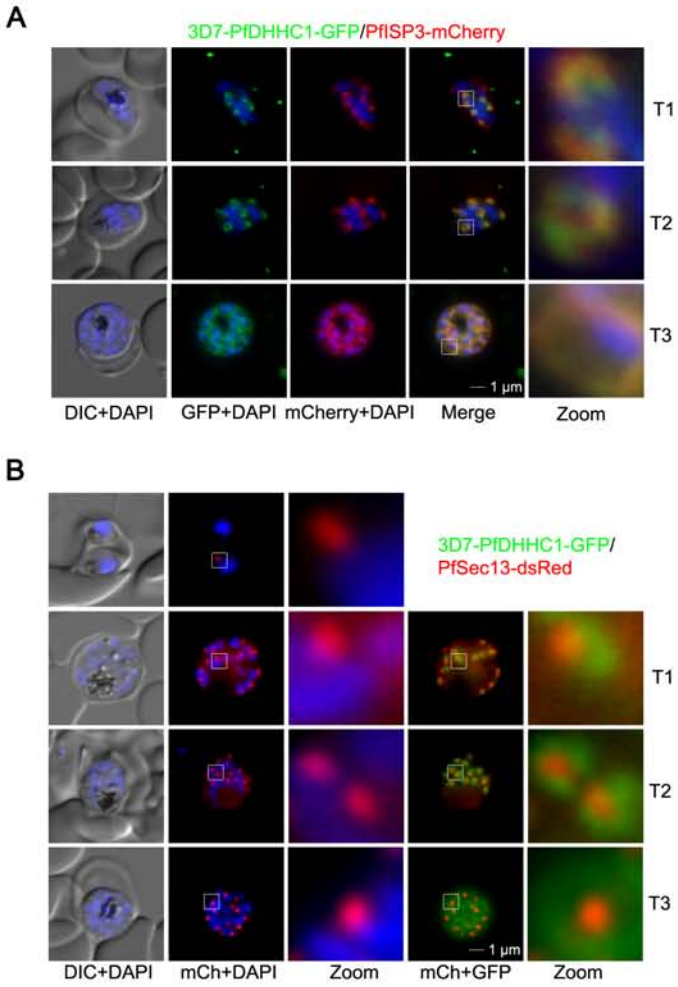

Figure 4.5 Co-localization of endogenous PfDHHC1-GFP with organelle markers. A. Co-localization with the IMC protein PfISP3-mCherry. PfISP3-mCherry was episomally co-expressed in 3D7-PfDHHC1-GFP parasites and shows identical spatial distribution compared with PfDHHC1-GFP. Nuclei were stained with DAPI. Enlargement of selected areas are marked with a white square and referred to as zoom. Scale bar, 1 µm. **B.** Co-localization with the trans-Golgi marker Sec13-dsRed. Sec13-dsRed was episomally co-expressed in 3D7-PfDHHC1-GFP parasites and shows distinct distribution compared to PfDHHC1-GFP. Nuclei were stained with DAPI. Enlargement of selected areas are marked with a white square and referred to as zoom. Scale bar, 1 µm.

4.2 Co-localization of PfISP3 with the IMC marker GAP45

IMC localization of PfISP3 was confirmed with two additional experiments: First, PfISP3 was endogenously tagged using the same 3' replacement approach described in 4.1.2. Importantly the dynamics and localization of endogenous PfISP3 is indistinguishable from the episomally expressed PfISP3 (please refer to Fig. 4.7 and 4.12 C).

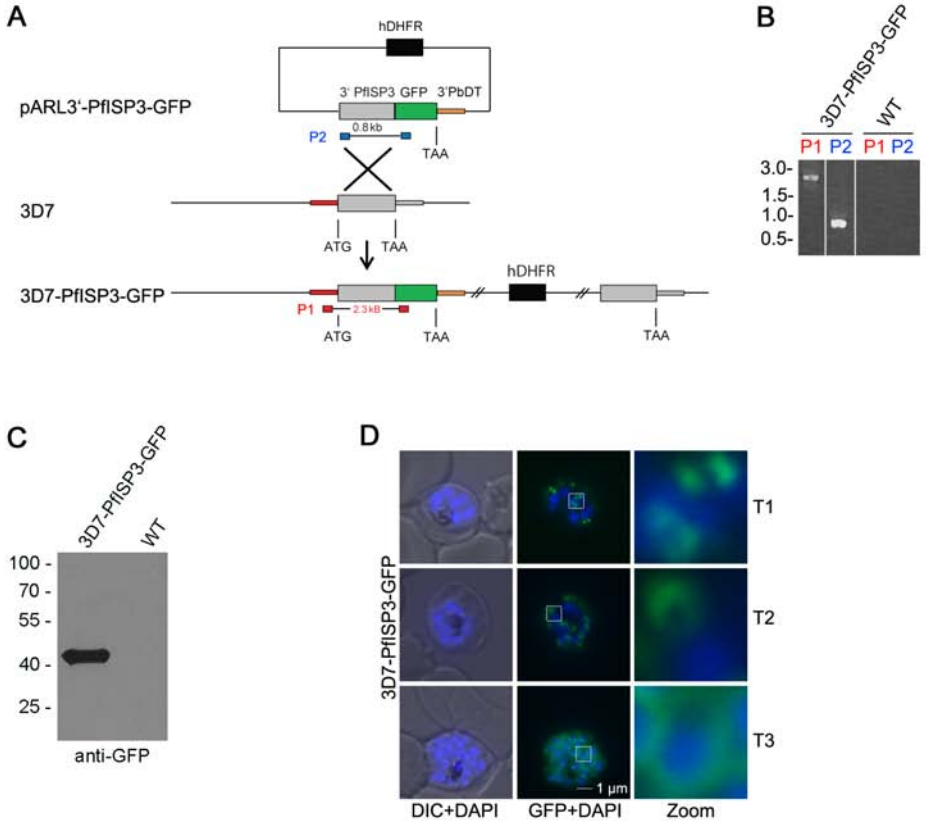

Figure 4.6 Localization of endogenous PfISP3. A. Schematic representation of the GFP replacement of the endogenous 3'end of PfISP3 creating a 3D7-PfISP3-GFP cell line. The vector encompasses the selection cassette (black), 500 bp of the PfISP3 gene (grey) was fused to GFP (green) accompanied by the 3'UTR of *Pb*DT (orange) without any promoter. Integration of the vector takes place by homologous recombination (cross) into the PfISP3 locus creating a full-length PfISP3-GFP fusion under the control of the endogenous promoter. **B.** Integration was confirmed by PCR using two different primer combinations on gDNA. One primer set (red) hybridizes in a PfISP3 region upstream of the integration and in the coding region of GFP. This primer combination can only amplify a 2.3 kb DNA fragment after recombination took place. The other set (blue) amplifies 0.8 kb of PfISP3 in the parental as well as in the transgenic parasite line. **C.** Expression of the transgene from the endogenous locus was shown by Western blot analysis using anti-GFP antibodies resulting in a fusion protein of approximately 45 kDa (calculated molecular weight 44 kDa). **D.** PfISP3-GFP was localized in unfixed late stage parasites showing characteristic IMC dynamics. Nuclei are stained with DAPI (blue). Enlargement of selected areas are marked with a white square and referred to as zoom. Scale bar, 1 µm.

Secondly, IMC localization was confirmed by co-localization with the IMC marker GAP45 (REF). This double-transgenic cell line was generated by transfecting GAP45-mCherry into the PfISP3-GFP cell line (following the principles explained above, 4.1.1). The latter cell line was previously generated by Dr. Susann Herrmann (Gilberger laboratory, McMaster University, Canada). Both proteins showed identical dynamics during IMC biogenesis (Fig. 4.7). Together, these results show that PfISP1 and PfISP3 (as well as PfDHHC1) are indeed IMC localized proteins.

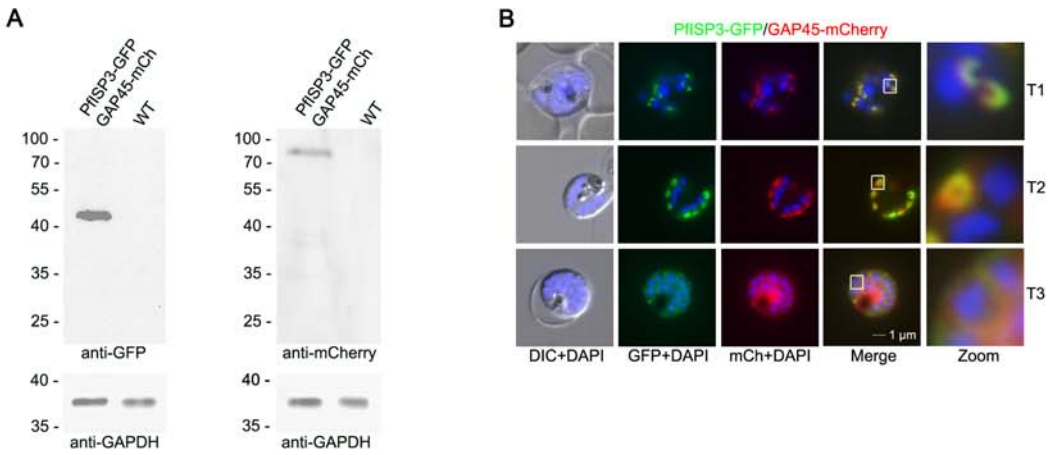

Figure 4.7 PfISP3 co-localizes with GAP45. A. Western blot analysis of parasites co-expressing PfISP3-GFP and GAP45-mCherry using either anti-GFP or anti-mCherry antibodies. Antibodies against the cytosolic protein GAPDH were used as control (bottom panels). **B.** Co-localization of PfISP3-GFP and GAP45-mCherry in unfixed parasites revealed their identical dynamic during schizogony. Enlargement of the selected areas are marked with a white square and referred to as zoom. Nuclei are stained with DAPI (blue). Scale bar, 1 µm.

4.3 Investigation of PfISP1, another peripheral dual acylated IMC protein

4.3.1 Localization of PfISP

PfISP1 (PF10_0107) is located on chromosome 13, has a predicted size of 903 basepairs (bp) (MW: 16.6 kDa) and four introns. It has neither a signal peptide nor a transmembrane domain and its expression profile shows an upregulation in late stages. PfISP1-peptides were detected by mass spectrometry in merozoites, gametocytes and salivary gland sporozoites. PfISP1 was first identified using BLAST search as a putative PfISP1/2 homologue (Beck et al., 2010). PfISP1 is predicted to be myristoylated (score: 1.5, predicted by NMT) and palmitoylated (Cys 7, score: 7.7; Cys 8, score 5.176; predicted by CSS-Palm version 3.0).

Table 4.2 Identities between TgISPs, PfGAP45, PfISP1 and PfISP3. Numbers represent percent identity. An identity of 25 % or higher implies similarity of function. 18-25% means similarity of structure or function. Numbers were retrieved using PSI-BLAST (PRALINE) homology-extended alignments (http://www.ibi.vu.nl/programs/pralinewww/).

	PfISP3	PfISP1	PfGAP45	TgISP1	TgISP2	TgISP3	TgISP4
PfIPS3	-	-	-	-	-	-	-
PfISP1	26 %	-	-	-	-	-	-
PfGAP45	19 %	16 %	-	-	-	-	-
TgISP1	23 %	44 %	9 %	-	-	-	-
TgISP2	20 %	33 %	11 %	38 %	-	-	-
TgISP3	31 %	24 %	11 %	26 %	24 %	-	-
TgISP4	16 %	22 %	14 %	26 %	22 %	18 %	-

PfISP1 was localized using episomal overexpression (Fig. 4.8) or endogenous tagging (Fig. 4.9). In both cases PfISP1 shows typical IMC localization.

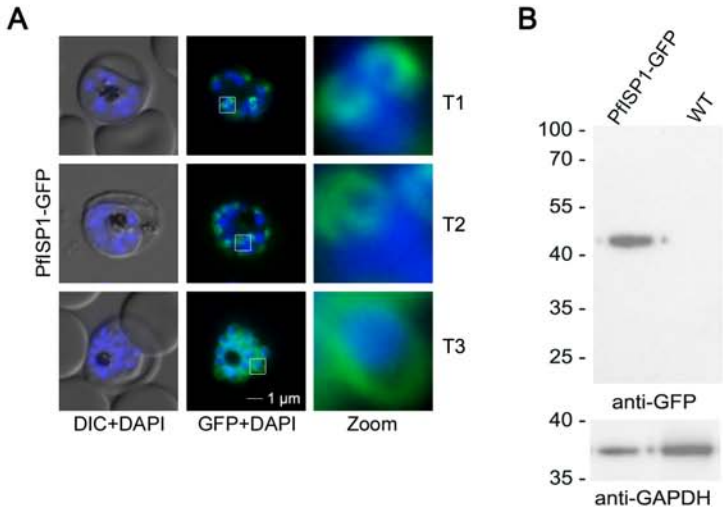

Figure 4.8 Over-expression of PfISP1. A. Western blot analysis using anti-GFP antibodies. A single protein band of about 45 kDa (expected MW: 43 kDa) was detected in the transgenic but not in the parental parasite line. **B.** Localization of PfISP1-GFP in unfixed parasites showing characteristic IMC dynamics during schizogony. Nuclei are stained with DAPI (blue). Enlargement of selected areas are marked with a white square and referred to as zoom. Scale bar, 1 µm.

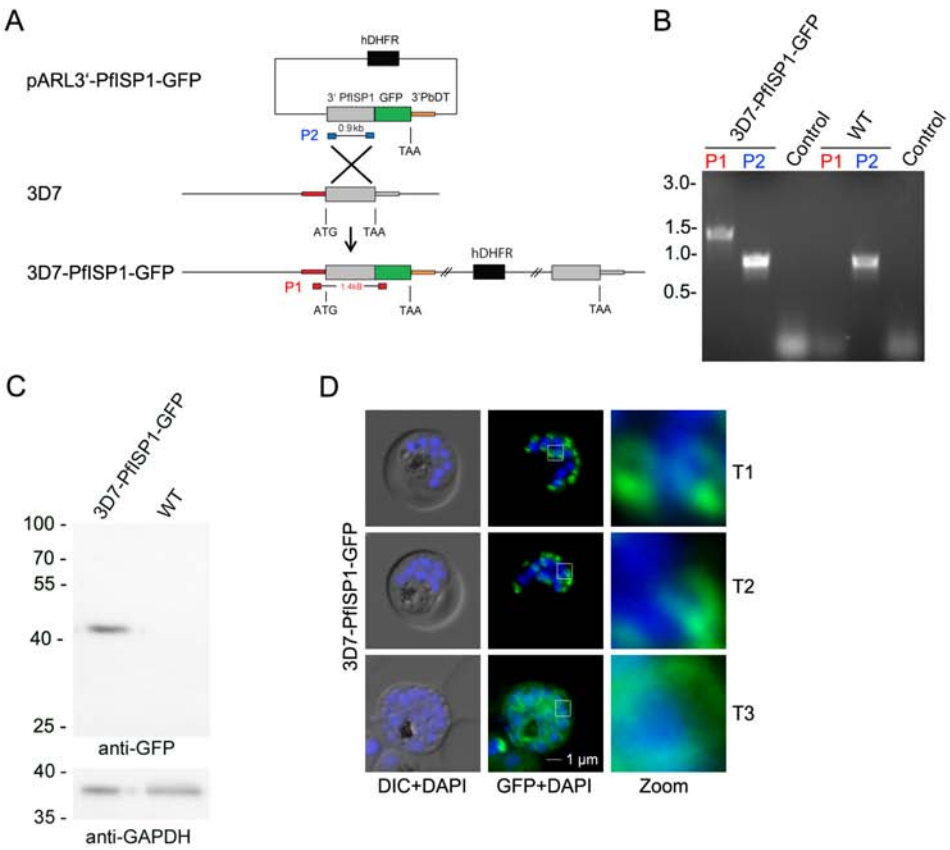

Figure 4.9 Endogenous PfISP1 localizes to the IMC. A. Schematic representation of the GFP replacement of the endogenous 3'end of PfISP1 creating a 3D7-PfISP1-GFP cell line. The vector encompasses the selection cassette (black), 900 bp of the PfISP1 gene (grey) was fused to GFP (green) accompanied by the 3'UTR of *Pb*DT (orange) without any promoter. Integration of the vector takes place by homologous recombination (cross) into the PfISP1 locus creating a full-length PfISP1-GFP fusion under the control of the endogenous promoter. **B.** Integration was confirmed by PCR using two different primer combinations on gDNA. One primer set (red) hybridizes in a PfISP1 region upstream of the integration and in the coding region of GFP. This primer combination can only amplify a 1.4 kb DNA fragment after recombination took place. The other set (blue) amplifies 0.9 kb of PfISP1 in the parental as well as in the transgenic parasite line. Control indicates PCRs with the red primer set in the absence of parasite DNA. **C.** Expression of the transgene from the endogenous locus was shown by Western blot analysis using anti-GFP antibodies (upper panel) resulting in a fusion protein of approximately 45 kDa (calculated molecular weight 43 kDa). Anti-GAPDH was used as a loading control. **D.** PfISP1-GFP was localized in unfixed late stage parasites showing characteristic IMC dynamics. Nuclei are stained with DAPI (blue). Enlargement of selected areas are marked with a white square and referred to as zoom. Scale bar, 1 µm.

In pre-sexual gametocyte stages (Fig. 4.10) PfISP1-GFP is not equally distributed within the nascent IMC. In stage III and IV gametocytes PfISP1-GFP appears more concentrated in the polar regions of the cell and additionally accumulates in transversal structures. Apical polarity was confirmed by confocal microscopy (data not shown). The transversal structures resemble the symmetric meshwork enclosing the gametocyte previously described as the localization of

the *Plasmodium*-specific IMC protein MAL13P1.228 (Kono et al., 2012) reflecting the sutures of individual IMC plates (Meszoely et al., 1987).

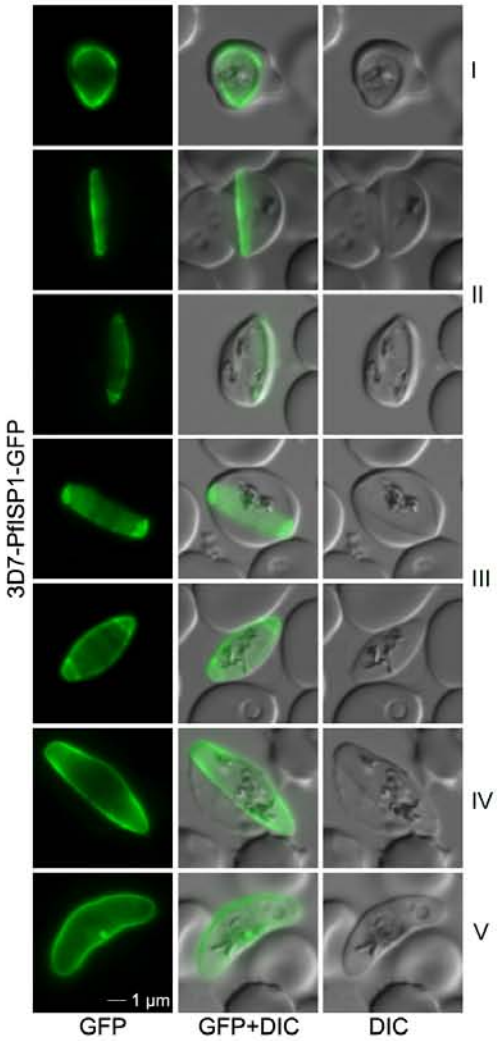

Figure 4.10 Localization of endogenously tagged PfISP1 in gametocytes. Localization of endogenously tagged PfISP1 during gametocyte development. Scale bar, 1 µm.

4.3.2 Co-localization of PfISP1 and PfISP3

PfISP3-mCherry was previously cloned and obtained from Dr. Maya Kono (BNI, Hamburg). The 3D7-PfISP1-3D7 parasites were transfected with the PfISP3-mCherry. Thereafter, it was possible to select for maintenance of both plasmids. PfISP1 and PfISP3 show identical localization during schizogony (Fig. 4.11). Unfortunately, the mCherry signal was hardly visible in gametocytes and the dynamics of both proteins could not be analyzed in those presexual stages.

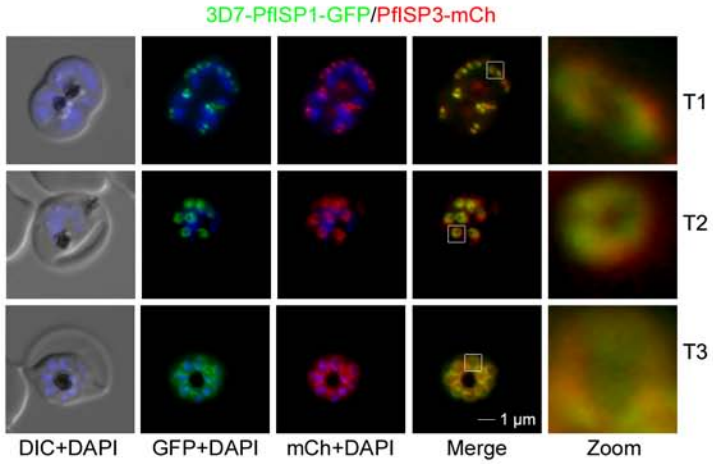

Figure 4.11 Co-localization of endogenous PfISP1-GFP with PfISP3-mCh. A. Co-localization with the IMC protein PfISP3-mCherry. PfISP3-mCherry was episomally co-expressed in 3D7-PfDHHC1-GFP parasites and shows identical spatial distribution compared with PfISP1-GFP. Nuclei were stained with DAPI. Enlargement of selected areas are marked with a white square and referred to as zoom. Scale bar, 1 µm.

4.4 Investigation of the IMC membrane recruitment of PfISP1 and PfISP3

4.4.1 N-terminal palmitoylation of PfISPs

Mutagenesis of N-terminal lipid acceptor sites leads to abolishment of membrane association of PfISPs

By using either full-length (Fig. 4.12 C-E; PfISP3-GFP, PfISP3$_{G2A}$-GFP, PfISP3$_{C5AC6A}$-GFP) or the N-terminal sequences (Fig. 4.12 G-I; $_{20}$PfISP1-GFP, $_{20}$PfISP1$_{G2A}$-GFP, $_{20}$PfISP1$_{C5AC6A}$-GFP), the role of palmitoylation (and myristoylation) for IMC membrane recruitment was verified by microscopy. The pertinent alanine substitutions led to the expected cytosolic distribution of the mutant proteins, underlining the synergistic effect of myristoylation and palmitoylation for membrane association (Fig. 4.12 D-I). This was additionally verified by solubilization assays performed with parasite material derived from PfISP3-GFP, PfISP3$_{G2A}$-GFP or PfISP3$_{C5AC6A}$-GFP expressing parasites (Fig. 4.12 F). While over-expressed PfISP3-GFP is mainly in the carbonate fraction confirming its membrane association, both mutants are exclusively found in the hypotonic fraction, resembling the cytosolic GAPDH control. Noteworthy, single point mutations of either C5 or C6 in PfISP3 do not interfere with IMC

membrane localization (Fig. 4.13). Taken together, these results show that IMC membrane recruitment of PfISP3 and PfISP1 depends on N-terminal lipid modification motifs.

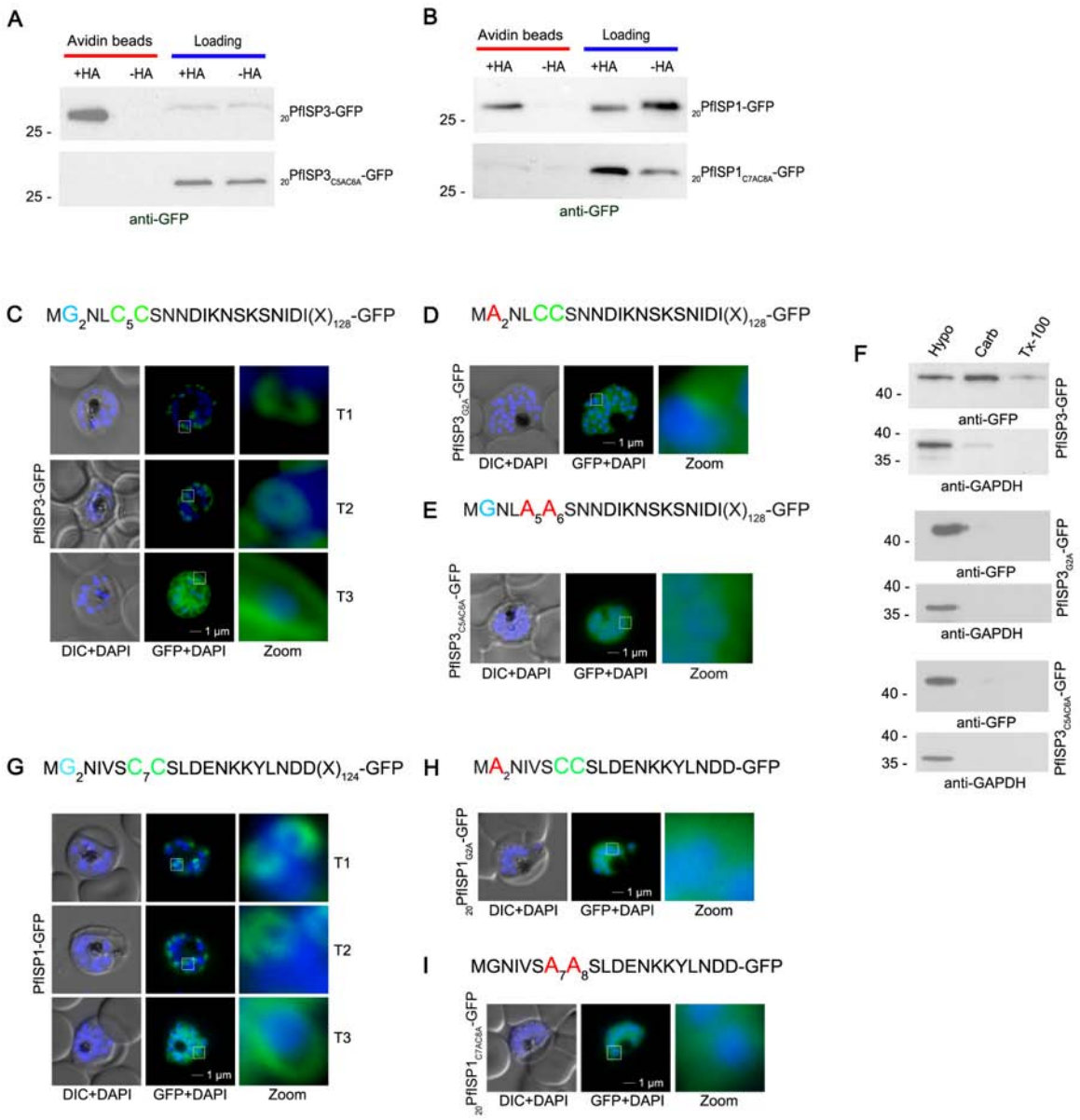

Figure 4.12 The role of N-terminal acylation for IMC membrane association of PfISP3 and PfISP1. A-B. Acyl biotin exchange assay. $_{20}$PfISP3-GFP, $_{20}$PfISP1 -GFP and the corresponding cysteine mutants $_{20}$PfISP3$_{C5AC6A}$-GFP and $_{20}$PfISP1$_{C7AC8A}$-GFP (as controls) were used in the switch experiments. Proteins were detected on Western blot using anti-GFP antibodies. **A.** $_{20}$PfISP3-GFP (upper panel) and $_{20}$PfISP3$_{C5AC6A}$-GFP (lower panel) fusion proteins are present in the two aliquots that were incubated with biotinylation reagent with or without hydroxylamine after NEM treatment ('Loading'). After elution from the NeutrAvidin beads ('Avidin beads'), only $_{20}$PfISP3-GFP but not the cysteine mutant $_{20}$PfISP3$_{C5AC6A}$-GFP is enriched in the hydroxylamine (+HA) treated sample when compared with the untreated sample (-HA). **B.** $_{20}$PfISP1-GFP and $_{20}$PfSP1$_{C7AC8A}$-GFP fusion proteins are present in the two aliquots that were incubated with biotinylation reagent with or without hydroxylamine after NEM treatment ('Loading'). After elution from the NeutrAvidin beads ('Avidin beads'), only $_{20}$PfISP1-GFP but not the cysteine mutant $_{20}$PfISP1$_{C7AC8A}$-GFP is enriched in the hydroxylamine (+HA) treated sample when compared with the untreated sample (-HA). **C.** Over-expression of PfISP3- showing characteristic IMC dynamics during schizogony (T1-T3). Scale bar, 1

µm. Putative myristoylation and palmitoylation sites are highlighted in light blue (G_2) or green (C_7C_8). **D-E.** IMC membrane association depends on the presence of N-terminal myristoylation and palmitoylation motifs. N-terminal myristoylation (**B,** PfISP3$_{G2A}$-GFP) and palmitoylation motif mutants (**C,** PfISP3$_{C5AC6A}$-GFP) were expressed in *P. falciparum* and localized in unfixed parasites. Mutation of either one of the acylation motifs resulted in a cytosolic distribution of the GFP-fusion protein (D1, E1). (**F**) This change in the localization pattern is supported by solubility assays. In contrast to the wild type proteins the mutant proteins are, like GAPDH (lower panels), exclusively detectable in the hypotonic fraction (soluble: H_2O/SN, carbonate Carb/SN and membrane Triton-X-100: Tx100/SN). **G.** Over-expression of the 20 amino acid N-terminus of PfISP1 ($_{20}$PfISP1-GFP) reveals identical IMC dynamic during schizogony as full-length PfISP3-GFP. **H-I.** Mutation of either one of the acylation motifs ($_{20}$PfISP1$_{G2A}$-GFP and $_{20}$PfISP1$_{C7AC8A}$-GFP) resulted in a cytosolic variant showed by microscopy. Scale bars, 1 µm.

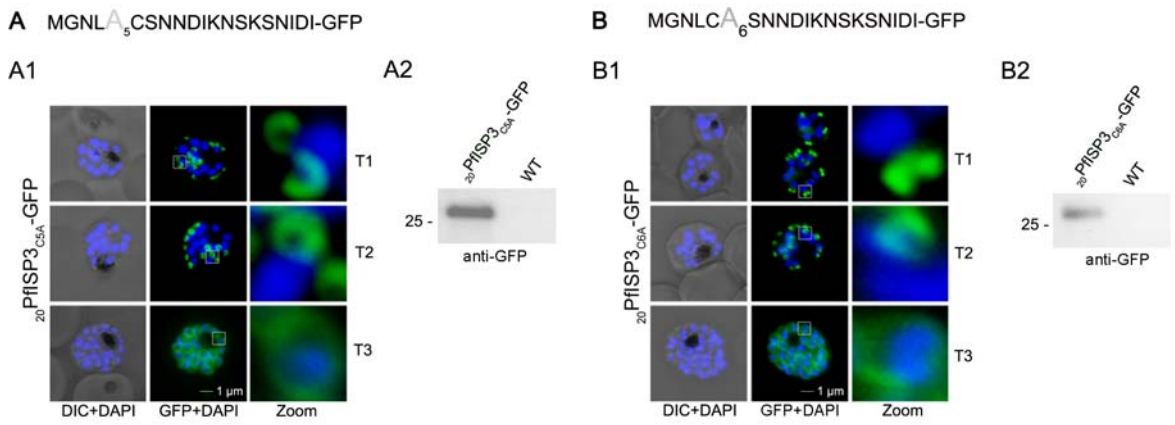

Figure 4.13 Expression and localization of the single cysteine mutants C5 and C6 in PfISP3. Neither the mutation C_5 (**A**) nor the mutation of C_6 (**B**) has an influence on IMC membrane attachment. $_{20}$PfISP3$_{C5A}$-GFP and $_{20}$PfISP3$_{C6A}$-GFP were localized in unfixed parasites (A1,B1) and display an identical IMC dynamic like the WT protein. Enlargement of selected areas are marked with white squares and referred as zoom. Nuclei stained with DAPI (blue). Scale bar, 1 µm. A2,B2. Western blot analysis of the expression using anti-GFP antibodies.

Direct evidence of N-terminal palmitoylation using acyl biotin exchange assays

To confirm the predicted palmitoylation *in vivo*, parasites expressing either the wild type sequence ($_{20}$PfISP3-GFP and $_{20}$PfISP1-GFP) or the corresponding cysteine/alanine substitutions ($_{20}$PfISP3$_{C5AC6A}$-GFP and $_{20}$PfISP1$_{C7AC8A}$-GFP) were used in acyl biotin exchange assays (ABEs) (Wan et al., 2007; Jones et al., 2012). This assay involves three main steps: I) blocking of free thiol side chains with N-ethylmaleimide, II) removal of palmitate from cysteines by thioester-cleavage using hydroxylamine, III) biotinylation of the exposed cysteines, wherefrom the thioester has been cleaved from. Treated protein samples can subsequently be used for affinity purification and Western blot analysis. These experiments showed that both PfISPs ($_{20}$PfISP3-GFP and $_{20}$PfISP1-GFP) are biotinylated and are enriched

in the fraction that is expected to contain all S-acylated proteins assayed by this method. The corresponding mutants without palmitoylation motifs were not enriched (Fig. 4.12 A, B).

4.4.2 Minimal sequence requirements for IMC targeting

PfISP1 and PfISP3 share a high degree of sequence similarity overall (Tab. 4.2) but within their fist 20 N-terminal amino acids in particular a myristoylated glycine (Wright et al., 2013) at position 2 and two predicted palmitoylated cysteines (Fig. 4.14). Moreover, the distribution of charged amino acids are comparable. Negatively charged amino acids frame positively charged lysines.

Figure 4.14 Comparison of the first 20 N-terminal amino acids of PfISP1 and PfISP3. Both amino acid sequences share a predicted myristoylation and palmitoylation motifand a similar patter of charged amino acids. Myristoylation sites were predicted using Myristoylator (www.expasy.org) or NMT (http://mendel.imp.ac.at/myristate/SUPLpredictor.htm). Palmitoylation sites were predicted using CSS-Palm 3.0 (Ren et al., 2008) (red: myristoylated glycine, palmitoylated cysteines; purple: negatively charged amino acids; light blue: positively charged amino acids).

Minimal sequence requirements for IMC localization of PfISP3

Although fatty acylation is essential for IMC localization of the PfISPs, it is unknown how the membrane specificity is achieved to exclusively trap these proteins at the IMC. Previous work showed that GFP tagged with the N-terminal 20 amino acids of dual acylated proteins are predominantly trafficked to the plasma membrane, but can also result in IMC (e.g. $_{20}$PfISP3) or rhoptry ($_{20}$PfARO) localization (Cabrera et al., 2012).

To identify potential sequence features that may contribute to IMC specific trafficking, a construct was generated, where the last 10 amino acids were exchanged to alanines ($_{20}$PfISP3$_{11\text{-}20A}$-GFP; Fig. 4.15 A). This mutant is still truthfully located at the IMC upon its expression in the parasite (Fig. 4.15 A) and associates with the specific intermediates (T1 and T2) of nascent IMC during schizogony. Hence, the N-terminal 10 amino acids are sufficient for mediating acylation and directing the ISP proteins to the IMC.

This was validated by the expression and localization of the first 10 amino acids of PfISP3 fused with GFP ($_{10}$PfISP3-GFP). Consistent with the previous findings, $_{10}$PfISP3-GFP is localized to the IMC (Fig. 4.15 B). Next, the only charged residue (D10) in the 10 amino acids was exchanged either to a neutral glycine (Fig. 4.15 C) or to a positively charged arginine (Fig. 4.15 D) or lysine (Fig. 4.15 E). While neither the exchange with glycine ($_{10}$PfISP3$_{D10G}$-GFP) nor arginine ($_{10}$PfISP3$_{D10R}$-GFP) interfered with correct targeting, the substitution with a lysine ($_{10}$PfISP3$_{D10K}$-GFP) led to a redirection of the GFP-fusion to the PM. IMC localization was excluded by performing immunofluorescence assays (IFAs) using the IMC marker GAPM2 (Kono et al., 2012). The two proteins do not co-localize in early schizont stage parasites (T1) (Fig. 4.15 E3) and only show co-localization at the very end of schizogony, where the IMC and the PM are hardly distinguishable (T3). Additionally, due to its PM association this mutant showed also some association with the food vacuole (Fig. 4.15 E1) with the residual body characterized by hemozoin (Ridzuan et al., 2012) that is not present in IMC targeted mutants (Fig. 4.15 and 4.16).

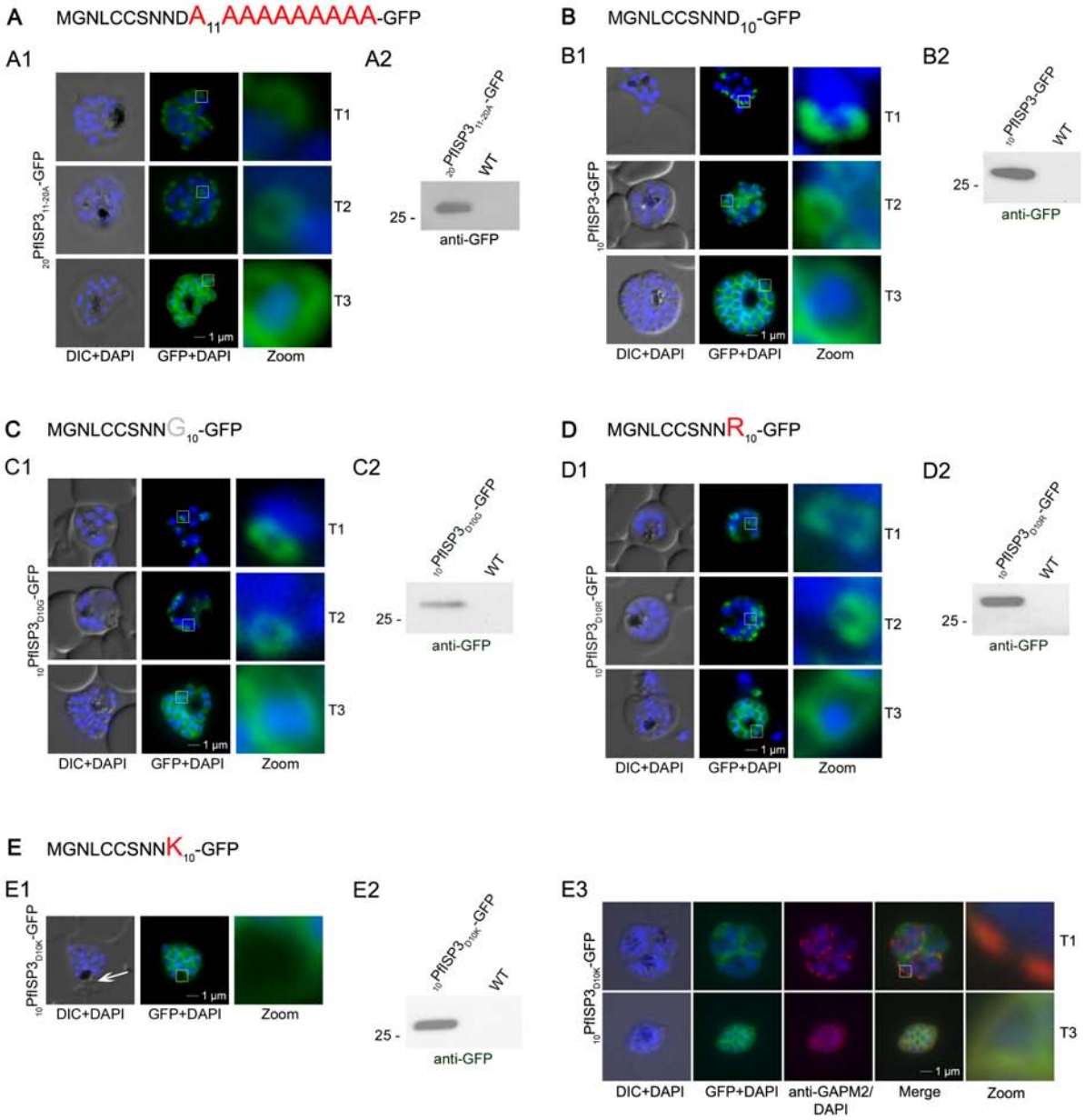

Figure 4.15 Mutational analysis of the minimal sequence requirements for IMC association of PfISP3. A-B. Expression and localization of the 20 amino acid N-terminus with the last 10 ($_{20}$PfISP3$_{11\text{-}20A}$-GFP) amino acids substituted with alanines. A1. $_{20}$PfISP3$_{11\text{-}20A}$-GFP was localized in unfixed parasites and showed an identical dynamic like the WT protein. A2. Western blot analysis of the expression using anti-GFP antibodies. **B.** The first 10 amino acids of PFISP3 ($_{10}$PfISP3-GFP) are sufficient for IMC localization (B1) B2. Western blot analysis of the expression $_{10}$PfISP3-GFP. **C-D.** Mutation of the sole charged residue D_{10} in to a neutral glycine ($_{10}$PfISP3$_{D10G}$-GFP, C1) or a positively charged arginine ($_{10}$PfISP3$_{D10R}$-GFP, D1) does not interfere with IMC targeting**.** Western blot analysis (C2, D2) of GFP-fusion protein expression **E.** Substitution of D_{10} with a positively charged lysine re-directs the GFP-fusion protein to the PM. The arrow and zoom highlights the additional association with the food vacuole membrane (E1). Western blot analysis (E2) of $_{10}$PfISP3$_{D10K}$-GFP. E3. Co-localization of the mutant with the IMCmarker GAPM2 (red) using anti-GAPM2 specific antibodies. Enlargement of selected areas are marked with white squares and referred as zoom. Nuclei stained with DAPI (blue). Scale bar, 1 µm.

Interestingly, previous work showed an essential role for an arginine and a lysine in close proximity downstream of the palmitoylated cysteine for rhoptry membrane targeting of PfARO (Cabrera et al., 2012). To probe into a putative discriminative role of an arginine in combination with a lysine, we attempted to re-direct $_{10}$PfISP3-GFP to the rhoptry membrane by the expression of mutants comprising both amino acids ($_{10}$PfISP3$_{N9RD10K}$-GFP). Indeed, these substitutions led to a partial redirection of GFP fusion to an apical structure that might resemble the rhoptry membrane (Fig. 4.16 B). As expected, the exchange of N9 with aspartate ($_{10}$PfISP3$_{N9D}$-GFP; Fig. 4.16 A) did not change IMC localization and the exchange of N9 and D10 with lysines ($_{10}$PfISP3$_{N9KD10K}$-GFP) redirected the protein to the PM (Fig. 4.16 C). IMC localization of this mutant was excluded by performing IFAs, which showed no co-localization of the two proteins in early schizont stage parasites (T1) (Fig. 4.16 C3) and only show co-localization at the very end of schizogony (T3).

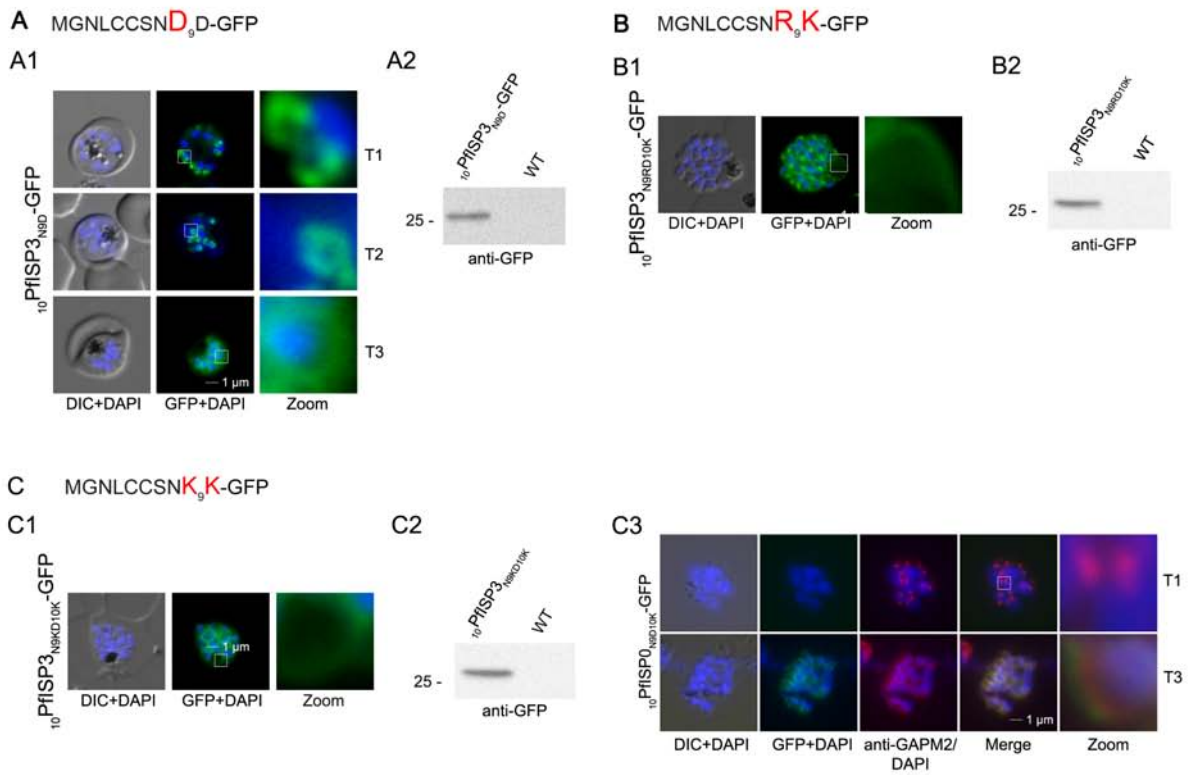

Figure 4.16 Redirection of the IMC $_{10}$PfISP3-GFP fusion protein to the rhoptry membrane. A. Substitution of N9 with D ($_{10}$PfISP3$_{N9D}$-GFP) does not interfere with correct IMC recruitment of the GFP-fusion protein (A1). **B.** Substitution of N_9 with arginine ($_{10}$PfISP3$_{N9RD10K}$-GFP) redirects the fusion protein to an apical membrane reminescent of the rhoptries with some additional PM localization. The zoom highlights the association with the food vacuole membrane (B1) **C.** The substitution of N_9 and D_{10} with lysine and its expression in the parasite ($_{10}$PfISP3$_{N9KD10K}$-GFP) leads to PM localization (C1). The arrow and zoom highlights the additional association of this mutant protein with the food vacuole membrane. C3. Co-localization of the mutant with the IMCmarker GAPM2 (red) using anti-GAPM2 specific antibodies. A2, B2 and C2. Western blot analysis using anti-GFP antibodies. Enlargement of selected areas are marked with white squares and referred as zoom. Nuclei stained with DAPI (blue). Scale bar, 1 µm.

Minimal sequence requirements for IMC localization of PfISP1

Given the similar N-terminal sequence signature of both PfISP proteins (Fig. 4.14), PfISP1 was also subject to mutational analysis of for minimal sequence requirements for IMC specific membrane recruitment (Fig. 4.17). First, the minimal targeting sequences were investigated by expressing only the first 11 (including the negatively charged residue) or the 10 amino acids of PfPfISP1. As expected from the previous results from PfISP3, both constructs, $_{11}$PfISP1-GFP and $_{10}$PfISP1-GFP, directed GFP to the IMC (Fig. 4.17 A, B). Again, the introduction of a lysine in this short targeting sequence ($_{11}$PfISP1$_{D11K}$-GFP) aborted IMC trafficking (Fig. 4.17 C) and led to a PM association. IMC localization was excluded by co-localization with the IMC marker GAPM2 (Fig. 4.17 E3), which showed no co-localization of the two proteins in early schizont stage parasites (T1) (Fig. 4.17 E3) and only show co-localization at the very end of schizogony (T3).

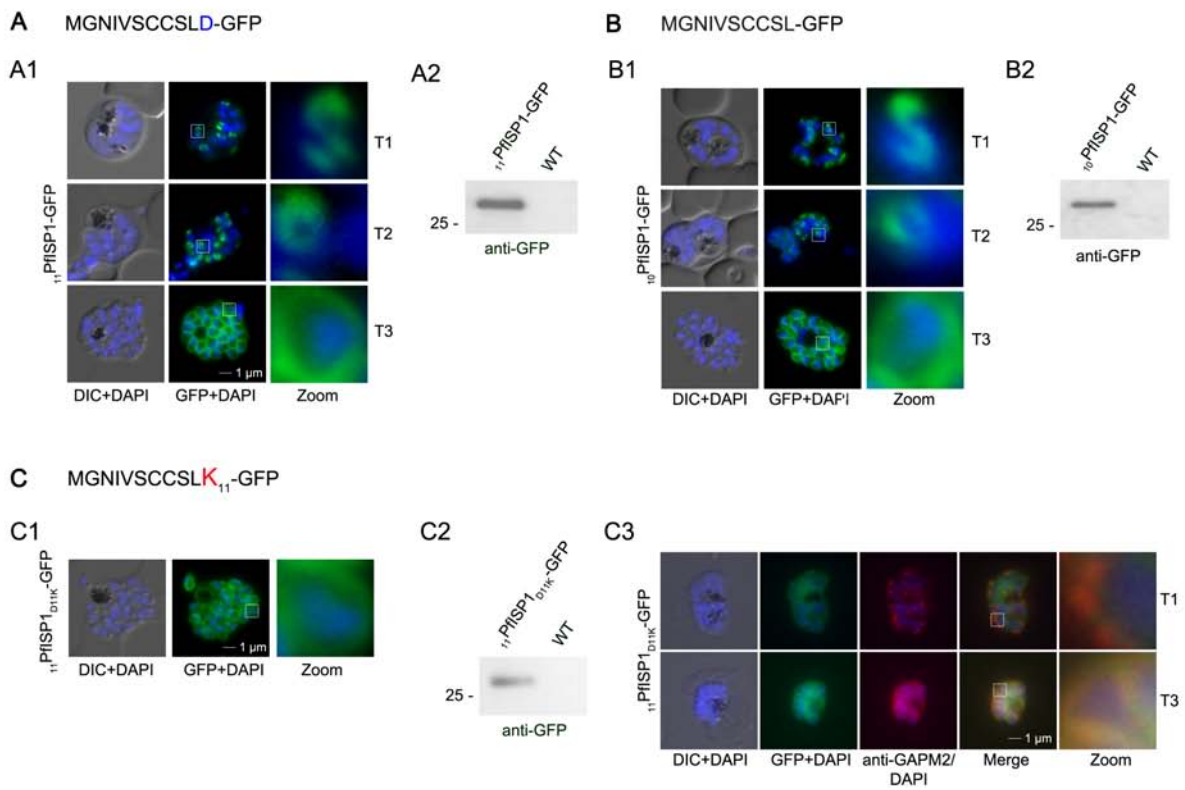

Figure 4.17 Localization and minimal sequence requirements for PfPfISP1. A. Expression of the first 11 ($_{11}$PfSP1-GFP, **A**) or 10 ($_{10}$PfISP1-GFP, **B**) amino acids are sufficient to direct GFP to the IMC (A1-B1). Western blot analysis using anti-GFP antibodies (A2-B2). **C.** Substitution of D_{11} with lysine ($_{11}$PfISP1$_{D11K}$-GFP, **C**) abolishes IMC targeting (C1) and leads to PM localization. The zoom highlights the additional association with the food vacuole membrane. **C2.** Western blot analysis using anti-GFP antibodies. C3. Co-localization of the mutant with the IMCmarker GAPM2 (red) using anti-GAPM2 specific antibodies. Enlargement of selected areas are marked with white squares and referred as zoom. Nuclei stained with DAPI (blue). Scale bar, 1 µm.

In summary, the mutational analysis revealed that the minimal sequence requirement of IMC recruitment of PfISPs does not depend on a net positive or negative charge in close proximity to the acylated cysteines. Only the introduction of a positively charged lysine leads to trapping of the protein at the PM. These concepts were also proven on a 20 amino acid background for both PfISPs (data not shown).

4.4.3 Retargeting of PfCDPK1 to the IMC

PfCDPK1 (PFB0815w) is localized at the PM, it is dually acylated at its N-terminus and the first 20 N-terminal amino acids localize to the PM (Möskes et al., 2004; Cabrera et al., 2012; Fig. 4.18 A). Furthermore, n order to validate, if this IMC trafficking information can be utilized in general to predict the localization of other dual acylated proteins, or even change their place of destination, amino acid substitutions were carried out to identify possible similarities in amino acid identity for trafficking to a particular membrane. Positively charged residues were exchanged with aspartate ($_{20}$CPDK1$_{K10DK13DR15D}$-GFP), which re-directs the protein to the IMC (Fig. 4.18 B).

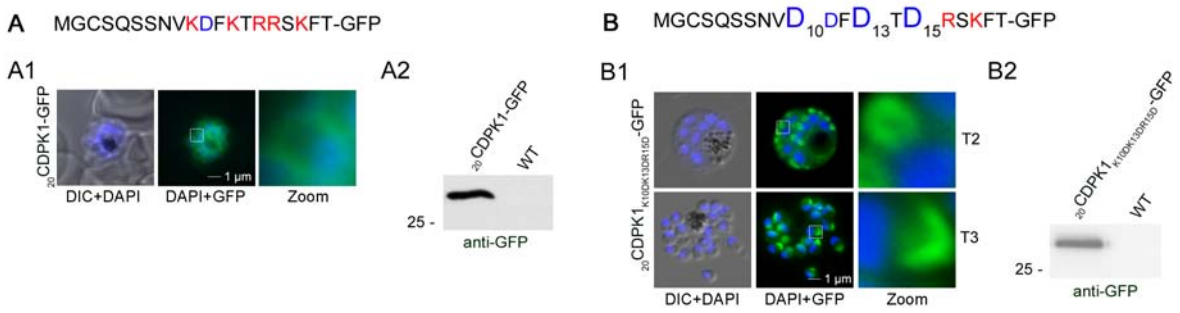

Figure 4.18 Redirection of the plasma membrane protein CDPK1 (PFB0815w) to the IMC. A. The GFP-tagged N-terminus of CDPK1 is localized at the parasites plasma membrane (A1). **A2** Western blot analysis using anti-GFP and anti-GAPDH antibodies as loading control. **B.** Exchange of the positively charged residues to aspartate and expression of $_{20}$CDPK1$_{K10DK13DR15D}$-GFP redirects the protein to the IMC (B1). Enlargement of selected areas are marked with a white square and referred to as zoom. Nuclei are stained with DAPI. Scale bars: 1 µm. **B2.** Western blot analysis using anti-GFP and anti-GAPDH antibodies as loading control.

4.5 Probing into PAT-substrate interactions

To provide direct evidence of interaction of *P. falciparum* PATs and ISP proteins differentially localized PATs were co-expressed with one putative substrate (PfISP3) in a yeast strain that is devoid of five (*akr1*Δ *akr2*Δ *pfa3*Δ *pfa4*Δ *pfa5*Δ) of its seven endogenous PATs (Hou et al., 2009). The molecular cloning part of this work was carried out in the Gilberger laboratory (McMaster University, Canada) while the expression of the plasmids in yeast, fluorescence microscopy and Western blot analysis was carried out in the Ungermann laboratory (University of Osnabrück, Germany). In addition to the IMC localized PfDHHC1, the PM associated PfDHHC3 and the apically localized PfDHHC9 were included in this experimental approach. All parasite PATs were expressed from chromosomally integrated plasmids with a C-terminal PR epitope. The N-terminus of PfISP3 ($_{20}$PfISP3) as well as two mutants – $_{20}$PfISP3$_{C5AC6A}$ and $_{20}$PfISP3$_{D10KD19K}$ – were co-expressed as GFP-fusions with the PATs. Although all genes were re-codonized to facilitate their heterologous expression in *S. cervesiae*, only the expression of PfDHHC3, PfDHHC9 as well as the expression of all substrates show abundant expression of the tagged proteins by Western blot analysis (with some degradation of PfDHHC9). The expression of the larger PAT PfDHHC1 was considerable lower (Fig. 4.19 A). Over-expression of PfDHHC1 from a high-copy plasmid did not result in higher expression (data not shown). Microscopic analysis of the $_{20}$PfISP3-GFP fusion proteins in the yeast cells showed that in the absence of the five endogenous ScPATs (or with the marginal expression of PfDHHC1), the GFP signal of all three substrates is cytosolic (Fig. 4.19 B). Whereas the co-expression of PfDHHC9 led to some re-distribution of wild type ISP3 as well as the $_{20}$PfISP3$_{D10KD19K}$-GFP substrate to the plasma membrane, the cysteine mutated version remained cytosolic in any co-expression with PfDHHC proteins. For PfDHHC1, a minor localization of PfISP3 to the plasma membrane was observed, which was even lower in the D10KD19K mutant. Importantly, co-expression of PfISP3 with PfDHHC3 led to a significant re-distribution of both wild-type PfISP3-GFP and of the $_{20}$PfISP3$_{D10KD19K}$ fusion protein to the plasma membrane of the yeast cells. This strongly suggests successful palmitoylation of ISP3 in this heterologous expression system by PfDHHC3. It also shows that yeast can be employed in the future to test for specificity of the PfDHHC proteins.

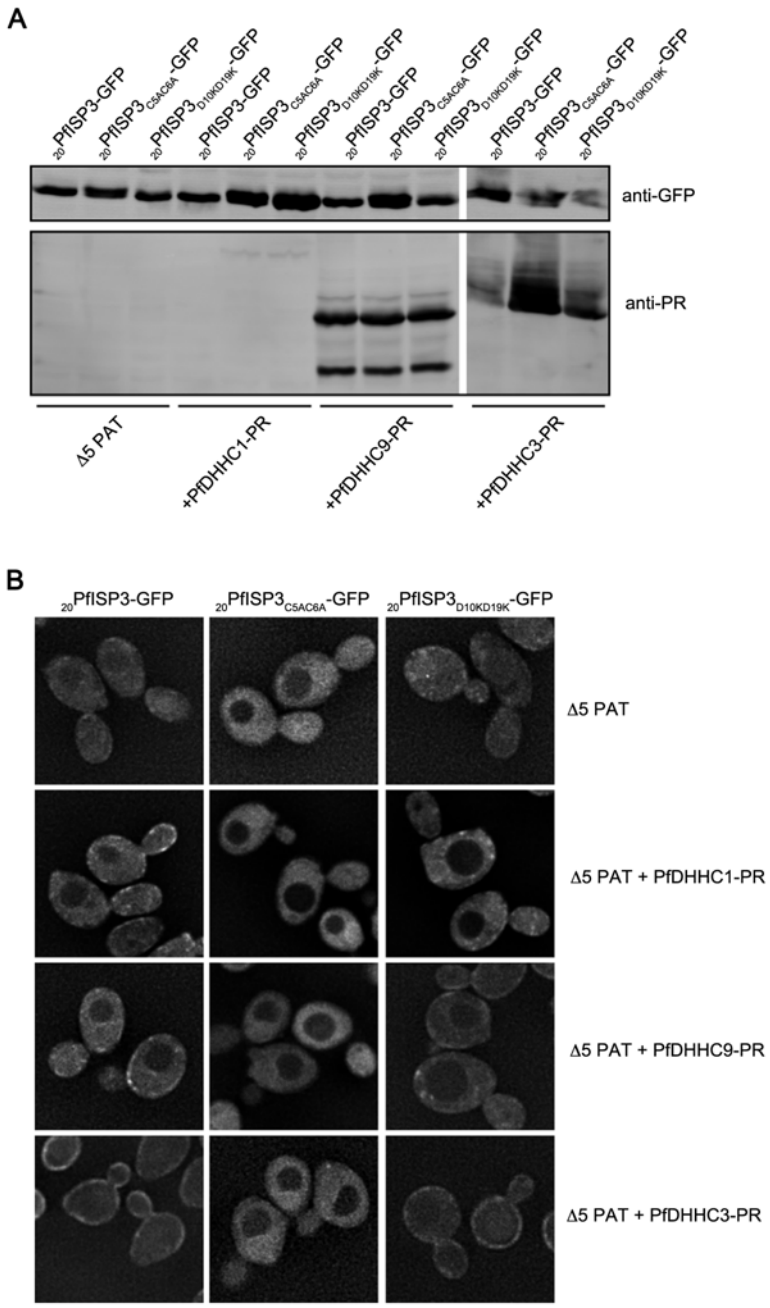

Figure 4.19 Membrane recruitment of PfISP3 by co-expression of PfPATs in yeast. A. Western blots of total cell lysates prepared from the 5 ×Δ DHHC yeast strains expressing different versions of the N-terminus of PFISP3 (wt: wild type; C5AC6A: $_{20}$PfISP3$_{C5AC6A}$ D10KD19K: $_{20}$PfISP3$_{D10KD19K}$) in combination with the Protein A-tagged PfPATs PfDHHC1, PfDHHC9 and PfDHHC3. Expression of PfDHHC9-PR, PfDHHC3-PR as well as the PfISP3 fusion proteins was verified by using anti-Protein A (anti-PR) or anti-GFP antibodies, expression of the larger PfDHHC1 was marginal. **B.** Microscopic analysis of the intracellular distribution of PfISP3-GFP proteins in PfPAT overexpressing strains. Cells were grown to mid-log phase in galactose containing medium and analyzed by fluorescence microscopy. Scale bar: 10 µm.

4.6 Analysis of putative acylprotein thioesterases (APTs)

An immediate consequence of analysis of the *P. falciparum* palmitoylation machinery is the investigation of the depalmitoylating enzymes. The parasite's APTs haven been annotated based on phylogenetic data from *T. gondii* (Kemp et al., 2013). A total number of four PfAPTs (PF11_0211/APT3; MAL8P1.66/APT1/2, MAL8P1.138/APT4) were suggested, wherefrom only PfAPT1 (MAL8P1.66) is upregulated in late parasite stages.

PfAPT1 (MAL8P1.66) is a conserved *Plasmodium* protein. APT1 is located on chromosome 8, has a size of 909 bp (MW: 34.9 kDa) and possesses eleven introns, a signal peptide and 1 transmembrane domain. It is expressed mostly in late parasite stages and gametocytes, but also shows slight upregulation in early ring stages. APT1-peptides were detected by mass spectrometry in schizonts, merozoites, oocytes and salivary gland sporozoites. The protein has an annotated α/β-hydrolase domain (predicted by SUPERFAMILY, E-value: 3.2 E-31).

PfAPT1 was cloned into pARL-1a-GFP and transfected into 3D7 wild type parasites. As previously reported (please refer to 4.1.1), overexpression of the GFP fusion protein is under the control of the *ama1* promoter. Using fluorescence microscopy in unfixed parasites, PfAPT1-GFP localizes to the parasite's PM (Fig. 4.23 A). Expression of the fusion proteins was confirmed by Western blot analysis (Fig. 4.23 B). PfAPT1 runs at 75 kDa and higher than its predicted MW (62 kDa) (Fig. 4.23 B), which might be due to the fact that PfATP1 is heavily phosphorylated (predicted by NetPhos 2.0; Blom et al., 1999).

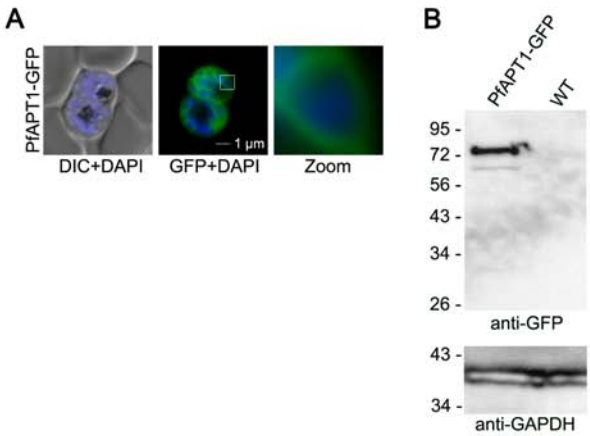

Figure 4.20 Localization pattern of PfAPT1. A. Expression of PfATP1-GFP. The protein reveals a peripheral distribution in unfixed schizont stage parasites. Enlargement of selected area is marked with a white square and referred to as zoom. Nuclei are stained with DAPI. Scale bar: 1 µm. **B.** Western blot analysis using anti-GFP antibodies. A single protein band of about 75 kDa (expected MW: 62 kDa) was detected in the transgenic but not in the parental parasite line.

5. Discussion

The survival of *Plasmodium falciparum* inside its human host ultimately depends on its ability to invade host cells. This process relies on the presence of apical secretory organelles and the inner membrane complex (IMC) (Baum et al., 2008). The IMC underlies the parasite's plasma membrane (PM) and serves as a scaffold during cytokinesis and, furthermore, provides stability to the merozoite during erythrocyte invasion. Correct protein recruitment to the IMC is a prerequisite for the function of this unique structure, which is only present in organisms belonging to the infra-kingdom Alveolata (Cavalier-Smith, 1993; Adl et al., 2005). A variety of IMC proteins were identified that bear different characteristics (Kono et al., 2012, 2013). Here, the focus lies on dual acylated IMC proteins that are potentially anchored to membranes by interaction with a cytoplasmic N-myristoyltransferase (NMT), followed by membrane locking by a specific palmitoyl acyltransferase (PAT).

5.1 Investigation of *Plasmodium falciparum* palmitoyl acyltransferases

The most common forms of protein lipid modification in eukaryotes are N-myristoylation and S-palmitoylation, which are catalyzed by NMTs and PATs, respectively. Protein palmitoylation is the only reversible post-translational lipid modification known and mediates protein-membrane attachment, subcellular trafficking of proteins, protein-protein interactions, protein stability and enrichment of proteins in microdomains on membranes. Palmitoylation is catalyzed by domain of approximately 51 amino acids, the DHHC-cysteine-rich domain (DHHC-CRD). Nevertheless, a consensus palmitoylation motif has not yet been identified and PATs are insufficiently described in *P. falciparum*. Noteworthy, PATs have not been investigated in Apicomplexa at the time when this study was initiated. The purpose of this investigation is to shed light on the mechanism on how membrane specificity for peripheral proteins is achieved, identify the enzymes responsible for this process, and to probe into specific sequence requirements for interaction of PAT-substrate pairs. While this part of the project was ongoing, the localization of PATs to different subcellular localizations in *Toxoplasma gondii* and *P. berghei* was published (Beck et al., 2013; Frénal et al., 2013). The PATs were named after their catalytic domain that consist of an asparagines-histidine-

histidine-cysteine motif (DHHC). Their findings include the existence of two IMC localized PATs in each species:

- TgDHHC2 (TGME49_278850, homologue of PfDHHC2) and
- TgDHHC14 (TGME49_293730, homologue of PfDHHC1) in *T. gondii* (Beck et al., 2013; Frénal et al., 2013)
- PbDHHC3 (PBANKA_092730, homologue of PfDHHC3) and
- PbDHHC9 (PBANKA_093210, homologue of PfDHHC9) in *P. berghei* (Frénal et al., 2013)

Those four PfPATs are late transcribed and also belong to the group of five PATs that were identified in our initial search.

5.1.1 Localization of PfPATs

PATs reside in different tissues and subcellular localizations in *Saccharomyces cerevisiae* and *Arabidopsis thaliana* (Roth et al., 2006; Batistic, 2012) and were recently shown to exhibit distinct organelle-specific localizations in the apicomplexan parasite *T. gondii*: 8 PATs were found at the Golgi complex, 3 at the endoplasmic reticulum (ER), 2 at the PM, 2 at the IMC, 1 PAT localized to the rhoptries (1), 2 PAT localization patterns remain unknown (Beck et al., 2013; Frénal et al., Traffic 2013). Five PATs were also localized in *P. berghei*, with two of them being IMC-localized (PbDHHC3 and PbDHHC9). Only one PAT was localized in *P. falciparum*: PfDHHC7 (Frénal et al., 2013). The overexpressed protein is localized to the rhoptries (Frénal et al., 2013). Moreover, PfDHHC7 was shown to be rhoptry localized in *P. berghei* as well (Beck et al., 2013; please refer to Tab. 5.1). Knockout (KO) of TgDHHC7 leads to scattered rhoptries within the parasite's cytosol (Frénal et al., 2013). Furthermore, TgDHHC7-KO parasites also show invasion defects (Frénal et al., 2013). These effects are most likely due to the failure to recruit proteins important for rhoptry biogenesis and organelle positioning at the apical pole of the parasites and not because TgDHHC7 has a role in the invasion process itself. Interestingly, these KO parasites show the same phenotype as TgARO-KO parasites (Mueller et al., 2013). This armadillo repeats only (ARO) protein is like the PfISPs myristoylated and palmitoylated at its N-terminus. The plasmodial homologue PfARO is recruited to the rhoptries in a sequence-dependent manner and is attached to the cytosolic face of the rhoptry membrane (Cabrera et al., 2012). Like its *T. gondii* homologue, it might be implicated in rhoptry biogenesis. This function could be mediated by its armadillo repeats, which function in protein-protein interaction (Tewari et al., 2010). For instance, the

yeast homologue of ARO, Vac8, is well characterized and essential for vacuole fusion and inheritance (Subramanian et al., 2006). PfDHHC7-dependent recruitment of ARO could fulfill a similar function by being important for membrane fusion of transport vesicle to the rhoptry membrane.

Table 5.1 List of PATs in *P. falciparum*, *P. berghei* and *T. gondii*. TgPATs without homologues in *P. falciparum* are not listed. IMC localization is indicated in light blue. Investigated PATs are marked in grey. Not expressed means that the endogenous protein was not detected by live cell fluorescence microscopy or Western blot analysis. N.d. = not defined. - = no homologue.

Name	*P. falciparum* localization	*P. berghei* localization/ essentiality	*T. gondii* homologue	*T. gondii* localization/ essentiality
PfDHHC1	IMC	n.d.	TgDHHC14	IMC/yes
PfDHHC2	ER	n.d	TgDHHC2	IMC/yes
PfDHHC3	PM	IMC/no	TgDHHC13	PM/no
PfDHHC4	n.d.	n.d.	TgDHHC4	PM/no
PfDHHC5	n.d.	ER/no	TgDHHC17	Golgi/no
PfDHHC6	n.d.	n.d.	TgDHHC15/ TgDHHC18	Golgi/n.d. No/n.d
PfDHHC7	n.d.	Rhoptry/no	TgDHHC1/ TgDHHC7	Golgi/no Rhoptries/yes
PfDHHC8	n.d.	Punctuate, not Golgi/n.d.	-	-
PfDHHC9	Apical	IMC/no	-	-
PfDHHC10	n.d.	n.d.	TgDHHC10	n.d
PfDHHC11	n.d.	n.d.	-	-
PfDHHC12	n.d.	-	-	-

PfDHHC1 is an IMC localized PAT

PfDHHC1 is annotated as a palmitoyltransferase and was unambigiously localized to the IMC of *P. falciparum* (Fig. 4.2, 4.3, 4.5). To further prove that PfDHHC1 is exclusively localized to the IMC and is not resident in the Golgi complex as suggested previously (Seydel et al., 2005), the tER marker PfSec13p-mCherry was transfected into the 3D7-PfDHHC1-GFP cell line. Live cell imaging reveals a localization of PfSec13p to the Golgi complex in trophozoite stage parasites without colocalizing with PfDHHC1 (Fig. 4.5 B). The previous study relied exclusively on the immunofluorescence assay (IFA) and co-localization studies with PfERD2. However, the specificity of the anti-PfDHHC1 was not rigorously confirmed (for instance by

a transgenic approach). Additionally, localization attempts of the endogenously tagged PfDHHC1 in earlier stages (e.g. trophozoites) revealed no detectable PfDHHC1. This is in agreement with the provided stage-specific Western blot (Fig. 4.3 D) and the published transcriptional profile of this gene (www.plasmodb.org).

Further, the provided localization analysis is in agreement with the localization data obtained from *T. gondii*, where the homologue TgDHHC14 also localizes to the IMC (Beck et al., 2013; Frénal et al., 2013). Noteworthy, the homologue in *T. gondii* was found to be essential for parasite survival (Frénal et al., 2013). Whether this is also true for the plasmodial homologue remains to be determined, however, it is highly likely that PfDHHC1 is essential, too. Since there are only six late transcribed PATs and PfDHHC1 is the only one that localizes to the IMC so far, it possible that it is the only IMC PAT in *P. falciparum* and, thus, has a crucial biological function.

Interestingly, in addition to the DHHC domain, PfDHHC1 also harbors ankyrin repeats that are stretched over 30 amino acids in proximity to the protein's N-terminus. Ankyrin repeats are found in other PATs in a variety of species, including *S. cerevisiae* (Akr1) and *Homo sapiens* (HIP14) (Roth et al., 2002; Singaraja et al., 2002). Importantly, the N-terminus, the DHHC-CRD and the C-terminus of PfDHHC1 are predicted to face the cytosolic face of the membrane. Hence, the ankyrin repeats might act in concert with the other cytosolic domains and facilitate substrate recognition (Gonzalez-Montoro et al., 2009; Beck et al., 2013). This dual step mechanism could provide additional control points. This is of great importance, because anchoring of arbitrary proteins to the IMC could negatively affect the proper function of the IMC.

The protein composition of the IMC of gametocytes is comparable to the IMC in merozoites with some exceptions (stage-specific expression of some alveolins). However, the gametocyte IMC has not been studied in great detail. Some structural insight into the IMC architecture was derived from early freeze-fracture studies and recent localization studies (Meszoely et al., 1987; Dearnley et al., 2011; Kono et al., 2012, 2013). The gametocyte IMC contains 10 – 15 cisternae that are connected at transverse sutures (Meszoely et al., 1987; Dearnley et al., 2011; Kono et al., 2012). This is in contrast to the architecture of the IMC in merozoites and the sporozoites, where the IMC appears to consist of one vesicle (Kono et al., 2012). The sutures give the gametocyte a segmented appearance. So far, only one the *Plasmodium*-specific protein MAL13P1.228 could be localized to these structures (Kono et al., 2012). PfDHHC1 shows a localization pattern resembling those sutures throughout gametocytogenesis (Fig.

4.4) although co-localization studies are needed to confirm this notion. It is interesting to speculate, why PfDHHC1 appears to accumulate in the sutures. Besides recruiting proteins to the IMC membrane, PfDHHC1 might be responsible for the linkage of the individual sutures either by physically connecting the membranes or by facilitating the recruitment of other proteins to the IMC that fulfill this task.

PfDHHC2, PfDHHC3 and PfDHHC9 do not localize to the IMC

Besides PfDHHC1, all other plasmodial PATs are all annotated as DHHC-type zinc finger proteins with unknown function. Zinc fingers usually bind DNA, RNA, proteins or other small molecules, and use one or more zinc ions or other metal ions to stabilize the fold (Hall, 2005; Brown, 2005; Gamsjaeger et al., 2007). Several classes of zinc fingers exist; most commonly they harbor a CCHH, CCHC or CCCC motif (C: cysteine, H: histidine; Laity et al., 2001). On the contrary, the DHHC motif shows a high level of conservation among eukaryotes (Putilina et al., 1999), suggesting a fundamental role of these amino acids and their secondary structure for PAT function.

None of the three other PfPATs analyzed in this study resemble IMC distribution as overexpressed proteins. However, they were not tagged endogenously. Future experiments are needed to localize the endogenous enzymes unambiguously. It will be particularly interesting to investigate PfDHHC9 in more detail, since it is essential for gametocyte development (Ikadai et al., 2013). Using transposon-mediated mutagenesis, *pfdhhc9* was identified among 15 other genes to be essential. Gene disruption led to an arrest of parasite development at stage I gametocytes, indicating that this PAT is probably important for gametocyte maturation (Ikadai et al., 2013).

Using the more recently established Flp/Cre-recombinase technique (O'Neill et al., 2011; Lacroix et al., 2011; Collins et al., 2013) or the FKBP system (Banaszynski et al., 2006; Armstrong and Goldberg, 2007) to study protein essentiality will give more insight into the function of PATs and their biological functions besides palmitoylation.

Taken together, this data demonstrates that *P. falciparum*, like other eukaryotic organisms, harbors a set of PATs that shows distinct subcellular localization (Ohno et al., 2006; Batistic, 2012; Frénal et al., 2013). However, the subcellular localization of the individual PATs should be analyzed by the expression of endogenously tagged proteins to deliver a spatial "PAT-map" in *P. falciparum.* Based on the palmitoyl proteome and independent studies

investigating single palmitoyl proteins, it is highly likely that PATs are also highly transcriptionally controlled, resulting also in a temporal PAT-map where individual PATs are restricted to gametocytes, sporozoites and oocystes (Bozdech et al., 2003; Corvi et al., 2011; Jones et al., 2012). The identification of a comprehensive spatio-temporal PAT map will also help to understand the specific mechanism for PAT-substrate interaction.

5.2 Characterization of PfISPs

Protein palmitoylation has recently gained increased attention in the malaria community with the publication of the *P. falciparum* palmitoyl proteome (Jones et al., 2012). Several IMC proteins were identified as palmitoyl proteins in that study, among those dual acylated proteins like PfISP1 (PF10_0107) and PfISP3 (PF14_0578), as well as the established IMC marker GAP45 and the aforementioned rhoptry protein PfARO. The PfISPs are homologues of the *T. gondii* ISPs and termed PfISP3 and PfISP1, respectively (Beck et al., 2010; Fung et al., 2012; Poulin et al., 2013). All ISPs, except TgISP4, display a similar amino acid motif in their N-terminus (Beck et al., 2010; Fung et al., 2012; Cabrera et al., 2012; Poulin et al., 2013).

5.2.1 Importance of myristoylation and palmitoylation for membrane attachment of PfISP1 and PfISP3

Full length and truncated versions of the PfISPs were previously analyzed in the Gilberger laboratory: the first 20 N-terminal amino acids of PfISP1 and PfISP3 were shown to be sufficient for IMC localization (Hu et al., 2010; Cabrera et al., 2012). PfISP3 and PfISP1 display a similar N-terminal amino acid sequence (Cabrera et al., 2012; Fig. 4.14). Using click chemistry and acyl-biotin exchange assays followed by mass spectrometry, both proteins were shown to be palmitoylated (Jones et al., 2012). Recently, they were also proven to be myristoylated (Wright et al., 2013). Noteworthy, these studies were published after the vast majority of experiments of this thesis were carried out.

Mutation of these lipid acceptor sites abolished IMC localization and led to an accumulation of the fusion proteins in the cytoplasm of the parasites (PfISP3$_{G2A}$-GFP, PfISP3$_{C5AC6A}$-GFP;

$_{20}$PfISP1$_{G2A}$-GFP, $_{20}$PfISP1$_{C7AC8A}$-GFP Fig. 4.12). Interestingly, mutation of only one of the palmitoylated cysteines does not render the localization of PfISP3 (Fig. 4.13), demonstrating that one palmitoylation site can compensate the function of the other. The fact that the PfISPs still harbor two palmitoylation sites, even though one is sufficient for membrane attachment might be due to the fact that a bipartite palmitoylation site promotes stronger membrane affinity. This aspect would favor a permanent IMC membrane attachment of the PfISPs over them being dynamically associated with the membrane by undergoing cycles of palmitoylation and depalmitoylation.

5.2.2 Mutational analysis of amino acid sequence to probe into membrane specificity of PfISPs

Palmitoylation and myristoylation sites are clearly of importance for membrane targeting of PfISPs, but it is not clear how sequence specificity is mediated. While a consensus motif for myristoylation has been described (Resh, 1999; Maurer-Stroh et al., 2002) as MGxxxC/S/T, an amino acid sequence for palmitoylation has not yet been identified. Since the first 20 N-terminal amino acids localize to the IMC, the minimal sequence for IMC targeting was further narrowed down: the first 10 amino acids are sufficient for IMC targeting of PfISP3 (Fig. 4.15). Similar results were obtained for PfISP1, where again 10 amino acids were sufficient for IMC localization of the fusion protein (Fig. 4.17). Consequently, future mutants were generated using these truncated versions. This is an advantage, since putative interference with other determinants for membrane specificity like protein-protein interaction or structural features can be excluded. Mutational analysis targeting the charged amino acids within that short stretch revealed that replacement of the asparagine with a neutral glycine or a positively charged arginine leaves the protein IMC-attached (Fig. 4.15). However, introducing a positively charged lysine led to a redistribution of the PfISPs to the PM (Fig. 4.15, 4.17). To further test whether these principles are also applicable to other dual acylated proteins, the calcium-dependent phosphokinase 1 (CDPK1; Möskes et al., 2004) was analyzed. Its first 20 N-terminal amino acids localize to the PM and have a predicted myristoylation and palmitoylation site (Cabrera et al., 2012). Mutating all positively charged amino acids into negatively charged asparagines led to a redistribution of the fusion protein to the IMC (Fig. 4.18). Future research dissecting the discriminative parameters between IMC and PM localized proteins will give further insight into determinants for palmitoylation by a specific PAT.

A recent study from our lab dissected the sequence requirements for rhoptry localization of the dual acylated PfARO (PFD0720w; Cabrera et al., 2012). Mutational analysis of the protein revealed an involvement of the positively charged arginine on position 9 in rhoptry targeting. Replacement of arginine 9 with glutamine resulted in a cytosolic localization, which implies that the positive charge of arginine at this particular position carries important trafficking-information (Cabrera et al., 2012). In agreement with this, all experimentally localized rhoptry fusion proteins (PF08_0062, PFL1110c), including PfARO, display an arginine two amino acids apart from the palmitoylated cysteines (Cabrera et al., 2012). To test if retargeting of PfISPs to the rhoptry membrane is possible, the amino acid sequence of PfARO was adapted to PfISP3, generating a construct mimicking the amino acid sequence of PfARO. Indeed, this mutant localized to the apical end of merozoites (Fig. 4.16) and showed some additional PM staining. In summary, targeting of dual acylated proteins to phylum-specific organelles seems to rely on complex trafficking information that is conserved within a short N-terminal amino acid stretch.

5.2.3 PfISPs – *sub*-compartment markers?

Besides similarities in protein composition, the general architecture of the IMC differs significantly among alveolate species (Kono et al., 2013): In *P. falciparum* blood stage parasites, the IMC appears to consist of a single vesicle (Raibaud et al., 2001; Kono et al., 2012), whereas the *T. gondii* tachyzoite consists of several vesicles. In *T. gondii*, the distribution of the individual ISPs are defining three sub-compartments: TgISP1 is localized to the apical cap, TgISP2 and TgISP4 are localized to the proximal part of the tachyzoite, and TgISP3 is localized to the proximal and basal regions (Beck et al., 2010; Fung et al., 2012). In *P. falciparum* merozoites, endogenously tagged PfISP1 and PfISP3 are evenly distributed within the cell (Fig. 4.6, 4.9). This again argues for only one spherical IMC vesicle with no sub-compartments. Nevertheless, in presexual gametocytes, PfISP1 appears to be more concentrated towards the poles of the developing gametocytes. Additionally, distinct stripe-like structures (Fig. 4.10) are visible. It remains to be determined, whether PfISP1 localizes to the same structures in gametocytes as PfDHHC1. But the pronounced polar distribution of PfISP1 in sexual blood stage parasites might define these sub-compartments.

Investigating the function of the PfISPs will be crucial to gain a better understanding of the IMC and, therefore, of the *P. falciparum* biology. Attempts to characterize the ISPs in more detail came from the *T. gondii* field (Beck et al., 2010, 2013). Based on the phylogenetic

conservation of this family, protein functions could possibly be conserved. In *T. gondii*, ISP2 has been implicated in cytokinesis, since deletion of the gene led to the production of parasites that have impaired replication, however, the remaining TgISPs were not essential (Beck et al., 2010; Fung et al., 2012). It is highly likely that TgISP2 carries out its roles in cytokinesis by interacting with other proteins. The protein has a predicted pleckstrin homology (PH) fold (E-value: 5.00e-29; predicted by SMART; Schultz et al., 1998; Letunic et al., 2012). Crystallization of TgISP1 and TgISP3 revealed that both proteins have a PH domain (Tonkin et al., 2014), which mediate protein-protein interactions. The plasmodial homologues also have predicted PH domains (see 1.3.2), which implicates that ISPs have conserved functions. By recruiting important interaction partners to the IMC, the family of ISP proteins might be involved in cytokinesis or in tethering of organelles to the IMC (Kudryashev et al., 2010). However, this tethering was so far only observed in sporozoites, where the nucleus, the mitochondrium, the apicoplast and microtubules were shown to be tethered to the IMC via linker molecules derived from the subpellicular network (SPN) (Kudryashev et al., 2010). It is likely that similar cellular features exist in other developmental stages, especially in gametocytes.

Another interesting feature of PfISP3 is its predicted phosphorylation site (serine 16) close to the palmitoylation site. This might represent a regulatory mechanism, similar to the one of phosphodiesterase 10A (PDE10A) (Charych et al., 2010): at low cAMP levels, PDE10A becomes palmitoylated and attached to the PM, where it regulates intracellular signaling. High cAMP levels promote phosphorylation of PDE10A by protein kinase A (PKA). Consequently, PDE cannot be palmitoylated since it is inaccessible to the PAT. PDE10A on the other hand has a catalytic activity and can regulate cAMP levels (Charych et al., 2010).

5.2.4 Model of membrane recruitment of dual acylated proteins by specific PATs

Trafficking of dual acylated proteins to their specific membrane has been described as the kinetic bilayer-trapping hypothesis, which postulates that a nascent protein is first myristoylated by a cytoplasmic N-myristoyl transferase (NMT) and transiently interacts with several membranes due to the increased lipophilicity. The protein will eventually get stably attached to a specific membrane after being recognized by a specific PAT (Fig. 5.1; Resh, 1999). This theory seems to be true for the PfISPs, since mutation of the myristoylated glycine leads to abolishment of membrane association. Furthermore, by mutating the palmitoylated cysteines and the charged amino acid residues or introducing an artificial

sequence, the proteins become cytosolic for the first case or have altered membrane specificity.

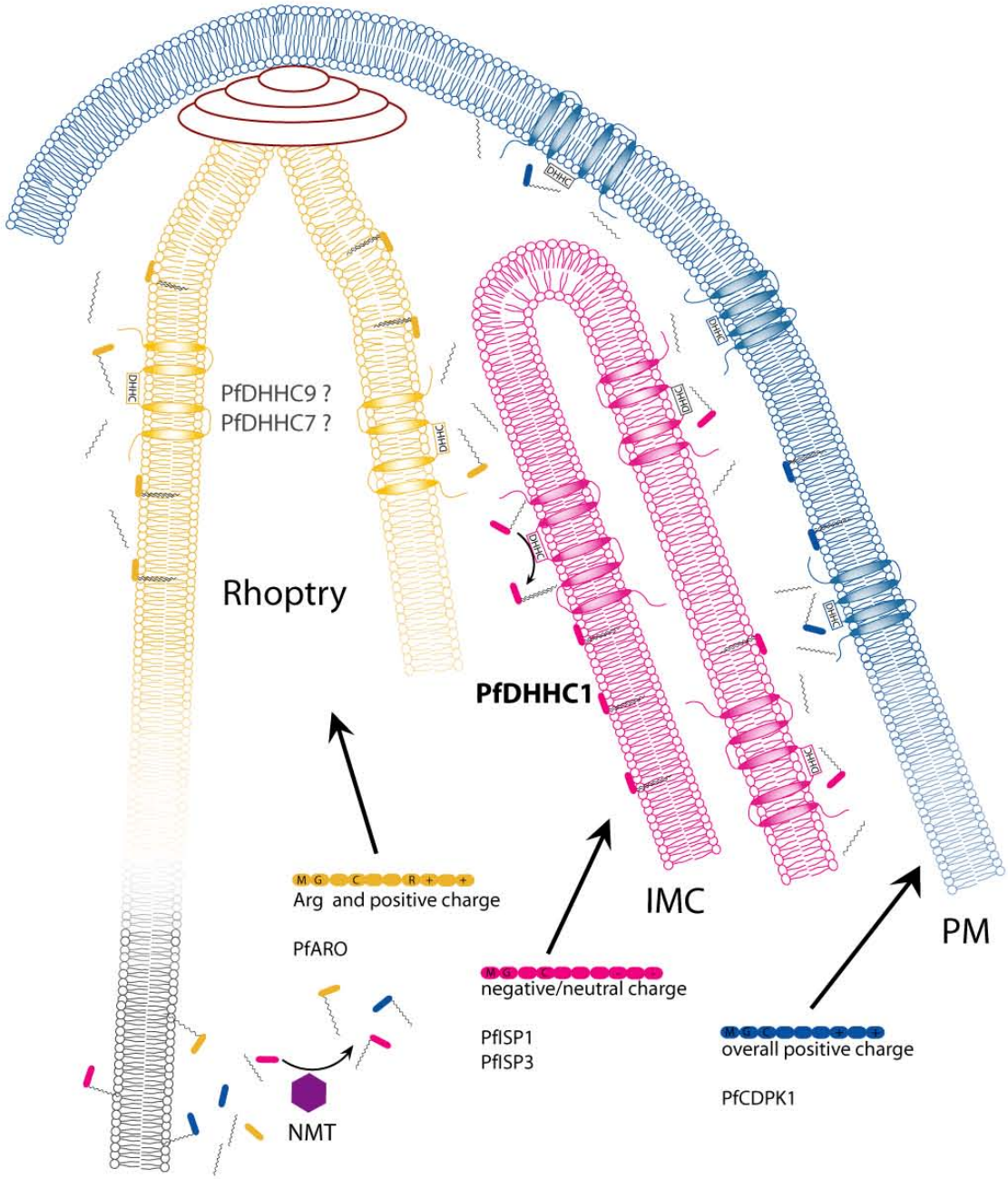

Figure 5.1 Trafficking model for membrane recruitment of dual acylated proteins to different endomembranes in *P. falciparum*. Proteins are cotranslationally myristoylated by the cytosolic NMT (bottom of the schematic). Myristoylated proteins encounter endomembrane-integrated PATs that palmitoylate their specific substrates. Palmitoylation of the now dual acylated proteins anchors them at the individual membranes. PM (blue), IMC (pink), rhoptries (yellow).

Interestingly, the depalmitoylating enzyme PfAPT1 (MAL8P1.66) is upregulated in late parasite stages and was localized to the parasite's PM in an overexpression cell line (Fig.

4.20). Localization of depalmitoylating enzymes to the PM could be an advantage because it mediates a highly dynamic regulation of proteins and their palmitoylation state.

5.3 Protein lipid modifications as drug targets

PATs are interesting drug targets since palmitoylation is needed to maintain basic cell function. PfDHHC1 resides in a phylum-specific membrane that is not present in any mammalian cell type. Five TgPATs were shown to be essential for parasite survival, among them the PfDHHC1 homologue TgDHHC14 (Frénal et al., 2013). This might be due to its role for recruitment of IMC proteins that support its role in motility, cell stability and cytokinesis. Unfortunately, established palmitoylation inhibitors seem to have a pleiotropic effect on the cell and further harbor and unknown mechanism of action (Draper and Smith, 2009; Jones et al., 2012). Future work is needed to identify more specific inhibitors to validate PfDHHC1 as a drug target.

Targeting myristoylation already show some promising results in anti-parasitic drug discover (Panethymitaki et al., 2006; Bowyer et al., 2007; Bowyer et al., 2008; Frearson et al., 2010; Crowther et al., 2011; Tate et al., 2014). A recently published study identified specific inhibitors of the *P. falciparum* NMT (Wright et al., 2014). Among several compounds, 2a was the most promising candidate that showed *in vivo* activity and interfere with the IMC targeting of PfISPs, GAP45 and MTIP (Wright et al., 2014).

5.4 A new experimental approach to study PAT-substrate interaction

The identification of organelle-specific PATs implicates a specific mechanism for PAT-substrate interaction and the possibility that specific PAT-substrate pairs exist. From the mutational analysis of amino acid residues of PfISPs, it is evident that the amino acid identity adjacent to palmitoylation sites has an impact on substrate targeting (see above, section 5.2.2). It was shown that amino acids flanking the palmitoylation sites need to be hydrophilic for palmitoylation to take place (El-Husseini et al., 2001). Other research groups show that sequences adjacent to palmitoylated cysteines are not important for substrate recognition in

mammalian cells (Rocks et al., 2006) or even that specific PATs have overlapping substrate-specificity (Roth et al., 2006; Hou et al., 2009; Huang et al., 2009). Even though it is not clear how substrate specificity is achieved on the amino acid sequence level, various PAT-substrate pairs have been identified (Linder and Deschenes, 2007; Huang et al., 2009; Salaun et al., 2010; Greaves and Chamberlain, 2011; Zhang et al., 2013). Two general approaches have been used to identify PAT-substrate pairs (reviewed in Planey and Zacharias, 2009): I) a PAT with specificity for a known palmitoyl protein via PICA (palmitoyl cysteine identification capture and analysis; Drisdel and Green, 2004; Zhang et al., 2008); II) identification of an unknown substrate of an individual PAT via metabolic labeling using radiolabeled palmitate (Fukata et al., 2006) or using bio-orthogonal probes (Kostiuk et al., 2008). Mammalian PAT-substrate pairs were mostly identified using a co-overexpression approach and revealed that some PATs have wide-ranging substrate specificity, while others seem to be more selective (Greaves and Chamberlain, 2011). Likewise, PAT substrates show different levels of specificity when interacting with PATs. One study used co-overexpression followed acyl-biotin exchange assay (ABE) to identify PAT-substrate pairs (Huang et al., 2009). Certain substrate specificity was identified for some human brain PATs that reside in the Golgi and specificity was further confirmed by siRNA-mediated knockdowns of endogenous PATs (Huang et al., 2009). Another study revealed that the synaptosomal-associated protein of 23 kDa (SNAP23) is palmitoylated by DHHC3. After exchange of the DHHC-CRD of DHHC3 with the one from DHHC15, the resulting chimeric PAT doesn't restore the enzyme's function and is no longer able to palmitoylate SNAP23 (Greaves et al., 2010). Specific PAT-substrate pairs also were identified in yeast using complex palmitoylation assays combined with mutational analysis (reviewed in Linder and Deschenes, 2007). Yeast PATs show a considerable substrate redundancy when over-expressed (Roth et al., 2006; Hou et al., 2009). For instance, Pfa3 and Erf2 function can be complemented by over-expression of other yeast PATs (Hou et al., 2009). In contrast, González-Montoro and colleagues showed that the yeast PAT Swf1 is highly specific from both the enzyme and substrate perspective (González-Montoro et al., 2011).

The above summarized efforts to study PAT-substrate interactions and PAT function is only a small part of the research carried out in the past years. Clearly, considerable efforts were undertaken to identify specific sequence requirements for substrate specificity of PATs, nonetheless a clear consensus sequence for individual PATs has not yet been identified, leaving us with the question how peripheral membrane proteins are recruited to specific membrane systems such as the IMC.

To experimentally probe into substrate selectivity some of the parasite PATs, the enzymes and putative substrates were co-expressed in a yeast strain devoid of five of its seven PATs (Fig. 4.19). This work was done in collaboration with the Ungermann laboratory in Osnabrück. In the absence of any heterologous expressed PAT in this yeast strain $_{20}$PfISP3-GFP remains cytosolic, showing that the endogenous PAT activity of the yeast does not lead to membrane association of the fusion protein. Although the experimental set up did not allow for strong expression of PfDHHC1, a significant difference in the membrane recruitment of $_{20}$PfISP3-GFP upon expression of either PfDHHC3 or PfDHHC9 was evident. Strong localization of PfISP3 to the yeast plasma membrane with PfDHHC3, and some with PfDHHC9 was observed. Given the similarity in size, topology and similar expression level of these two enzymes in the yeast heterologous system (Fig. 4.19), this difference might point towards distinct substrate specificity. Coincidentally, over-expressed PfDHHC3 is localized in the plasma membrane of the parasite that was previously shown to be the default pathway for dual lipidated proteins (Cabrera et al., 2012). The default pathway would require a PAT with broad substrate specificity or additional PATs with complementing specificity. Then again, association with the rhoptry membrane needs very specific sequence requirements like an arginine in close proximity to the palmitoylated cysteine; PfDHHC9 might be associated with the rhoptry membrane. Future work exploiting this co-expression system with its visual read-out might be instrumental for comprehensively addressing the substrate specificity of the PATs. It could be also instrumental for screening approach investigating specific sequence requirements for individual PATs of the parasite localized to different membranous systems.

The establishment of a yeast system to study specific PAT-substrate pair represents new means to comprehend the precise interactions of a PAT with one or more potential substrate. Even though protein expression needs to be optimized for scarcely expressed protein candidates, it is evident that this new strategy to study interaction patterns represents a powerful tool to investigate protein palmitoylation in *P. falciparum* as well as in other organisms.

5.6 Conclusion and outlook

The findings help not only to understand the parasite biology in general, but also have specific implications in better understanding the IMC and its highly diverse set of proteins. Furthermore, partial analysis of the enzymatic machinery that carries out protein palmitoylation in *P. falciparum* indicates that the parasite uses this lipid modification to recruit proteins to its unique set of organelles. However, confirmation of *in vivo* enzyme activities, functional studies and further research concerning the parasite's complete PAT repertoire and their potential substrates is necessary. The results and transgenic cell lines generated in this project provide important tools to analyze the function of the parasite's IMC in more detail. With the newly established cell lines, detailed functional analysis of proteins can be accomplished. Special focus on the function of PfISPs in asexual blood stages as well as in presexual gametocyte stages will further evaluate the importance of the IMC of the parasite. This is of major interest, since especially the *P. falciparum* gametocyte architecture in respect of the IMC is exceptional and almost unexplored.

The establishment of a yeast system to study specific PAT-substrate pair represents new means to comprehend the precise interactions of a PAT with one or more potential substrate. Even though protein expression needs to be optimized for scarcely expressed protein candidates, it is evident that this new strategy to study interaction patterns represents a powerful tool to investigate protein palmitoylation in *P. falciparum* as well as in other organisms.

6. References

Abrahamsen, M. S., Templeton, T. J., Enomoto, S., Abrahante, J. E., Zhu, G., Lancto, C. A., ... and Kapur, V. (2004). Complete genome sequence of the apicomplexan, Cryptosporidium parvum. Science. 304, 441-445.

Adl, S., and Leander, B. (2007). Diversity, nomenclature, and taxonomy of protists. Syst. Biol. *56*, 684–689.

Adl, S.M., Simpson, A.G.B., Farmer, M.A., Andersen, R.A., Anderson, O.R., Barta, J.R., Bowser, S.S., Brugerolle, G., Fensome, R.A., Fredericq, S., et al. (2005). The new higher level classification of eukaryotes with emphasis on the taxonomy of protists. J. Eukaryot. Microbiol. *52*, 399–451.

Agnandji, S.T., Lell, B., Fernandes, J.F., Abossolo, B.P., Methogo, B.G.N.O., Kabwende, A.L., Adegnika, A.A., Mordmüller, B., Issifou, S., Kremsner, P.G., et al. (2012). A phase 3 trial of RTS,S/AS01 malaria vaccine in African infants. N. Engl. J. Med. *367*, 2284–2295.

Aicart-Ramos, C., Valero, R.A., and Rodriguez-Crespo, I. (2011). Protein palmitoylation and subcellular trafficking. Biochim. Biophys. Acta *1808*, 2981–2994.

Alonso, a M., Coceres, V.M., De Napoli, M.G., Nieto Guil, a F., Angel, S.O., and Corvi, M.M. (2012). Protein palmitoylation inhibition by 2-bromopalmitate alters gliding, host cell invasion and parasite morphology in *Toxoplasma gondii*. Mol. Biochem. Parasitol. *184*, 39–43.

Amino, R., Thiberge, S., Martin, B., Celli, S., Shorte, S., Frischknecht, F., and Ménard, R. (2006). Quantitative imaging of *Plasmodium* transmission from mosquito to mammal. Nat. Med. 12, 220-224.

Anderson-White, B.R., Ivey, F.D., Cheng, K., Szatanek, T., Lorestani, A., Beckers, C.J., Ferguson, D.J.P., Sahoo, N., and Gubbels, J. (2012). A family of intermediate filament-like proteins is sequentially assembled into the cytoskeleton of *Toxoplasma gondii*. Cell. Microbiol. *13*, 18-31.

Aneck-Hahn, N.H., Schulenburg, G.W., Bornman, M.S., Farias, P., and de Jager, C. (2007). Impaired semen quality associated with environmental DDT exposure in young men living in a malaria area in the Limpopo Province, South Africa. J. Androl. *28*, 423–434.

Aravind, L., Iyer, L., Wellems, T., and Miller, L. (2003b) *Plasmodium* Biology: Genomic Gleanings. Cell, 115, 771-785.

Armstrong, C.M., and Goldberg, D.E. (2007). An FKBP destabilization domain modulates protein levels in *Plasmodium falciparum*. Nat. Methods. *4*, 1007–1009.

Babu, P., Deschenes, R.J., Robinson, L.C. (2004). Akr1p-dependent palmitoylation of Yck2p yeast casein kinase 1 is necessary and sufficient for plasma membrane targeting. J. Biol. Chem. 279, 27138–27147.

Baker, D.A. (2010). Malaria gametocytogenesis. Mol. Biochem. Parasitol. *172*, 57–65.

Banaszynski, L.A., Chen, L.-C., Maynard-Smith, L.A., Ooi, A.G.L., and Wandless, T.J. (2006). A rapid, reversible, and tunable method to regulate protein function in living cells using synthetic small molecules. Cell *126*, 995–1004.

Bannister, L.H., Hopkins, J.M., Fowler, R.E., Krishna, S., and Mitchell, G.H. (2000) Ultrastructure of rhoptry development in *Plasmodium falciparum* erythrocytic schizonts. Parasitology 121 (Part 3): 273–287.

Bannister, L.H., Hopkins, J.M., Dluzewski, A.R., Margos, G., Williams, I.T., Blackman, M.J., Kocken, C.H., Thomas, A.W., and Mitchell, G.H. (2003). *Plasmodium falciparum* apical membrane antigen 1 (PfAMA-1) is

translocated within micronemes along subpellicular microtubules during merozoite development. J. Cell Sci. *116*, 3825–3834.

Barker, R.H., Urgaonkar, S., Mazitschek, R., Celatka, C., Skerlj, R., Cortese, J.F., Tyndall, E., Liu, H., Cromwell, M., Sidhu, A.B., et al. (2011). Aminoindoles, a novel scaffold with potent activity against *Plasmodium falciparum*. Antimicrob. Agents Chemother. *55*, 2612–2622.

Bartels, D.J., Mitchell, D.A., Dong, X., Deschenes, R.J., Bartels, D.J., Mitchell, D.A., and Dong, X. (1999). Erf2, a Novel Gene Product That Affects the Localization and Palmitoylation of Ras2 in *Saccharomyces cerevisiae* Erf2 , a Novel Gene Product That Affects the Localization and Palmitoylation of Ras2 in Saccharomyces cerevisiae. Mol. Cell. Biol. 19, 6775-6787.

Bartoloni, A., and Zammarchi, L. (2012). Clinical aspects of uncomplicated and severe malaria. Mediterr. J. Hematol. Infect. Dis. *4*, e2012026.

Batistic, O. (2012). Genomics and localization of the Arabidopsis DHHC-cysteine-rich domain S-acyltransferase protein family. Plant Physiol. *160*, 1597–1612.

Baum, J., Papenfuss, A.T., Baum, B., Speed, T.P., and Cowman, A.F. (2006). Regulation of apicomplexan actin-based motility. Nat. Rev. Microbiol. *4*, 621–628.

Baum, J., Gilberger, T.-W., Frischknecht, F., and Meissner, M. (2008). Host-cell invasion by malaria parasites: insights from *Plasmodium* and *Toxoplasma*. Trends Parasitol. *24*, 557–563.

Beck, J.R., Rodriguez-Fernandez, I. a, Cruz de Leon, J., Huynh, M.-H., Carruthers, V.B., Morrissette, N.S., and Bradley, P.J. (2010). A novel family of Toxoplasma IMC proteins displays a hierarchical organization and functions in coordinating parasite division. PLoS Pathog. *6*, e1001094.

Beck, J.R., Fung, C., Straub, K.W., Coppens, I., Vashisht, A. a, Wohlschlegel, J. a, and Bradley, P.J. (2013). A Toxoplasma Palmitoyl Acyl Transferase and the Palmitoylated Armadillo Repeat Protein TgARO Govern Apical Rhoptry Tethering and Reveal a Critical Role for the Rhoptries in Host Cell Invasion but Not Egress. PLoS Pathog. *9*, e1003162.

Bhatnagar, R.S., Fütterer, K., Farazi, T. a, Korolev, S., Murray, C.L., Jackson-Machelski, E., Gokel, G.W., Gordon, J.I., and Waksman, G. (1998). Structure of N-myristoyltransferase with bound myristoylCoA and peptide substrate analogs. Nat. Struct. Biol. *5*, 1091–1097.

Blom, N., Gammeltoft, S., and Brunak, S. (1999). Sequence- and structure-based prediction of eukaryotic protein phosphorylation sites. J. Molec. Biol. 294, 1351-1362.

Bowyer, P.W., Gunaratne, R.S., Grainger, M., Withers-Martinez, C., Wickramsinghe, S.R., Tate, E.W., Leatherbarrow, R.J., Brown, K.A., Holder, A.A., and Smith, D.F. (2007). Molecules incorporating a benzothiazole core scaffold inhibit the N-myristoyltransferase of *Plasmodium falciparum*. Biochem. J. *408*, 173–180.

Bowyer, P.W., Tate, E.W., Leatherbarrow, R.J., Holder, A.A., Smith, D.F., and Brown, K.A. (2008). N-myristoyltransferase: a prospective drug target for protozoan parasites. ChemMedChem *3*, 402–408.

Bozdech, Z., Llinás, M., Pulliam, B.L., Wong, E.D., Zhu, J., and DeRisi, J.L. (2003). The Transcriptome of the Intraerythrocytic Developmental Cycle of *Plasmodium falciparum*. PLoS Biol. *1*, E5.

Brown, R. S. (2005). Zinc finger proteins: getting a grip on RNA. Curr. Opin. Struct. Biol. 15, 94-98.

Bullen, H.E., Tonkin, C.J., O'Donnell, R. a, Tham, W.-H., Papenfuss, A.T., Gould, S., Cowman, A.F., Crabb, B.S., and Gilson, P.R. (2009). A Novel Family of Apicomplexan Glideosome-associated Proteins with an Inner Membrane-anchoring Role. J. Biol. Chem. *284*, 25353–25363.

Butler, N.S., Schmidt, N.W., Vaughan, A.M., Aly, A.S., Kappe, S.H.I., and Harty, J.T. (2011). Superior antimalarial immunity after vaccination with late liver stage-arresting genetically attenuated parasites. Cell Host Microbe *9*, 451–462.

Cabrera, A., Herrmann, S., Warszta, D., Santos, J.M., John Peter, A.T., Kono, M., Debrouver, S., Jacobs, T., Spielmann, T., Ungermann, C., et al. (2012). Dissection of minimal sequence requirements for rhoptry membrane targeting in the malaria parasite. Traffic. *13*, 1335-1350.

Cavalier-Smith, T. (1993). Kingdom protozoa and its 18 phyla. Microbiol. Rev. *57*, 953–994

Charych, E.I., Jiang, L.-X., Lo, F., Sullivan, K., and Brandon, N.J. (2010). Interplay of palmitoylation and phosphorylation in the trafficking and localization of phosphodiesterase 10A: implications for the treatment of schizophrenia. J. Neurosci. *30*, 9027–9037.

Child, M.A., Hall, C.I., Beck, J.R., Ofori, L.O., Albrow, V.E., Garland, M., Bowyer, P.W., Bradley, P.J., Powers, J.C., Boothroyd, J.C., et al. (2013). Small-molecule inhibition of a depalmitoylase enhances *Toxoplasma* host-cell invasion. Nat. Chem. Biol. *9*, 651–656.

Chowdhury, D.R., Angov, E., Kariuki, T., and Kumar, N. (2009). A potent malaria transmission blocking vaccine based on codon harmonized full length Pfs48/45 expressed in Escherichia coli. PLoS One *4*, e6352.

Collins, W. E., and Jeffery, G. M. (2007). *Plasmodium* malariae: parasite and disease. Clin Microbio Rev. 20, 579-592.

Collins, C.R., Das, S., Wong, E.H., Andenmatten, N., Stallmach, R., Hackett, F., Herman, J.-P., Müller, S., Meissner, M., and Blackman, M.J. (2013). Robust inducible Cre recombinase activity in the human malaria parasite *Plasmodium falciparum* enables efficient gene deletion within a single asexual erythrocytic growth cycle. Mol. Microbiol.

Corvi, M.M., Alonso, A.M., and Caballero, M.C. (2012). Protein palmitoylation and pathogenesis in apicomplexan parasites. J. Biomed. Biotechnol. 483969, doi:10.1155

Counihan, N.A., Kalanon, M., Coppel, R.L., and de Koning-Ward, T.F. (2013). *Plasmodium* rhoptry proteins: why order is important. Trends Parasitol. 1–9.

Cowman, A.F., and Crabb, B.S. (2006). Invasion of red blood cells by malaria parasites. Cell *124*, 755–766.

Cowman, A.F., Berry, D., and Baum, J. (2012). The cellular and molecular basis for malaria parasite invasion of the human red blood cell. J. Cell Biol. *198*, 961–971.

Crowther, G. J., Napuli, A. J., Gilligan, J. H., Gagaring, K., Borboa, R., Francek, C., ... and Kuhen, K. L. (2011). Identification of inhibitors for putative malaria drug targets among novel antimalarial compounds. Molec. Biochem. Parasitol. 175, 21-29.

Dearnley, M.K., Yeoman, J.A., Hanssen, E., Kenny, S., Turnbull, L., Whitchurch, C.B., Tilley, L., and Dixon, M.W. (2012). Origin, composition, organization and function of the inner membrane complex of *Plasmodium falciparum* gametocytes. J. Cell Sci. *125*, 2053–2063.

Delves, M., Plouffe, D., Scheurer, C., Meister, S., Wittlin, S., Winzeler, E. A., ... and Leroy, D. (2012). The activities of current antimalarial drugs on the life cycle stages of *Plasmodium*: a comparative study with human and rodent parasites. PLoS Med. *9*, e1001169.

Devadas, B., Lug, T., Katohp, A., Kishore, N.S., Wade, A.C., Mehta, P.P., Rudnickt, D.A., Bryant, M.L., Adam, S.P., Lij, Q., et al. (1992). Substrate Specificity of *Saccharomyces cerevisiae* Myristoyl-CoA:Protein N-Myristoyltransferase. J. Biol. Chem., 267, 7224-7239.

Dietrich, L.E.P., and Ungermann, C. (2004). On the mechanism of protein palmitoylation. EMBO Rep. *5*, 1053–1057.

Dixon, M.W.A., Thompson, J., Gardiner, D.L., and Trenholme, K.R. (2008). Sex in *Plasmodium*: a sign of commitment. Trends Parasitol. *24*, 168–175.

Dondorp, A.M., Fairhurst, R.M., Slutsker, L., Macarthur, J.R., Breman, J.G., Guerin, P.J., Wellems, T.E., Ringwald, P., Newman, R.D., and Plowe, C.V. (2011). The threat of artemisinin-resistant malaria. N. Engl. J. Med. *365*, 1073–1075.

Van Dooren, G. G., Stimmler, L. M., and McFadden, G. I. (2006). Metabolic maps and functions of the *Plasmodium* mitochondrion. FEMS Microbiol. Rev. 30, 596-630.

Van Dooren, G.G., and Striepen, B. (2013). The algal past and parasite present of the apicoplast. Annu. Rev. Microbiol. *67*, 271–289.

Drakeley, C., Sutherland, C., Bousema, J. T., Sauerwein, R. W., and Targett, G. A. (2006). The epidemiology of *Plasmodium falciparum* gametocytes: weapons of mass dispersion. Trends Parasitol. *22*, 424-430.

Draper, J.M., and Smith, C.D. (2009). Palmitoyl acyltransferase assays and inhibitors. Mol. Membr. Biol. *26*, 5–13.

Drisdel, R.C., and Green, W.N. (2004) Labeling and quantifying sites of protein palmitoylation. Biotechniques. 36, 276-285.

Dubremetz, J., and Torpier, G. (1978) Freeze fracture study of the pellicle of an eimerian sporozoite (Protozoa, Coccidia). J Ultrastruct Res. *62*, 94–109.

Ducker, C.E., Stettler, E.M., French, K.J., Upson, J.J., and Smith, C.D. (2004). Huntingtin interacting protein 14 is an oncogenic human protein: palmitoyl acyltransferase. Oncogene *23*, 9230–9237.

Ducker, C.E., Griffel, L.K., Smith, R.A., Keller, S.N., Zhuang, Y., Xia, Z., Diller, J.D., and Smith, C.D. (2006). Discovery and characterization of inhibitors of human palmitoyl acyltransferases. Mol. Cancer Ther. *5*, 1647–1659.

El-Husseini, A. E. D., Craven, S. E., Brock, S. C., and Bredt, D. S. (2001). Polarized targeting of peripheral membrane proteins in neurons. J. Biol. Chem. 276, 44984-44992.

Enayati, A., and Hemingway, J. (2010). Malaria management: past, present, and future. Annu. Rev. Entomol. *55*, 569–591.

Epp, C., Raskolnikov, D., and Deitsch, K. (2008) A regulatable transgene expression system for cultured *Plasmodium falciparum* parasites. Malaria Journal. *7*, 86.

Epstein, J.E., Tewari, K., Lyke, K.E., Sim, B.K.L., Billingsley, P.F., Laurens, M.B., Gunasekera, a, Chakravarty, S., James, E.R., Sedegah, M., et al. (2011). Live attenuated malaria vaccine designed to protect through hepatic $CD8^+$ T cell immunity. Science *334*, 475–480.

Fidock, D., and Wellems, T. (1997) Transformation with human dihydrofolate reductase renders malaria parasites insensitive to WR99210 but does not affect the intrinsic activity of proguanil. Proc. Natl. Acad. Sci. *94*, 10931–10936.

Fidock, D. A., Rosenthal, P. J., Croft, S. L., Brun, R., and Nwaka, S. (2004). Antimalarial drug discovery: efficacy models for compound screening. Nat Rev Drug Discov. *3*, 509-520.

Fivelman, Q.L., McRobert, L., Sharp, S., Taylor, C.J., Saeed, M., Swales, C.A, Sutherland, C.J., and Baker, D.A. (2007). Improved synchronous production of *Plasmodium falciparum* gametocytes in vitro. Mol. Biochem. Parasitol. *154*, 119–123.

Florens, L., Washburn, M.P., Raine, J.D., Anthony, R.M., Grainger, M., Haynes, J.D., Moch, J.K., Muster, N., Sacci, J.B., Tabb, D.L., et al. (2002). A proteomic view of the *Plasmodium falciparum* life cycle. Nature *419*, 520–526.

Flueck, C., Bartfai, R., Niederwieser, I., Witmer, K., Alako, B.T.F., Moes, S., Bozdech, Z., Jenoe, P., Stunnenberg, H.G., and Voss, T.S. (2010) A major role for the *Plasmodium falciparum* ApiAP2 protein PfSIP2 in chromosome end biology. PLoS Pathog. doi:10.1371/journal.ppat.1000784

Frearson, J. a, Brand, S., McElroy, S.P., Cleghorn, L.A.T., Smid, O., Stojanovski, L., Price, H.P., Guther, M.L.S., Torrie, L.S., Robinson, D.A., et al. (2010). N-myristoyltransferase inhibitors as new leads to treat sleeping sickness. Nature *464*, 728–732.

Frénal, K., Polonais, V., Marq, J.-B., Stratmann, R., Limenitakis, J., and Soldati-Favre, D. (2010). Functional dissection of the apicomplexan glideosome molecular architecture. Cell Host Microbe *8*, 343–357.

Frénal, K., Tay, C.L., Mueller, C., Bushell, E.S., Jia, Y., Graindorge, A., Billker, O., Rayner, J.C., and Soldati-Favre, D. (2013). Global analysis of apicomplexan protein S-acyl transferases reveals an enzyme essential for invasion. Traffic *14*, 895–911.

Frénal, K., Kemp, L.E., and Soldati-Favre, D. (2014). Emerging roles for protein S-palmitoylation in *Toxoplasma* biology. Int. J. Parasitol. *44*, 121–131.

Fukata, Y., Iwanaga, T., and Fukata, M. (2006). Systematic screening for palmitoyl transferase activity of the DHHC protein family in mammalian cells. Methods, 40, 177-182.

Fung, C., Beck, J.R., Robertson, S.D., Gubbels, M.-J., and Bradley, P.J. (2012). *Toxoplasma* ISP4 is a central IMC Sub-compartment Protein whose localization depends on palmitoylation but not myristoylation. Mol. Biochem. Parasitol. *184*, 99–108.

Gamsjaeger, R., Liew, C. K., Loughlin, F. E., Crossley, M., and Mackay, J. P. (2007). Sticky fingers: zinc-fingers as protein-recognition motifs. Trends Biochem. Sci. 32, 63-70.

Gardner, M.J., Hall, N., Fung, E., White, O., Berriman, M., Hyman, R.W., Carlton, J.M., Pain, A., Nelson, K.E., Bowman, S., et al. (2002). Genome sequence of the human malaria parasite *Plasmodium falciparum*. Nature *419*, 498–511.

Gaskins, E., Gilk, S., DeVore, N., Mann, T., Ward, G., and Beckers, C. (2004). Identification of the membrane receptor of a class XIV myosin in *Toxoplasma gondii*. J. Cell Biol. *130*, 285–297.

Gavin, A.-C., Bösche, M., Krause, R., Grandi, P., Marzioch, M., Bauer, A., Schultz, J., Rick, J.M., Michon, A.-M., Cruciat, C.-M., et al. (2002). Functional organization of the yeast proteome by systematic analysis of protein complexes. Nature *415*, 141–147.

Gething, P.W., Patil, A.P., Smith, D.L., Guerra, C. a, Elyazar, I.R.F., Johnston, G.L., Tatem, A.J., and Hay, S.I. (2011). A new world malaria map: *Plasmodium falciparum* endemicity in 2010. Malar. J. *10*, 378.

Gething, P.W., Elyazar, I.R.F., Moyes, C.L., Smith, D.L., Battle, K.E., Guerra, C. a, Patil, A.P., Tatem, A.J., Howes, R.E., Myers, M.F., et al. (2012). A long neglected world malaria map: *Plasmodium vivax* endemicity in 2010. PLoS Negl. Trop. Dis. *6*, e1814.

González Montoro, A., Quiroga, R., Maccioni, H.J.F., and Valdez Taubas, J. (2009). A novel motif at the C-terminus of palmitoyltransferases is essential for Swf1 and Pfa3 function in vivo. Biochem. J. *419*, 301–308.

González Montoro, A., Chumpen Ramirez, S., Quiroga, R., and Valdez Taubas, J. (2011). Specificity of transmembrane protein palmitoylation in yeast. PLoS One *6*, e16969.

Gordon, J.L., Beatty, W.L., and Sibley, L.D. (2008) A novel actin-related protein is associated with daughter cell formation in *Toxoplasma gondii*. Eukaryot Cell 7: 1500–1512.

Gould, S.B., Tham, W.-H., Cowman, A.F., McFadden, G.I., and Waller, R.F. (2008). Alveolins, a new family of cortical proteins that define the protist infrakingdom Alveolata. Mol. Biol. Evol. *25*, 1219–1230.

Gould, S.B., Kraft, L.G.K., Van Dooren, G.G., Goodman, C.D., Ford, K.L., Cassin, A.M., Bacic, A., McFadden, G.I., and Waller, R.F. (2011). Ciliate pellicular proteome identifies novel protein families with characteristic repeat motifs that are common to alveolates. Mol. Biol. Evol. *28*, 1319–1331.

Greaves, J., and Chamberlain, L.H. (2011). DHHC palmitoyl transferases: substrate interactions and (patho)physiology. Trends Biochem. Sci. *36*, 245–253.

Greenwood, B. M., Fidock, D. A., Kyle, D. E., Kappe, S. H., Alonso, P. L., Collins, F. H., and Duffy, P. E. (2008). Malaria: progress, perils, and prospects for eradication. J Clin Invest. *118*, 1266-1276.

Gubbels, M.-J., Wieffer, M., and Striepen, B. (2004). Fluorescent protein tagging in *Toxoplasma gondii*: identification of a novel inner membrane complex component conserved among Apicomplexa. Mol. Biochem. Parasitol. *137*, 99–110.

Gunaratne, R.S., Sajid, M., Ling, I.T., Tripathi, R., Pachebat, J.A., and Holder, A.A. (2000) Characterization of N-myristoyltransferase from *Plasmodium falciparum.* Biochem. J. 348, 459-463.

Gupta, P., Soyombo, A.A., Atashband, A., Wisniewski, K.E., Shelton, J.M., Richardson, J.A., Hammer, R.E., and Hofmann, S.L. (2001). Disruption of PPT1 or PPT2 causes neuronal ceroid lipofuscinosis in knockout mice. 2–7.

Hall, T. M. T. (2005). Multiple modes of RNA recognition by zinc finger proteins. Curr. Opin. Struct. Biol. 15, 367-373.

Hay, S. I., Sinka, M. E., Okara, R. M., Kabaria, C. W., Mbithi, P. M., Tago, C. C., ... and Godfray, H. C. J. (2010). Developing global maps of the dominant *Anopheles* vectors of human malaria. PLoS Med. 7, e1000209.

Hemingway, J., Hawkes, N. J., McCarroll, L., & Ranson, H. (2004). The molecular basis of insecticide resistance in mosquitoes. Insect Biochem. Molec. Biol. 34, 653-665.

Heuckeroth, R.O., Glaser, L., and Gordon, J.I. (1988). Heteroatom-substituted fatty acid analogs as substrates for N-myristoyltransferase: an approach for studying both the enzymology and function of protein acylation. Proc. Natl. Acad. Sci. *85*, 8795–8799.

Hill, A.V.S. (2011). Vaccines against malaria. Philos. Trans. R. Soc. London - Ser. B Biol. Sci. *366*, 2806–2814.

Hou, H., John Peter, A.T., Meiringer, C., Subramanian, K., and Ungermann, C. (2009). Analysis of DHHC acyltransferases implies overlapping substrate specificity and a two-step reaction mechanism. Traffic. *10*, 1061–1073.

Hu, K., Mann, T., Striepen, B., Beckers, C. J., Roos, D. S., and Murray, J. M. (2002). Daughter Cell Assembly in the Protozoan Parasite*Toxoplasma gondii*. Mol. Biol. Cell. 13, 593-606.

Hu, G., Cabrera, A., Kono, M., Mok, S., Chaal, B.K., Haase, S., Engelberg, K., Cheemadan, S., Spielmann, T., Preiser, P.R., et al. (2010). Transcriptional profiling of growth perturbations of the human malaria parasite *Plasmodium falciparum*. Nat. Biotechnol. *28*, 91–98.

Huang, K., Yanai, A., Kang, R., Arstikaitis, P., Singaraja, R.R., Metzler, M., Mullard, A., Haigh, B., Gauthier-Campbell, C., Gutekunst, C.A., Hayden, M.R., El-Husseini, A. (2004) Huntingtin-interacting protein HIP14 is a palmitoyl transferase involved in palmitoylation and trafficking of multiple neuronal proteins. Neuron. 44, 977-986.

Ikadai, H., Shaw Saliba, K., Kanzok, S.M., McLean, K.J., Tanaka, T.Q., Cao, J., Williamson, K.C., and Jacobs-Lorena, M. (2013). Transposon mutagenesis identifies genes essential for *Plasmodium falciparum* gametocytogenesis. Proc. Natl. Acad. Sci. 1–9.

Jones, M.L., Collins, M.O., Goulding, D., Choudhary, J.S., and Rayner, J.C. (2012) Analysis of protein palmitoylation reveals a pervasive role in *Plasmodium* development and pathogenesis.Cell Host Microbe. 12, 246–258.

Kang, R., Wan, J., Arstikaitis, P., Takahashi, H., Huang, K., Bailey, A.O., Thompson, J.X., Roth, A.F., Drisdel, R.C., Mastro, R., et al. (2008). Neural palmitoyl-proteomics reveals dynamic synaptic palmitoylation. Nature *456*, 904–909.

Kayser, F., Böttger, E., Zinkernagel, R., Haller, O., Eckert, J., and Deplazes, P. (2005) Taschenlehrbuch Medizinische Mikrobiologie. Georg Thieme Verlag, Stuttgart.

Keeling, P.J. (2009). Chromalveolates and the evolution of plastids by secondary endosymbiosis. J. Eukaryot. Microbiol. *56*, 1–8.

Kemp, L.E., Rusch, M., Adibekian, A., Bullen, H.E., Graindorge, A., Freymond, C., Rottmann, M., Braun-Breton, C., Baumeister, S., Porfetye, A.T., et al. (2013). Characterization of a serine hydrolase targeted by acyl-protein thioesterase inhibitors in *Toxoplasma gondii*. J. Biol. Chem. *288*, 27002–27018.

Khan, S.M., Janse, C.J., Kappe, S.H.I., and Mikolajczak, S.A. (2012). Genetic engineering of attenuated malaria parasites for vaccination. Curr. Opin. Biotechnol. *23*, 908–916.

Khater, E.I., Sinden, R.E., and Dessens, J.T. (2004). A malaria membrane skeletal protein is essential for normal morphogenesis, motility, and infectivity of sporozoites. J. Cell Biol. *167*, 425–432.

Kishore, N.S., Woods, D.C., Mehta, P.P., Wade, A.C., Lun, T., Gokeln, G.W., and Gordon, I. (1993). Comparison of the Acyl Chain Specificities of Human Myristoyl-CoA Synthetase and Human Myristoyl-CoA : Protein. *268*, 4889–4902.

Kono, M., Herrmann, S., Loughran, N.B., Cabrera, A., Engelberg, K., Lehmann, C., Sinha, D., Prinz, B., Ruch, U., Heussler, V., et al. (2012). Evolution and Architecture of the Inner Membrane Complex in Asexual and Sexual Stages af the Malaria Parasite. Mol. Biol. Evol. *29*, 1–20.

Kono, M., Prusty, D., Gilberger, T.W. (2013) A membranous system in the spotlight: The apicomplexan inner membrane complex and its adaptation to an endoparasitic life style. Front Biosci. 18, 982-992.

Kostiuk, M.A, Corvi, M.M., Keller, B.O., Plummer, G., Prescher, J.A, Hangauer, M.J., Bertozzi, C.R., Rajaiah, G., Falck, J.R., and Berthiaume, L.G. (2008). Identification of palmitoylated mitochondrial proteins using a bio-orthogonal azido-palmitate analogue. FASEB J. *22*, 721–732.

Kudryashev, M., Lepper, S., Stanway, R., Bohn, S., Baumeister, W., Cyrklaff, M., and Frischknecht, F. (2010). Positioning of large organelles by a membrane- associated cytoskeleton in *Plasmodium* sporozoites. Cell. Microbiol. *12*, 362–371.

Kyes, S.A., Kraemer, S.M., and Smith, J.D. (2007) Antigenic Variation in *Plasmodium falciparum*: Gene Organization and Regulation of the var Multigene Family. Eukar. Cell, 6, 1511-1520.

Labaied, M., Harupa, a., Dumpit, R.F., Coppens, I., Mikolajczak, S. a., and Kappe, S.H.I. (2007). *Plasmodium* yoelii Sporozoites with Simultaneous Deletion of P52 and P36 Are Completely Attenuated and Confer Sterile Immunity against Infection. Infect. Immun. *75*, 3758–3768.

Lacroix, C., Giovannini, D., Combe, A., Bargieri, D.Y., Späth, S., Panchal, D., Tawk, L., Thiberge, S., Carvalho, T.G., Barale, J.-C., et al. (2011). FLP/FRT-mediated conditional mutagenesis in pre-erythrocytic stages of *Plasmodium berghei*. Nat. Protoc. *6*, 1412–1428.

Laity, J. H., Lee, B. M., and Wright, P. E. (2001). Zinc finger proteins: new insights into structural and functional diversity. Curr. Opin. Struct. Biol. 11, 39-46.

Lamarque, M., Besteiro, S., Papoin, J., Roques, M., Vulliez-Le Normand, B., Morlon-Guyot, J., Dubremetz, J.-F., Fauquenoy, S., Tomavo, S., Faber, B.W., et al. (2011). The RON2-AMA1 interaction is a critical step in moving junction-dependent invasion by apicomplexan parasites. PLoS Pathog. *7*, e1001276.

Lambros, C., and Vanderberg, J.P. (1979) Synchronization of *Plasmodium falciparum* Erythrocytic Stages in Culture. J. Parasitol. *65*, 418-420.

Lengeler, C. (2004). Insecticide-treated bed nets and curtains for preventing malaria. Cochrane Database Syst Rev. 2, CD000363.

Letunic, I., Doerks, T., and Bork, P. (2012). SMART 7: recent updates to the protein domain annotation resource. Nucl. Acids Res. 40, D302-D305.

Linder, M.E., and Deschenes, R.J. (2007). Palmitoylation: policing protein stability and traffic. Nat. Rev. Mol. Cell Biol. *8*, 74–84.

Linder, M.E., and Jennings, B.C. (2013). Mechanism and function of DHHC S-acyltransferases. Biochem. Soc. Trans. *41*, 29–34.

Lobo, S., Greentree, W.K., Linder, M.E., and Deschenes, R.J. (2002). Identification of a Ras palmitoyltransferase in *Saccharomyces cerevisiae*. J. Biol. Chem. *277*, 41268–41273.

Malpede, B.M., and Tolia, N.H. (2014). Malaria adhesins: structure and function. Cell. Microbiol. *16*, 621–631.

Mann, T., and Beckers, C. (2001). Characterization of the subpellicular network, a filamentous membrane skeletal component in the parasite *Toxoplasma gondii*. Mol Biochem Parasitol *115*, 257–268.

Mansouri, M.R., Marklund, L., Gustavsson, P., Davey, E., Carlsson, B., Larsson, C., White, I., Gustavson, K.-H., and Dahl, N. (2005). Loss of ZDHHC15 expression in a woman with a balanced translocation t(X;15)(q13.3;cen) and severe mental retardation. Eur. J. Hum. Genet. *13*, 970–977.

Maund, S. J., Campbell, P. J., Giddings, J. M., Hamer, M. J., Henry, K., Pilling, E. D., ... and Wheeler, J. R. (2012). Ecotoxicology of synthetic pyrethroids. In *Pyrethroids* (pp. 137-165). Springer Berlin Heidelberg.

Maurer-Stroh, S., Eisenhaber, B., and Eisenhaber, F. (2002). N-terminal N-myristoylation of proteins: refinement of the sequence motif and its taxon-specific differences. J. Mol. Biol. *317*, 523–540.

Ménard, R., Tavares, J., Cockburn, I., Markus, M., Zavala, F., and Amino, R. (2013). Looking under the skin: the first steps in malarial infection and immunity. Nat. Rev. Microbiol. *11*, 701–712.

Mendis, K., Sina, B., Marchesini, P., and Carter, R. (2001) The neglected burden of *Plasmodium vivax* malaria. Am. J. Trop. Med. Hyg. *64*, 97-106.

Meszoely, C., Erbe, E., Steere, R., Trosper, J., Beaudoin, R.L. (1987) *Plasmodium falciparum*: freeze-fracture of the gametocyte pellicular complex. Exp. Parasitol. 64, 300–309.

Mitchell, D. a, Vasudevan, A., Linder, M.E., and Deschenes, R.J. (2006). Protein palmitoylation by a family of DHHC protein S-acyltransferases. J. Lipid Res. *47*, 1118–1127.

Mitchison, H.M., Lim, M.J., and Cooper, J.D. (2004). Selectivity and Types of Cell Death in the Neuronal Ceroid Lipofuscinoses (NCLs). Brain Pathology. 14, 86-96.

Möskes, C., Burghaus, P.A., Wernli, B., Sauder, U., Dürrenberger, M., and Kappes, B. (2004). Export of *Plasmodium falciparum* calcium-dependent protein kinase 1 to the parasitophorous vacuole is dependent on three N-terminal membrane anchor motifs. Mol. Microbiol. 54, 676-691.

Moore, R.B., Oborník, M., Janouskovec, J., Chrudimský, T., Vancová, M., Green, D.H., Wright, S.W., Davies, N.W., Bolch, C.J.S., Heimann, K., et al. (2008). A photosynthetic alveolate closely related to apicomplexan parasites. Nature *451*, 959–963.

Morrissette, N. S., Murray, J. M., and Roos, D. S. (1997). Subpellicular microtubules associate with an intramembranous particle lattice in the protozoan parasite *Toxoplasma gondii*. J. Cell Sci. 110, 35-42.

Morrissette, N.S., and Sibley, L.D. (2002). Cytoskeleton of apicomplexan parasites. Microbiol. Mol. Biol. Rev. *66*, 21–38.

Mueller, C., Klages, N., Jacot, D., Santos, J.M., Cabrera, A., Gilberger, T.W., Dubremetz, J.-F., and Soldati-Favre, D. (2013). The *Toxoplasma* Protein ARO Mediates the Apical Positioning of Rhoptry Organelles, a Prerequisite for Host Cell Invasion. Cell Host Microbe *13*, 289–301.

Mukai, J., Liu, H., Burt, R. a, Swor, D.E., Lai, W.-S., Karayiorgou, M., and Gogos, J.A. (2004). Evidence that the gene encoding ZDHHC8 contributes to the risk of schizophrenia. Nat. Genet. *36*, 725–731.

Naik, R.S., Venkatesan, M., and Gowda, D.C. (2001). *Plasmodium falciparum*: the lethal effects of tunicamycin and mevastatin on the parasite are not mediated by the inhibition of N-linked oligosaccharide biosynthesis. Exp. Parasitol. *98*, 110–114.

Noedl, H., Se, Y., Schaecher, K., Smith, B.L., Socheat, D., and Fukuda, M.M. (2008). Evidence of artemisinin-resistant malaria in western Cambodia. N. Engl. J. Med. *359*, 2619–2620.

Nussenzweig, R.S., Vanderberg, J., Most, H., and Orton, C. (1967). Protective immunity produced by the injection of x-irradiated sporozoites of *Plasmodium berghei*. Nature. 216, 160 - 162

Nussenzweig, V., and Nussenzweig, R. S. (1989). Rationale for the development of an engineered sporozoite malaria vaccine. Advances Immunol. 45, 283-334.

O'Neill, M.T., Phuong, T., Healer, J., Richard, D., and Cowman, A.F. (2011). Gene deletion from *Plasmodium falciparum* using FLP and Cre recombinases: implications for applied site-specific recombination. Int. J. Parasitol. *41*, 117–123.

Ohno, Y., Kihara, A., Sano, T., and Igarashi, Y. (2006). Intracellular localization and tissue-specific distribution of human and yeast DHHC cysteine-rich domain-containing proteins. Biochim. Biophys. Acta *1761*, 474–483.

Oyama, T., Miyoshi, Y., Koyama, K., Nakagawa, H., Yamori, T., Ito, T., Matsuda, H., Arakawa, H., and Nakamura, Y. (2000). Isolation of a novel gene on 8p21.3-22 whose expression is reduced significantly in human colorectal cancers with liver metastasis. Genes. Chromosomes Cancer *29*, 9–15.

Panethymitaki, C., Bowyer, P.W., Price, H.P., Leatherbarrow, R.J., Brown, K. a, and Smith, D.F. (2006). Characterization and selective inhibition of myristoyl-CoA:protein N-myristoyltransferase from *Trypanosoma brucei* and *Leishmania major*. Biochem. J. *396*, 277–285.

Pedro, M.P., Vilcaes, A.A., Tomatis, V.M., Oliveira, R.G., Gomez, G.A., and Daniotti, J.L. (2013). 2-Bromopalmitate Reduces Protein Deacylation by Inhibition of Acyl-Protein Thioesterase Enzymatic Activities. PloS One, 8, e75232.

Van Pelt-Koops, J.C., Pett, H.E., Graumans, W., van der Vegte-Bolmer, M., van Gemert, G.J., Rottmann, M., Yeung, B.K.S., Diagana, T.T., and Sauerwein, R.W. (2012). The spiroindolone drug candidate NITD609 potently inhibits gametocytogenesis and blocks *Plasmodium falciparum* transmission to anopheles mosquito vector. Antimicrob. Agents Chemother. *56*, 3544–3548.

Phyo, A.P., Nkhoma, S., Stepniewska, K., Ashley, E.A., Nair, S., McGready, R., ler Moo, C., Al-Saai, S., Dondorp, A.M., Lwin, K.M., et al. (2012). Emergence of artemisinin-resistant malaria on the western border of Thailand: a longitudinal study. Lancet *379*, 1960–1966.

Planey, S.L., and Zacharias, D.A. (2009). Palmitoyl acyltransferases, their substrates, and novel assays to connect them. Mol. Membr. Biol. *26*, 14–31.

Planey, S.L., and Zacharias, D.A. (2010). Identification of targets and inhibitors of protein palmitoylation. Expert Opin. Drug Discov. *5*, 155–164.

Pluess, B., Tanser, F.C., Lengeler, C., and Sharp, B.L. (2010). Indoor residual spraying for preventing malaria Cochrane Database Syst Rev. doi: 10.1002/14651858.CD006657.pub2.

Poulin, B., Patzewitz, E.-M., Brady, D., Silvie, O., Wright, M.H., Ferguson, D.J.P., Wall, R.J., Whipple, S., Guttery, D.S., Tate, E.W., et al. (2013). Unique apicomplexan IMC sub-compartment proteins are early markers for apical polarity in the malaria parasite. Biol. Open *2*, 1160–1170.

Porchet, E. and Torpier, G. (1977) Etude du germe infectieux de *Sarcocystis tenella* et *Toxoplasma gondii* par la technique du cryodécapage. Z. Parasitenk. *54*, 101-124.

Prudêncio, M., Rodriguez, A., and Mota, M.M. (2006). The silent path to thousands of merozoites: the *Plasmodium* liver stage. Nat. Rev. Microbiol. *4*, 849–856.

Putilina, T., Wong, P., and Gentleman, S. (1999). The DHHC domain: a new highly conserved cysteine-rich motif. Mol. Cell. Biochem. *195*, 219–226.

Raibaud, A., Lupetti, P., Paul, R., Mercati, D., Brey, P., Sinden, R., Heuser, J., Dallai, R. (2001) Cryofracture electron microscopy of the ookinete pellicle of *Plasmodium gallinaceum* reveals the existence of novel pores in the alveolar membranes. J Struct Biol. 135, 47–57.

Ranson, H., N'Guessan, R., Lines, J., Moiroux, N., Nkuni, Z., and Corbel, V. (2011). Pyrethroid resistance in African anopheline mosquitoes: what are the implications for malaria control? Trends Parasitol, 27, 91-98.

Rayavara, K., Rajapandi, T., Wollenberg, K., Kabat, J., Fischer, E.R., and Desai, S.A. (2009). A complex of three related membrane proteins is conserved on malarial merozoites. Mol. Biochem. Parasitol. *167*, 135–143.

Raymond, F.L., Tarpey, P.S., Edkins, S., Tofts, C., O'Meara, S., Teague, J., Butler, A., Stevens, C., Barthorpe, S., Buck, G., et al. (2007). Mutations in ZDHHC9, which encodes a palmitoyltransferase of NRAS and HRAS, cause X-linked mental retardation associated with a Marfanoid habitus. Am. J. Hum. Genet. *80*, 982–987.

Rees-Channer, R., Martin, S., Green, J., Bowyer, P., Grainger, M., Molloy, J., Holder, A. (2006) Dual acylation of the 45 kDa gliding-associated protein (GAP45) in *Plasmodium falciparum* merozoites. Mol Biochem Parasitol. 149, 113–116.

Ren, J., Wen, L., Gao, X., Jin, C., Xue, Y., and Yao, X. (2008). CSS-Palm 2.0: an updated software for palmitoylation sites prediction. Protein Eng. Des. Sel. *21*, 639–644.

Resh, M.D. (1997). Fatty acylation of proteins: New insights into membrane targeting of myristoylated and palmitoylated proteins. Biochim. Biophys. Acta 1451, 1-16

Resh, M.D. (2006). Trafficking and signaling by fatty-acylated and prenylated proteins. Nat. Chem. Biol. *2*, 584–590.

Ridzuan, M. a M., Moon, R.W., Knuepfer, E., Black, S., Holder, A. a, and Green, J.L. (2012). Subcellular location, phosphorylation and assembly into the motor complex of GAP45 during *Plasmodium falciparum* schizont development. PLoS One *7*, e33845.

Robert, V., Macintyre, K., Keating, J., Trape, J. F., Duchemin, J. B., Warren, M., and Beier, J. C. (2003). Malaria transmission in urban sub-Saharan Africa. Am J Trop Med Hyg. *68*, 169-176.

Rocks, O., Peyker, A., and Bastiaens, P. I. (2006). Spatio-temporal segregation of Ras signals: one ship, three anchors, many harbors. Curr. Opin. Cell Biol. 18, 351-357.

Rocks, O., Gerauer, M., Vartak, N., Koch, S., Huang, Z.-P., Pechlivanis, M., Kuhlmann, J., Brunsveld, L., Chandra, A., Ellinger, B., et al. (2010). The palmitoylation machinery is a spatially organizing system for peripheral membrane proteins. Cell *141*, 458–471.

Roth, A.F., Feng, Y., Chen, L., and Davis, N.G. (2002). The yeast DHHC cysteine-rich domain protein Akr1p is a palmitoyl transferase. J. Cell Biol. *159*, 23–28.

Roth, A.F., Wan, J., Bailey, A.O., Sun, B., Kuchar, J. a, Green, W.N., Phinney, B.S., Yates, J.R., and Davis, N.G. (2006). Global analysis of protein palmitoylation in yeast. Cell *125*, 1003–1013.

Rottmann, M., McNamara, C., Yeung, B.K.S., Lee, M.C.S., Zou, B., Russell, B., Seitz, P., Plouffe, D.M., Dharia, N. V, Tan, J., et al. (2010). Spiroindolones, a potent compound class for the treatment of malaria. Science *329*, 1175–1180.

Rudnick, D.A., McWherter, C.A., Rocque, W.J., Lennon, P.J., Getman, D.P., Gordon, J.I. (1991) Kinetic and structural evidence for a sequential ordered Bi Bi mechanism of catalysis by *Saccharomyces cerevisiae* myristoyl-CoA:protein N-myristoyltransferase. J. Biol. Chem. 266, 9732-9739.

Russo, I., Oksman, A., and Goldberg, D.E. (2009). Fatty acid acylation regulates trafficking of the unusual *Plasmodium falciparum* calpain to the nucleolus. Mol. Microbiol. *72*, 229–245.

Sachs, J., and Malaney, P. (2002) The economic and social burden of malaria. Nature *415*, 680-685.

Salaun, C., Greaves, J., and Chamberlain, L.H. (2010). The intracellular dynamic of protein palmitoylation. J. Cell Biol. *191*, 1229–1238.

Santos, J.M., Lebrun, M., Daher, W., Soldati, D., and Dubremetz, J.-F. (2009). Apicomplexan cytoskeleton and motors: key regulators in morphogenesis, cell division, transport and motility. Int. J. Parasitol. *39*, 153–162.

Saxon, E., and Bertozzi, C.R. (2000). Cell surface engineering by a modified Staudinger reaction. Science. *287*, 2007–2010.

Scherf, A., Hernandez-Rivas, R., Buffet, P., Bottius, E., Benatar, C., Pouvelle, B., Gysin, J., and Lanzer, M. (1998) Antigenic variation in malaria: in situ switching, relaxed and mutually exclusive transcription of var genes during intra-erythrocytic development in *Plasmodium falciparum*. EMBO Journal. 17, 5418-5426.

Schultz, J., Milpetz, F., Bork, P., & Ponting, C. P. (1998). SMART, a simple modular architecture research tool: identification of signaling domains. PNAS, 95, 5857-5864.

Seder, R. A., Chang, L. J., Enama, M. E., Zephir, K. L., Sarwar, U. N., Gordon, I. J., ... and Wilson, B. (2013). Protection against malaria by intravenous immunization with a nonreplicating sporozoite vaccine. Science. *341*, 1359-1365.

Selvakumar, P., and Sharma, R.K. (2006). Phosphorylation and dephosphorylation of human myristoyltransferase type 1. Can. J. Physiol. Pharmacol. 84, 707-712.

Seydel, K.B., Gaur, D., Aravind, L., Subramanian, G., and Miller, L.H. (2005). *Plasmodium falciparum*: characterization of a late asexual stage golgi protein containing both ankyrin and DHHC domains. Exp. Parasitol. *110*, 389–393.

Shahinian, S., and Silvius, J.R. (1995). Doubly-lipid-modified protein sequence motifs exhibit long-lived anchorage to lipid bilayer membranes. Biochemistry *34*, 3813–3822.

Shekalaghe, S., Rutaihwa, M., Billingsley, P.F., Chemba, M., Daubenberger, C.A., James, E., Mpina, M., Ali Juma, O., Schindler, T., Huber, E., et al. (2014). Controlled Human Malaria Infection of Tanzanians by Intradermal Injection of Aseptic, Purified, Cryopreserved *Plasmodium falciparum* Sporozoites. Am. J. Trop. Med. Hyg. 4–6.

Sibley, L.D. (2004). Intracellular parasite invasion strategies. Science. *304*, 248–253.

Silvestrini, F., Lasonder, E., Olivieri, A., Camarda, G., van Schaijk, B., Sanchez, M., Younis Younis, S., Sauerwein, R., and Alano, P. (2010). Protein export marks the early phase of gametocytogenesis of the human malaria parasite *Plasmodium falciparum*. Mol. Cell. Proteomics *9*, 1437–1448.

Sinka, M. E., Bangs, M. J., Manguin, S., Rubio-Palis, Y., Chareonviriyaphap, T., Coetzee, M., ... and Hay, S. I. (2012). A global map of dominant malaria vectors. Parasit Vectors. 5, 69.

Singaraja, R. R., Hadano, S., Metzler, M., Givan, S., Wellington, C. L., Warby, S., ... and Hayden, M. R. (2002). HIP14, a novel ankyrin domain-containing protein, links huntingtin to intracellular trafficking and endocytosis. Human Molec. Gen. 11, 2815-2828.

Singh, B., Sung, L.K., Matusop, A., Radhakrishnan, A., Shamsul, S.S., Cox-Singh, J., Thomas, A., and Conway, D.J. (2004) A large focus of naturally acquired *Plasmodium knowlesi* infections in human beings. The Lancet. *363*, 1017-1024.

Sinnis, P., and Zavala, F. (2012). The skin: where malaria infection and the host immune response begin. In Seminars in immunopathology (Vol. 34, No. 6, pp. 787-792). Springer-Verlag.

Smotrys, J.E., and Linder, M.E. (2004). Palmitoylation of intracellular signaling proteins: regulation and function. Annu. Rev. Biochem. *73*, 559–587.

Snow, R.W., Guerra, C.A., Noor, A.M., Myint, H.Y., and Hay, S.I. (2005) The global distribution of clinical episodes of *Plasmodium falciparum* malaria. Nature. *434*, 214-217.

Soldati, D., Foth, B.J., and Cowman, A.F. (2004). Molecular and functional aspects of parasite invasion. Trends Parasitol. *20*, 567–574.

Spring, M., Murphy, J., Nielsen, R., Dowler, M., Bennett, J.W., Zarling, S., Williams, J., de la Vega, P., Ware, L., Komisar, J., et al. (2013). First-in-human evaluation of genetically attenuated *Plasmodium falciparum* sporozoites administered by bite of Anopheles mosquitoes to adult volunteers. Vaccine *31*, 4975–4983.

Stewart, M. J., and Vanderberg, J. P. (1988). Malaria Sporozoites Leave Behind Trails of Circumsporozoite Protein During Gliding Motility. J. Protozool. *35*, 389-393.

Struck, N.S., de Souza Dias, S., Langer, C., Marti, M., Pearce, J.A., Cowman, A.F., and Gilberger, T.W. (2005) Re-defining the Golgi complex in *Plasmodium falciparum* using the novel Golgi marker PfGRASP. J. Cell Science. 118, 5603-5613.

Struck, N.S., Herrmann, S., Schmuck□Barkmann, I., de Souza Dias, S., Haase, S., Cabrera, A.L., ... and Gilberger, T. W. (2008). Spatial dissection of the cis□and trans□Golgi compartments in the malaria parasite *Plasmodium falciparum*. Molec. Microbiol. 67, 1320-1330.

Subramanian, K., Dietrich, L.E.P., Hou, H., LaGrassa, T.J., Meiringer, C.T.A., and Ungermann, C. (2006). Palmitoylation determines the function of Vac8 at the yeast vacuole. J. Cell Sci. *119*, 2477–2485.

Tate, E.W., Bell, A.S., Rackham, M.D., and Wright, M.H. (2014). N-Myristoyltransferase as a potential drug target in malaria and leishmaniasis. Parasitology *141*, 37–49.

Tewari, R., Bailes, E., Bunting, K. A., and Coates, J. C. (2010). Armadillo-repeat protein functions: questions for little creatures. Trends Cell Biol. 20, 470-481.

Tonkin, M.L., Brown, S., Beck, J.R., Bradley, P.J., and Boulanger, M.J. (2012). Purification, crystallization and preliminary X-ray diffraction analysis of inner membrane complex (IMC) sub-compartment protein 1 (ISP1) from *Toxoplasma gondii*. Acta Crystallogr. Sect. F. Struct. Biol. Cryst. Commun. *68*, 832–834.

Tonkin, M.L., Beck, J.R., Bradley, P.J., and Boulanger, M.J. (2014). The Inner Membrane Complex Sub-compartment Proteins Critical for Replication of the Apicomplexan Parasite *Toxoplasma gondii* Adopt a Pleckstrin Homology Fold. J. Biol. Chem. *289*, 13962–13973.

Trager, W., and Jensen, J.B. (1976). Human malaria parasites in continuous culture. Science. *193*, 673-675.

Treeck, M., Zacherl, S., Herrmann, S., Cabrera, A., Kono, M., Struck, N.S., Engelberg, K., Haase, S., Frischknecht, F., Miura, K., et al. (2009). Functional analysis of the leading malaria vaccine candidate AMA-1 reveals an essential role for the cytoplasmic domain in the invasion process. PLoS Pathog. *5*, e1000322.

Turusov, V., Rakitsky, V., and Tomatis, L. (2002). Dichlorodiphenyltrichloroethane (DDT): ubiquity, persistence, and risks. Environ Health Perspect. 111, 125.

Vanbuskirk, K.M., Neill, M.T.O., La, P. De, Maier, A.G., Krzych, U., Williams, J., Dowler, M.G., Sacci, J.B., Kangwanrangsan, N., Tsuboi, T., et al. (2009). falciparum vaccine candidates by design. Proc. Natl. Acad. Sci. *106*, 13004-13009.

Vesa, J., Hellsten, E., Verkruyse, L.A., Camp, L.A., Rapola, J., Santavuori, P., Hofmann, S.L., Peltonen, L. (1995) Mutations in the palmitoyl protein thioesterase gene causing infantile neuronal ceroid lipofuscinosis. Nature. 376, 584-587.

Volkman, S. K., Hartl, D. L., Wirth, D. F., Nielsen, K. M., Choi, M., Batalov, S., ... and Winzeler, E. A. (2002). Excess polymorphisms in genes for membrane proteins in *Plasmodium falciparum*. Science. 298, 216-218.

Wan, J., Roth, A.F., Bailey, A.O., Davis, N.G. (2007) Palmitoylated proteins: purification and identification. Nat. Protoc. *2*, 1573-1584.

Weston, S.A., Camble, R., Colls, J., Rosenbrock, G., Taylor, I., Egerton, M., Tucker, A.D., Tunnicliffe, A., Mistry, A., Mancia, F., et al., (1998) Crystal structure of the anti-fungal target N-myristoyl transferase. Nat. Struct. Biol. 5, 213-221.

White, N.J., Pukrittayakamee, S., Hien, T.T., Faiz, M.A., Mokuolu, O.A., and Dondorp, A.M. (2014). Malaria. 383, 723–735.

WHO World Malaria Report, 2013

Wilson, R.J.M., Denny, P. W., Preiser, P. R., Rangachari, K., Roberts, K., Roy, A., Whyte, A., ... and Williamson, D. H. (1996). Complete Gene Map of the Plastid-like DNA of the Malaria Parasite *Plasmodium falciparum*. J Mol Biol, 261, 155-172.

Wolters, J. (1991). The troublesome parasites--molecular and morphological evidence that Apicomplexa belong to the dinoflagellate-ciliate clade. Biosystems. *25*, 75–83.

Wright, M.H., Heal, W.P., Mann, D.J., and Tate, E.W. (2010). Protein myristoylation in health and disease. J. Chem. Biol. *3*, 19–35.

Wright, M.H., Clough, B., Rackham, M.D., Rangachari, K., Brannigan, J. a, Grainger, M., Moss, D.K., Bottrill, A.R., Heal, W.P., Broncel, M., et al. (2014). Validation of N-myristoyltransferase as an antimalarial drug target using an integrated chemical biology approach. Nat. Chem. *6*, 112–121.

Wu, Y., Sifri, C.D., Lei, H.H., Su, X.Z., and Wellems, T.E. (1995) Transfection of *Plasmodium falciparum* within human red blood cells. Proc. Natl. Acad. Sci.. *92*, 973-977.

Xue, Y., Chen, H., Jin, C., Sun, Z., Yao, X. (2006) NBA-Palm: prediction of palmitoylation site implemented in Naïve Bayes algorithm. BMC Bioinformatics. 7, 458.

Yamamoto, Y., Nishiyama, Y., Ishikawa, S., Nakano, J., Chang, S.S., Bandoh, S., Kanaji, N., Haba, R., Kushida, Y., and Ohkawa, M. (2007). Correlation of 18F-FLT and 18F-FDG uptake on PET with Ki-67 immunohistochemistry in non-small cell lung cancer. Eur. J. Nucl. Med. Mol. Imaging *34*, 1610–1616.

Yanai, A., Huang, K., Kang, R., Singaraja, R.R., Arstikaitis, P., Gan, L., Orban, P.C., Mullard, A., Cowan, C.M., Raymond, L.A., et al. (2006). Palmitoylation of huntingtin by HIP14 is essential for its trafficking and function. Nat. Neurosci. *9*, 824–831.

Yeh, E., and DeRisi, J. L. (2011). Chemical rescue of malaria parasites lacking an apicoplast defines organelle function in blood-stage *Plasmodium falciparum*. PLoS Biol. 9, e1001138.

Yeoman, J. a, Hanssen, E., Maier, A.G., Klonis, N., Maco, B., Baum, J., Turnbull, L., Whitchurch, C.B., Dixon, M.W.A., and Tilley, L. (2011). Tracking Glideosome-associated protein 50 reveals the development and organization of the inner membrane complex of *Plasmodium falciparum*. Eukaryot. Cell *10*, 556–564.

Young, F.B., Butland, S.L., Sanders, S.S., Sutton, L.M., and Hayden, M.R. (2012). Putting proteins in their place: palmitoylation in Huntington disease and other neuropsychiatric diseases. Prog. Neurobiol. *97*, 220–238.

Zhang, M.M., Wu, P.-Y.J., Kelly, F.D., Nurse, P., and Hang, H.C. (2013). Quantitative control of protein S-palmitoylation regulates meiotic entry in fission yeast. PLoS Biol. *11*, e1001597

7. Publication

Wetzel J, Hermann S, Seshadri LS, Prusty D, Peter ATJ, Kono M, Saini S, Nellimarla S, Wong T, Wilcke L, Ramsay O, Cabrera A, Biller L, Mossman K, Spielmann T, Ungermann C, Parkinson J, Gilberger TW. The role of palmitoylation for protein recruitment to the inner membrane complex of the malaria parasite. Journal of Biological Chemistry. 2014; jbc-M114

8. Acknowledgements

First and foremost I would like to thank my thesis supervisor Prof. Dr. Tim Gilberger for giving me the opportunity to realize my PhD project in his laboratory. He provided ideas and enthusiasm, supported me whenever necessary and was a great supervisor, patient and open minded, but critical as well as helpful in any aspect. Without his help, this work wouldn't have been possible. Once again many thanks! Furthermore, I would like to thank Prof. Dr. Egbert Tannich for his co-supervision. A big "thank you" also goes to my former committee members Prof. Dr. Gerry Wright and Prof. Dr. Brian Coombes for their co-supervision of my thesis work while I was at McMaster University in Hamilton, Ontario.

I want to thank the whole Gilberger group for the friendly and inspiring atmosphere in the lab, sit-ins on "the bench" and the entertaining moments not always related to lab activities. Namely, I thank: Dr. Ana Cabrera for always having an open ear and helping to solve problems; Dr. Dhaneswar Prusty for letting me see many things with a different view, sharing fun times and great food; Tatianna Wong, for being a wonderful bench mate and providing great feedback early on; Louisa Wilcke for sharing good times and memories during that hot summer, Dr. Maya Kono for all her help, Dorothee Heincke and Viola Ladenburger for being great lab and desk mates and Dr. Susann Herrmann for letting me be part of her project. Special thanks goes to the Spielmann group – it was great sharing a variety of very small rooms with you guys!

The years I spent in Canada are so memorable to me, which has a lot to do with the great people I was lucky to meet. Namely, I thank Vagmi Patel, Jann Ang and Sidharth Saini for being so welcoming and helpful during the first months and for the great times spent together later on. I thank Olivia Ramsay and for being an amazing friend and bench mate! Big thanks go out to Juliane Wunderlich, Kathrin Stamms, and Joshua Emery. Also, I would like to thank all the lovely people in the Wright Lab, the Brown Lab, the Sloboda lab and the CMCB staff for sharing their expert opinions, relaxing coffee breaks and after work beers at the Phoenix.

Last but not least I'd like to thank my family and friends for all their encouragement and support not only during my PhD years – I thank you so much for listening to me talking about science, the lab and life, and not walking out of the room!!

Language certificate

October 8, 2014

To Whom it May Concern:

I am a native speaker, have read the PhD thesis authored by Johanna Wetzel, and hereby confirm that it complies with the rules of the English language.

Sincerely,

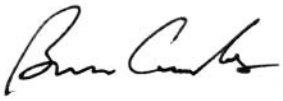

Canada Research Chair in Infectious Disease Pathogenesis
Associate Professor and Associate Chair
Department of Biochemistry & Biomedical Sciences

Dr. Brian K. Coombes, PhD., Department of Biochemistry & Biomedical Sciences
McMaster University, Health Sciences Centre, Room 4H17, 1200 Main Street West, Hamilton, Ontario L8N 3Z5
Ph: 905-525-9140 ext. 22159. Fax: 905-522-9033
e: coombes@mcmaster.ca. web: www.coombeslab.com

Declaration on oath

I hereby declare, on oath, that I have written the present dissertation on my own and have not used other than the acknowledged resources and aids.

_____ _____

City, date Signature